CHARACTERIZATION OF GENES IN THE CYCLOHEXANOL OPERON OF *POLAROMONAS* SP. STRAIN JS666

A Dissertation

Presented to the Faculty of the Graduate School

of Cornell University

In Partial Fulfillment of the Requirements for the Degree of

Doctor of Philosophy

by

Wan Lutfi bin Wan Johari

May 2012

CHARACTERIZATION OF GENES IN THE CYCLOHEXANOL OPERON OF *POLAROMONAS* SP. STRAIN JS666

Wan Lutfi bin Wan Johari, Ph.D.

Cornell University 2012

Polaromonas sp. strain JS666 is the only isolate capable of growth through the aerobic oxidation of *cis*-dichloroethene (cDCE). Study of the JS666 genome, along with previous results from transcriptomics and proteomics studies, have suggested the involvement of a cyclohexanone monooxygenase gene *(chmo, chnB,* Bpro_5565) in the process. Specifically, CHMO was hypothesized to catalyze the epoxidation of cDCE. We successfully inactivated the *chmo* gene through use of a suicide vector, and the resulting *chmo*-knockout strain (KO) was incapable of growth on cyclohexanone (CYHX), cDCE, ethanol (EtOH) and cyclohexanol. The overexpressed CHMO in *Escherichia coli* showed activity on CYHX; nonetheless, no activity was confirmed with cDCE. This suggests that CHMO is not involved in the first step of cDCE degradation, however, differences in cellular environments (i.e. pH, protein folding and post-translational modification) between the *E. coli* and JS666 strains could have contributed to the outcome. Genes in the same operon with *chmo*, namely the adjacent, upstream hydrolase (*chnC,* Bpro_5566) and two adjacent, downstream alcohol dehydrogenases (*chnD* and *chnA*, Bpro_5563 and Bpro_5564, respectively) may serve important roles in cDCE degradation. When CYHX or EtOH was supplied as co-substrate, wild-type JS666 (WT) quickly exhibited cDCE degradation and sustained it through multiple additions, but not when succinate or acetate was co-administered, suggesting that CYHX and EtOH

each elevate expression of proteins involved in cDCE metabolism. ChnD overexpressed in *E. coli* showed activity not only on EtOH and cyclohexanol, but also on 2,2-dichloroacetaldehyde (DCAL), which is a hydroxylation product of cDCE by cyctochrome P450 (Bpro_5301), reducing it to 2,2-dichloroethanol. This suggests that ChnD is involved in cDCE degradation — not as a first step, but in subsequent steps.

Changes in proteome levels during cDCE-degradation were explored using a quantitative shotgun proteomics technique, Isobaric Tag for Relative and Absolute Quantitation (iTRAQ). iTRAQ studies showed that genes adjacent to *chmo* were still translated in the KO, but with reduced protein abundance, particularly with respect to downstream genes. Given that we demonstrated ChnD (and possibly ChnA) acts on alcohol, and given that the KO lost ability to degrade alcohol and cDCE, it is therefore reasonable to propose that the lower abundance of ChnD (and presumably ChnA) in KO is the explanation for the differing behaviors of KO vs. WT strains. Through iTRAQ studies, we found that cDCE increased the relative abundances of proteins involved in glyoxylate metabolism. Several proteins that may be involved in cDCE-degradation pathways were also identified, such as an aldehyde dehydrogenase (Bpro_3952) and enzymes that are hypothetically involved in glyoxal metabolism. This also supports a hypothesis of a cDCE-degradation pathway involving glyoxal formation from hydrolysis of cDCE-epoxide. Collectively, data gathered from these studies suggest possible roles of genes in the cyclohexanol operon and update our understanding on multiple pathways of cDCE-biodegradation in JS666.

BIOGRAPHICAL SKETCH

Wan Lutfi did his undergraduate study at The Ohio State University. He graduated in 2003 with bachelor's degree in Civil and Environmental Engineering & Geodetic Science. He came to Cornell in 2005 and worked under supervision of Prof. Leonard Lion, modeling nanoparticle-facilitated contaminant transport. He received his master's degree in 2007. He returned home for a semester before decided to come back to Ithaca and continued his academic journey under Prof. James Gossett, working with JS666. In his free time, he enjoys traveling, cooking, reading and illustrating.

ACKNOWLEDGMENTS

First and foremost, I would like to express my gratitude to my advisor, Jim Gossett for his invaluable advice and sincere concern throughout my PhD training. I would like to thank Ruth Richardson and Jim Bisogni for serving as my committee members, providing resourceful input and supporting me throughout my studies. My appreciation also goes to my academic sibling, Cloelle Giddings, for her help on everything to do with JS666 and her qPCR work on *chmo*-knockout strain. I would like to acknowledge my friends in Cornell Environmental Processes Lab: Annie Rowe, Iman El-Gheriany, Gabi Hidalgo, Gretchen Heavner, Cresten Mansfeldt, Fang Liu and Deborah Sills for providing assistance and expertise in the use of many instruments, and for countless suggestions for the genetic, RNA and protein works. My thanks go to Eugene Madsen and his students from Cornell Department of Microbiology for providing us with the suicide vector (pVIK110) and helps with the initial GC-MS works.

Credits also go to Jim Spain, his colleagues and students: Shirley Nishino, Zohre Kurt and Marco Minoia, for helping me getting started at Georgia Institute of Technology, Atlanta, GA. I have obtained valuable information and knowledge throughout my stay there. Identification of putative epoxide peaks was also conducted in Spain's lab. They also provided us with *p450* clones that were used in this study. This dissertation has also benefitted from the iTRAQ work and suggestions from Sheng Zhang, James McCardle and Wei Chen at The Proteomics and Mass Spectrometry Core Facility. To our colleagues in University of Toronto, Canada: Elizabeth Edwards and Peter Chan, thank you for providing us with Bpro_4478 clone used in our study.

I would like to acknowledge friends and families for providing moral support. Special thanks go to Adi Md. Sikin and Mohd Zafri Hassan for their support and encouragement. I would also like to express my gratitude to the people in Department of Environmental Sciences, Faculty of Environmental Studies, Universiti Putra Malaysia: Dr. M. Nasir Shamsudin, Dr. Mohd Kamil Yusoff, Dr. Puziah Latif and Dr. Mohamad Pauzi Zakaria.

Last but not least, I would like to express appreciation to my sponsors: Malaysian Ministry of Higher Education and Universiti Putra Malaysia. Financial support for this work was funded by a research contract between Cornell University and Geosyntec, Inc. The ultimate source of the funds is from Geosyntec's contract (ER-1557) with the U.S. Strategic Environmental Research & Development Program (SERDP).

TABLE OF CONTENTS

LIST OF TABLES

LIST OF FIGURES

LIST OF ABBREVIATIONS

1,1-DCE	1,1-dichloroethene
2D	Two Dimensional
6-HHA	6-hydroxyhexanoic Acid
bp	Basepairs
CAP	ε-caprolactone
cDCE	*cis*-dichloroethene
cDCE-epoxide	*cis*-dichloroepoxyethane
cDNA	Complementary Deoxyribonucleic Acid
CHMO	Cyclohexanone Monooxygenase (Bpro_5565)
CI	Confidence Interval
CoA	Coenzyme A
CYHX	Cyclohexanone
DCA	1,2-dichloroethane
DCAA	2,2-dichloroacetic acid
DCAL	2,2-dichloroacetaldehyde
DCET	2,2-dichloroethanol
DNA	Deoxyribonucleic Acid
EF	Error Factor
Et_2O	Diethyl Ether
EtOAc	Ethyl Acetate
EtOH	Ethanol
FAD	Flavin Adenine Dinucleotide
FID	Flame Ionization Detector
FMO	Flavin Monooxygenase
GC	Gas Chromatography or Gas Chromatograph
GC-MS	Gas Chromatography-Mass Spectrometry
GST	Glutathione S-Transferase
HAD	Haloacid Dehalogenase (Bpro_0530, Bpro_5186)
HCl	Hydrochloric Acid
IPTG	Isopropyl β-D-1-Thiogalactopyranoside
iTRAQ	Isobaric Tag for Relative and Absolute Quantitation
kbp	Kilobase Pairs
KO	*chmo*-knockout JS666 strain
LB	Lysogeny Broth (Miller)
LC	Liquid Chromatography
Mbp	Megabase Pairs
mCPBA	*meta*-chloroperoxybenzoic acid, 3-chloroperoxybenzoic acid
MEHQ	Hydroquinone Monomethyl Ether

MS	Mass Spectrometry
MSM	Minimal Salts Medium
NAD^+	Nicotinamide Adenine Dinucleotide (oxidized)
NADH	Nicotinamide Adenine Dinucleotide (reduced)
NaOH	Sodium Hydroxide
OD_{600}	Optical Density measured at 600 nm
P450	Cytochrome P450 (Bpro_5301)
PA	Peak Area
PCE	Tetrachloroethene, Perchloroethylene
PCR	Polymerase Chain Reaction
rRNA	Ribosomal Ribonucleic Acid
Taq	*Thermus aquaticus*
TCA	Tricarboxylic Acid (Cycle)
TCAL	2,2,2-trichloroacetaldehyde
TCE	Trichloroethene, Trichloroethylene
TCET	2,2,2-trichloroethanol
tDCE	*trans*-dichloroethene
T_m	Melting Temperature
TOM-Green	Evolved Toluene *ortho*-Monooxygenase
TRK	¼ -TSA plate with rifampicin and kanamycin
TRT	¼ -TSA plate with rifampicin and tetracycline
TSA	Trypticase Soy Agar
TSB	Trypticase Soy Broth
USEPA	The United States Environmental Protection Agency
VC	Chloroethene, Vinyl Chloride
WT	Wild-type JS666 strain

CHAPTER 1

1. INTRODUCTION

Chlorinated ethenes, such as tetrachloroethene (PCE) and trichloroethene (TCE), are persistent in the environment because of their extensive use (as dry cleaning solvents and metal degreasers) and improper disposal. Accumulation of *cis*-dichloroethene (cDCE) has been reported at sites where contaminated plumes have migrated into aerobic zones following the incomplete reductive dechlorination of higher-chlorinated ethenes (i.e., PCE and TCE) in upgradient, anaerobic regions (Duba et al., 1996; Bradley, 2003). The United States Environmental Protection Agency (USEPA) has listed cDCE as a priority pollutant due to its suspected carcinogenicity and toxicity, and has enforced 70 μg/L as the maximum contaminant level for cDCE in public drinking water systems (USEPA, 2011).

Polaromonas sp. strain JS666 is the first isolated aerobic bacterium capable of growth on cDCE as a sole carbon and energy source (Coleman et al., 2002a). cDCE-grown cells can transform *trans*-DCE (tDCE), TCE, vinyl chloride (VC), or ethene, although they are incapable of growth on these substrates as sole carbon source (Coleman et al., 2002a). This ability to transform other chlorinated hydrocarbons may be useful at sites where mixtures of these compounds occur. The 16S rRNA of JS666 shares 97% nucleotide identity with *Polaromonas naphthalenivorans* CJ2, a naphthalene degrader (Jeon et al., 2006). The genome of JS666 consists of circular chromosome (5.2 Mbp) and two plasmids (360 kbp and 338 kbp) (Coleman et al., 2002a). Genomic analysis revealed no obvious cDCE-degradation operon, rather genes potentially involved in cDCE

degradation, such as monooxygenases and dehalogenases, were scattered among the chromosome and two plasmids (Jennings et al., 2009). Proteomic and transcriptomic analyses revealed genes that were upregulated during cDCE degradation (Jennings et al., 2009). Two-dimensional gel electrophoresis identified proteins upregulated by cDCE (compared to the results obtained with two reference substrates) such as putative enzymes of glutathione S-transferase (GST, Bpro_0645) and flavin-containing cyclohexanone monooxygenase (CHMO, encoded by *chnB*, Bpro_5565). The proteomic results were confirmed with data from microarray studies (Jennings et al., 2009). Other transcripts upregulated by cDCE were genes that confer putative hydrolase (*chnC*, Bpro_5566), alcohol dehydrogenase (*chnA*, Bpro_5564), cytochrome P450 (Bpro_5301), heme peroxidase (Bpro_2396), ABC transporters and transposases (Jennings et al., 2009).

Detection of epoxides when JS666 cells were incubated with ethene and propene has confirmed the activities of monooxygenases (Coleman et al., 2002a). In strain JS666, it is possible that CHMO catalyzes the formation of cDCE-epoxide analogous to toluene *ortho*-monooxygenase from *Burkholderia cepacia* G4 (Rui et al., 2004b). Besides, production of epoxide by chemically-synthesized methyllumiflavin supports the possibility of epoxidation by the hydroperoxyflavin group of flavin-containing monooxygenases (Bruice et al., 1983). Akin to this reaction, peracid produces epoxides when reacted with several chlorinated ethenes (Liebler and Guengerich, 1983; Janssen et al., 1988; Verce et al., 2002).

Genes in the same operon with *chmo*, namely hydrolase (*chnC*, Bpro_5566) and dehydrogenases (*chnD* and *chnA*, Bpro_5563 and Bpro_5564, respectively), may also serve important roles, especially in detoxification of byproducts from cDCE-degradation.

Hydrolase is postulated to catalyze the hydrolysis of epoxide, and dehydrogenases may react with chlorinated alcohols or alkanals.

In this study, we report the cloning and functional analysis of the *chmo* (or *chnB*) and other genes in the cyclohexanol operon of strain JS666 during aerobic cDCE-degradation. Results from this study are used to update the cDCE-degradation pathways and understand the detoxification mechanism during degradation. The objectives of the study are laid out in the following:

1.1 Objective 1: Determining the involvement of the *chmo* gene during cDCE degradation and developing a genetic system for JS666.

The first objective of this study is to determine the involvement of the *chmo* gene during cDCE degradation by knocking out the *chmo* homolog of JS666, and comparing the abilities of the wild-type strain and the *chmo*-knockout mutant to degrade cDCE and other substrates. Results from knockout experiments will help to identify genes essential for cDCE degradation and may allow the inference of enzyme function through monitoring the accumulation of intermediates. If more than one cDCE-degradation pathway were present, knocking out this one putative pathway may still allow cDCE degradation.

Developing a genetic system for JS666 is important in order to understand the cDCE-degradation pathway and to pave the way for future gene-based investigations of this important organism. Several steps for developing a genetic system are as follows: (i) successful incorporation of foreign genetic materials into JS666; (ii) knockout of a target gene; and (iii) reintroduction of a functional gene into a knockout mutant.

1.2 Objective 2: Characterizing the roles of enzymes in the cyclohexanol operon (Bpro_5566 to Bpro_5563) during aerobic cDCE-degradation.

The second objective of this study is to characterize the functions of enzymes putatively associated with the cyclohexanol degradation pathway and to determine their roles (if any) in aerobic cDCE degradation. Out of five genes that are putatively linked to the conversion of cyclohexanol to adipic acid in JS666, only four are located in the same operon. They are genes annotated as putative hydrolase (Bpro_5566), *chmo* (Bpro_5565), short-chain dehydrogenase (Bpro_5564) and alcohol dehydrogenase (Bpro_5563). The genes will be cloned and transformed into *E. coli* cells as both individual genes and as the operon ensemble and tested with various substrates, such as cDCE and its metabolites.

1.3 Objective 3: Understanding the translational changes in strain JS666 in the presence of cDCE and during cDCE degradation.

The third objective is to study the proteome differences between wild-type and *chmo*-negative mutant strains of JS666 during identical substrate conditions. We will use the iTRAQ labeling method to monitor important proteins. One issue in producing a knockout strain is that, even though the insert is designed to target a specific gene, expression of adjacent genes might have been affected by the insert. Can differences in substrate utilization by wildtype vs. knockout strains be confidently attributed to the

presence/absence of the targeted gene only? Using iTRAQ, we will quantify the relative productions from genes adjacent to *chmo* in knockout vs. wildtype strains. Several "missing" proteins in the cDCE-biodegradation pathways also might be recognized in this study, such as aldehyde dehydrogenases or hydrolases. Data from iTRAQ study can help us to better interpret the results from Objective 1, and can conceivably be used to update the cDCE-metabolic pathways in strain JS666.

CHAPTER 2

2. BACKGROUND

Accumulation of dichloroethenes (DCEs) has been observed in field and laboratory enrichment cultures and it is often linked to incomplete anaerobic dechlorination of high-chlorinated ethenes and ethanes such as tetrachloroethene (PCE), tetrachloroethane and trichloroethene (TCE) (Bagley and Gossett, 1990; Sharma and McCarty, 1996; Holliger et al., 1998a; Lorah and Olsen, 1998; Lorah and Voytek, 2004; Darlington et al., 2008). Several causes of incomplete reduction of PCE and TCE include: (i) the absence or scarcity of appropriate electron donor species required by the microbial populations (Holliger et al., 1993; Neumann et al., 1994); (ii) the abundance of other substrates that are thermodynamically favored by degraders; (iii) the absence of appropriate bacteria that are capable of converting past DCEs (Sharma and McCarty, 1996; Miller et al., 1997; Holliger et al., 1998a; Holliger et al., 1998b; Harkness et al., 1999); (iv) slow removal of DCEs (Rosner et al., 1997); and (v) migration of contaminated plumes from anaerobic to aerobic zones (Duba et al., 1996; Bradley, 2003).

Aerobic oxidation of less-chlorinated ethenes is common, and these compounds can be degraded by microorganisms either growth-coupled or co-metabolically. Bacteria such as *Mycobacterium* spp., *Nocardioides* sp. JS614, *Pseudomonas aeruginosa* MF1 can easily utilize vinyl chloride (VC) as carbon and energy source under aerobic conditions (Hartmans and De Bont, 1992; Verce et al., 2000; Coleman et al., 2002b; Gossett, 2010). Numerous aerobic bacteria are capable of co-metabolizing chlorinated solvents, including

bacteria that oxidize ammonia (Vannelli et al., 1990), ethene or ethane (Coleman et al., 2011), methane (Janssen et al., 1988; Little et al., 1988; Oldenhuis et al., 1989) and toluene (Nelson et al., 1987; Wackett and Gibson, 1988). Several microbial populations can co-metabolize DCEs in the presence of other substrates (Gao and Skeen, 1999; Verce et al., 2002; Elango et al., 2011), and this is usually associated with the activity of monooxygenases (Ensign et al., 1992; van Hylckama Vlieg et al., 1996; Vancheeswaran et al., 1999; Kim and Semprini, 2005). However, co-oxidation of chlorinated compounds can be detrimental to cells or enzymes due to the toxicity of substrates (at high concentrations) or the presence of intermediates, thus reducing or inhibiting degradation activity (Alvarez-Cohen and McCarty, 1991; Oldenhuis et al., 1991; Landa et al., 1994). Furthermore, the bacteria may not possess genes capable of handling metabolites and byproducts of chlorinated compounds, such as chlorinated epoxides, alkanals (aldehydes) and alcohols. TCE and its degradation products were found to be toxic to methane-oxidizing *Methylosinus trichosporium* OB3b due to non-specific conjugation of metabolites to the cellular proteins (Oldenhuis et al., 1991). Competitive enzyme inhibition can occur with the presence of multiple substrates. The competition between primary substrate (growth substrate) and the substrate of interest (co-metabolic substrate or targeted contaminant) for the enzyme's primary active site will decrease the enzyme's affinity for each substrate, consequently reducing transformation rates. Toluene/*o*-xylene monooxygenase from *Pseudomonas stutzeri* OX1, for example, not only can hydroxylize toluene, but also a number of other substrates, such as styrene, naphthalene, 1,1-DCE and TCE (Chauhan et al., 1998), and the presence of mixtures of chlorinated ethenes affects the degradation rates of individual substrates (Shim and Wood, 2000).

2.1 *Polaromonas* sp. strain JS666

Several studies have demonstrated that microorganisms can utilize cDCE as sole carbon and energy source for growth (Bradley and Chapelle, 1999; Coleman et al., 2002a; Schmidt et al., 2010). Bacterial populations from black-water stream sediments have shown the ability to degrade cDCE under aerobic conditions; although no cDCE-degrader was isolated (Bradley and Chapelle, 1999). Coleman et al. (2002b) successfully isolated several aerobic bacteria capable of degrading VC, but only one unique isolate capable of utilizing cDCE as sole source for carbon and energy (2002a). *Polaromonas* sp. strain JS666 was isolated from an enrichment culture that was inoculated with granular activated carbon from an industrial plant that processed contaminated groundwater. Due to its ability to degrade cDCE — and since growth-coupled oxidation of cDCE does not appear to be common at field sites — strain JS666 is a prime candidate for bioaugmentation at sites where cDCE has accumulated in aerobic zones (Coleman et al., 2002a; Giddings et al., 2010).

The minimum doubling time of strain JS666 grown solely on cDCE is 73 ± 7 hours, and its growth yield is 6.1 g protein/mole cDCE at 20°C. The optimum growth conditions for cDCE degradation are 20 – 25°C and pH 7.2. Complete dechlorination of cDCE occurs during growth producing 1.94 mol of Cl^- per mol of cDCE degraded. The half-velocity constant of JS666 during cDCE metabolism is 1.6 ± 0.2 μM and the maximum specific substrate-utilization rate ranges from 12.6-16.8 nmole/min/mg of protein at 20°C (Coleman et al., 2002a). According to Coleman et al. (2002a), strain JS666 is incapable of growth on *trans*-DCE (tDCE), TCE, VC, 1,2-dichloroethane (DCA) or ethene as carbon source, but cDCE-grown cells can transform these substrates. Further

investigation has determined that strain JS666 can grow on DCA and has a complete set of DCA catabolic genes (Mattes et al., 2008). The ability to transform other chlorinated hydrocarbons may be useful at sites where mixtures of these compounds occur.

The 16S rRNA gene of JS666 shares 97% nucleotide identity with *Polaromonas vacuolata*, an Antarctic marine isolate (Irgens et al., 1996) and *Polaromonas naphthalenivorans* CJ2, a naphthalene degrader incapable of cDCE degradation (Jeon et al., 2006). The genome of strain JS666 has been fully sequenced by the Joint Genome Institute (Copeland et al., 2006) and consists of a circular chromosome (5.2 Mbp) and two circular plasmids, pPol360 (360 kbp) and pPol338 (338 kbp). These two plasmids persist in strain JS666 despite an extended enrichment and isolation process (Coleman et al., 2002a). Genomic analysis revealed no obvious cDCE-degradation operon, rather genes potentially involved in cDCE degradation, such as monooxygenases and dehalogenases, are scattered among the chromosome and two plasmids (Jennings et al., 2009).

Strain JS666 has shown two phenotypical behaviors during cDCE-degradation: (i) so-called "good behavior," which has high maximum specific degradation rate and is characterized by growth-coupled degradation; and (ii) "bad behavior," which is slower, cometabolic-like, and exhibits a transformation capacity (Jennings, 2005). H^+ accumulation as a result of cDCE degradation has caused significant decrease in cDCE-degradation rates, and degradation resumed when pH was restored to the initial neutral value. Nevertheless, low pH is not the only condition that causes the degradation to decline. High levels of oxygen and previously growth on alternative substrates, such as succinate, acetate or glycolate, can also promote the bad phenotypical behavior (Jennings,

2005). Our colleagues at Georgia Institute of Technology found the accumulation of chloride ion to be an issue and were only able to grow JS666 to high density by exchange with fresh medium (Nishino, personal communication).

The inconsistent behaviors observed during the culturing of strain JS666 may be due to the involvement of many enzymes in the initiation of cDCE-degradation and the presence of multiple degradation pathways, suggesting that the strain might have limited regulation of a newly acquired pathway. Support for this comes from observation that there are 55 genes from different types of transposable elements present in the genome (Mattes et al., 2008). The production of the expected *cis*-1,2-dichloroepoxyethane (cDCE-epoxide) intermediate might be detrimental to the cells and detoxification mechanisms are poorly established. Other metabolites, such as chlorinated alkanals and alcohols, may contribute to poor cDCE-degradation performance as well.

2.2 Exploring bacterial behavior through omics-based approaches

Comparative genomic studies have shown shared genes (68.21%) in the chromosomes of JS666 and CJ2 strains, as well as genes that are totally unique to each strain. It may be more likely that genes present in strain JS666 but not in strain CJ2 are involved in cDCE degradation (Jennings, 2009; Yagi et al., 2009). There are 55 genes from different types of transposable elements present in the genome, and transposons are often associated with evolution of pathways involved in xenobiotics-biodegradation or -detoxification. The presence of several catabolic genes located near mobile genetic elements suggests that they were recently acquired (Mattes et al., 2008). Other genes that

may be involved in xenobiotic or hydrocarbon metabolism in strain JS666 are 59 oxygenases, 21 glutathione S-transferases, 111 hydrolases, 27 hydratases and 9 dehalogenases (Mattes et al., 2008). The genome contains complete glycolytic and Entner-Doudoroff pathways and the tricarboxylic acid (TCA) cycle. Genes involved in the glyoxylate pathway are present, such as the gene that confers isocitrate lyase (*aceA*, Bpro_2101), which is expected for an organism isolated on a C_2 compound (i.e. cDCE) (Mattes et al., 2008).

Proteomic and transcriptomic techniques were utilized to identify induction of genes as clues of JS666's response to growth on cDCE, versus non-chlorinated substrates such as glycolate and acetate (Jennings et al., 2009). For proteomic analysis, proteins from cultures grown in cDCE and acetate or glycolate were extracted and compared by overlaying the individual two-dimensional (2D) gel separations. Subsequently the proteins that were differentially expressed in cDCE gel were excised and analyzed using liquid chromatography (LC) and tandem mass spectrometry (MS/MS) and identified using the NCBI database. The analysis revealed induction of genes annotated as encoding glutathione S-transferase-like protein (*gst*, Bpro_0645), cyclohexanone monooxygenase (*chnB* or *chmo*, Bpro_5565) and haloacid dehalogenase (*had*, Bpro_5186) (Figure 2.1 and Table 2.1). These findings were confirmed by DNA microarray experiments. Upregulated transcripts include *gst*, pyridoxamine 5'-phosphate oxidase (*pnpox*, Bpro_0646), *chmo*, cytochrome P450 (*p450*, Bpro_5301), ABC transporters and two haloacid dehalogenases (Bpro_0530 and Bpro_5186). Selected upregulated transcripts in strain JS666 when grown on cDCE versus the reference substrate glycolate are summarized in Table 2.2.

Overall, 2D gel analysis and the microarray approach were not sufficient to elucidate the cDCE-degradation pathways in strain JS666. Several involved proteins may be overlooked due to their highly acidic or basic properties. The upregulation of transcripts (mRNAs) does not always reflect the activity of the corresponding proteins. For example, the transcripts of *p450* were upregulated by cDCE less than the transcripts of *chmo* or *gst* (Table 2.2); nevertheless a study by Shin (2010) showed that P450 initiates attack on cDCE, and no activity on cDCE has yet been demonstrated for CHMO (Alexander, 2010) or GST (Jennings et al., 2009).

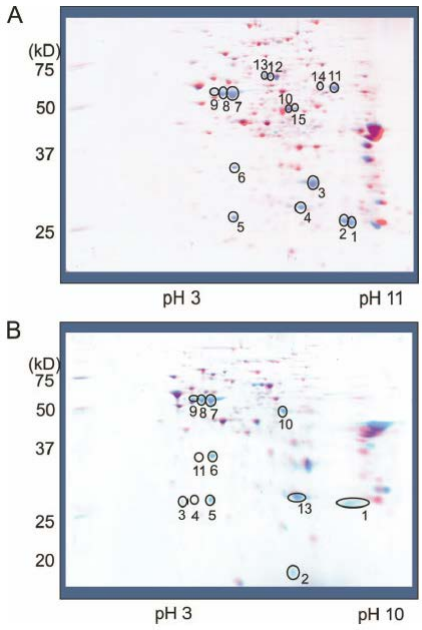

Figure 2.1. Overlays of 2D gel images comparing proteins extracted from cDCE-grown (blue) cells to proteins extracted from acetate-grown (red) cells (A) and proteins extracted from cDCE-grown (blue) cells to proteins extracted from glycolate-grown (red) cells (B). Differentially expressed spots in cDCE gels that were subsequently analyzed by MS are circled and reported in Table 2.1. Adapted from Jennings et al. (2009).

Table 2.1. Proteins upregulated in cells grown on cDCE compared to cells grown on acetate[a] Adapted from Jennings et al. (2009). Sample numbers correspond to the numbers in Figure 2.1. Corresponding transcripts reported in Table 2.2 are bolded.

Sample	Locus tag	Putative enzyme function[b]	Protein score[c]	Peptide count[d]
1	Bpro_0645	**GST-like protein**	115	1
2	Bpro_0645	**GST-like protein**	181	1
2	Bpro_3647	3-Oxoacyl-(acyl carrier protein) reductase	143	1
3	Bpro_4563	2-Hydroxy-3-oxopropionate reductase	547	4
4	Bpro_4562	Hydroxypyruvate isomerase	435	5
4	Bpro_2567	Short-chain dehydrogenase/reductase	144	2
4	Bpro_4841	Peroxidase	126	1
5	Bpro_5186	**HAD, type II**	110	1
6	Bpro_0646	**PNPox-related protein**	85	1
10	Bpro_0650	DEAD/DEAH box helicase-like protein	256	2
12	Bpro_4561	Glyoxylate carboligase	614	6
13	Bpro_4561	Glyoxylate carboligase	564	4

[a] There were no significant JS666 hits for samples 7 to 9, 11, 14, and 15.
[b] Annotations were derived from the DOE JGI Integrated Microbial Genomes database.
[c] The protein score (or Mowse score) is -10log (P), where P is the probability that the observed match is a random event.
[d] Number of peptides with an expectation value of 0.01 as identified using LC-MS/MS. The expectation value corresponds to the number of matches that are expected to occur by chance alone.

Table 2.2. Selected transcripts upregulated in cells grown on cDCE compared to cells grown on glycolate (Jennings et al., 2009).

Locus tag	P value	Change (fold)	Region or putative enzyme function
Bpro_3336	0.005	111	ABC transporter, extracellular receptor
Bpro_0645	0.012	99.8	GST-like protein
Bpro_0646	0.012	87.5	PNPox-related protein
Bpro_3335	0.009	70	ABC transporter, inner membrane translocator
Bpro_0530	0.011	53.3	HAD, type II
Bpro_5186	0.013	51.5	HAD, type II
Bpro_0532	0.007	42.7	Hypothetical protein
Bpro_0531	0.015	40.9	Sodium/solute symporter
Bpro_5185	0.017	39.2	Sodium/solute symporter
Bpro_3334	0.010	30.8	ABC transporter, inner membrane translocator
Bpro_3333	0.013	27.1	ABC transporter, ATPase component
Bpro_0529	0.013	24.3	Conserved hypothetical protein
Bpro_5184	0.004	19	Predicted membrane protein
Bpro_3332	0.005	18.3	ABC transporter, ATPase component
Bpro_2731	0.016	17.9	Conserved hypothetical protein
Bpro_2396	0.017	14.8	Heme peroxidase
Bpro_0577	0.025	10.4	CO dehydrogenase
Bpro_5565	0.024	10.1	CHMO
Bpro_5566	0.056	7.3	Hydrolase
Bpro_5564	0.010	6.3	Short-chain dehydrogenase
Bpro_3866	0.027	3.6	Universal stress protein
Bpro_5301	0.010	3.5	Cytochrome P450
Bpro_2732	0.018	3.4	Transposase
Bpro_4792	0.030	3.2	Transposase
Bpro_4575	0.024	3.1	Transposase
Bpro_3227	0.040	3	Universal stress protein

The complexity of bacterial metabolic pathways and identification of stress-related proteins can be studied through isobaric tags for relative and absolute quantitation (iTRAQ). This multiplexed isobaric tagging method uses a set of isobaric mass labels as reporters at the N terminal and lysine side chains of peptides. The labels containing the reporter groups range in mass from *m/z* 114.1 to 117.1, and the balance group of each is formulated such that the combined mass is 145.1 Da for each of the four reagents, thereby minimizing analytical bias. Four different samples, each containing digested proteins from cells grown under a different condition, can each be labeled with one of the four tags, and the four samples are subsequently combined. The derivatized peptides in the mixture are then identified and quantified chromatographically. One sample type is chosen as the basis for comparison (the denominator in calculated ratios). The ratio of a particular peptide's abundance in any other sample type to that in the basis sample is then presumed to be the same as the ratio of their observed, tag-types associated with that peptide (Ross et al., 2004). This approach has been successfully used to monitor variations in protein abundance level in a particular bacterial species under different biological conditions, such as in the study discussed in the following.

An *Escherichia coli* strain was engineered to metabolize cDCE through expression of an evolved toluene *ortho*-monooxygenase (TOM-Green) from *Burkholderia cepacia* G4, which consists of a mutated hydroxylase subunit, a NADH-oxidoreductase and an electron-transfer protein. The mutation in the hydroxylase resulted in an improved activity towards chlorinated ethenes, producing corresponding epoxides (Canada et al., 2002a). The research continued with the detoxification of epoxides using an epoxide hydrolase, EchA, from *Agrobacterium radiobacter* AD1 and several of its

mutated enzymes (Rui et al., 2004a). In another study, the cDCE-epoxide generated by a similar monooxygenase was subsequently catalyzed by a GST system (IsoILR1) (Rui et al., 2004b).

iTRAQ was used to monitor the proteome changes in these metabolically engineered *E. coli* strains during aerobic mineralization of cDCE. TOM-Green was utilized to initiate attack on cDCE, producing cDCE-epoxide, which was then detoxified by either a glutathione system or an epoxide hydrolase. The monooxygenase-and-glutathione system demonstrated induction of proteins involved in an oxidative defense mechanism, pyruvate metabolism and glutathione synthesis. On the other hand, fatty-acid synthesis, gluconeogenesis and the TCA cycle were repressed. In the same study, the researchers compared the evolved EchA and its wild-type analog, yet no as conclusive result was reported (Lee et al., 2006).

In addition to the proteomic analysis, Lee et al. (2010) performed a whole-transcriptome study to determine the impact of cDCE degradation in engineered *E. coli* strains. More than 4200 transcripts were identified compared to 364 proteins in the quantitative proteome study. In the monooxygenase-and-glutathione system (compared to a strain with no cloned genes), eight out of 46 significantly upregulated proteins were also induced in the whole-transcriptome analysis. 30 stress-related genes were identified in the transcriptomic study while only five stress response proteins were identified in their previous study.

In the strain with an epoxide hydrolase (EchA) addition (compared to a strain with monooxygenase only), the effects of epoxide hydrolysis were studied. 21 stress-

related genes as well as genes involved in glyoxylate metabolism were among those that were induced. The induction of *gloA* (encodes glyoxalase I) and *glxA23* genes (encode ureidoglycolate hydrolase and a repressor) in this strain support the hypothesis of glyoxal formation from 1,2-dichloroethane-1,2-diol (Rui et al., 2004a). The monooxygenase-and-hydrolase system demonstrated a strong stress response similar to heat shock and oxidative stress. Transcriptome analysis revealed inductions of genes that encode stress-related proteins, heat shock proteins, ribosomal proteins and several hypothetical proteins. Other stress-related genes were further studied by whole-transcriptome analyses of single-gene knockout mutants [Keio Collection (Baba et al., 2006)] (Lee et al., 2010).

2.3 Monooxygenases

A monooxygenase incorporates one oxygen atom into substrates using NADH or NADPH as a donor by utilizing variety of enzymatic reaction mechanisms. Many xenobiotic-degrading bacteria contain multiple oxygenases. *Mycobacterium chubuense* strain NBB4, for example, contains several monooxygenases, such as ethane monooxygenase (*etnABCD*), propene and propane monooxygenases, butane monooxygenase, alkene monooxygenase (alkB) and P450 (Coleman et al., 2011).

Genomic analysis revealed that JS666 has 16 monooxygenases, 4 P450s and 43 dioxygenases (Mattes et al., 2008), though few of these putative annotations of function have been confirmed. Flavin-containing monooxygenase (FMO) and P450 act on diverse substrates including alkanes, aromatics and heterocyclics. FMO catalyzes oxidation of various compounds through Baeyer-Villiger oxidation, which is commonly known for

conversion of ketones to esters or cyclic ketones into lactones by peroxy acids, such as potassium monopersulfate or *meta*-chloroperoxybenzoic acid (mCPBA) (Baeyer and Villiger, 1899; Meunier, 1992). The production of epoxide from alkene's reaction with peracid is also well-established (Prileschajew, 1909). During ethene transformation by strain JS666, the formation of epoxyethane was reported (Coleman et al., 2002a), and we observed cDCE-epoxide during the growth of strain JS666 on cDCE (for details on chemically synthesized cDCE-epoxide, see Appendix B), which suggests activity of monooxygenases (Guengerich, 1991; Ensign, 2001) that may include P450s and/or FMOs. This enzymatic epoxidation mechanism may mimic the oxidation mechanism by peracid.

2.3.1 Cyclohexanone monooxygenase (CHMO)

CHMO (EC: 1.14.13.22) is a flavin-containing enzyme capable of converting cyclohexanone (CYHX) to ε-caprolactone (CAP) via Baeyer-Villiger oxidation. CHMO from *Acinetobacter* sp. NCIMB 9871 is the most studied CHMO and has been tested on numerous chemical compounds (Donoghue and Trudgill, 1975). The versatility of CHMO from *Acinetobacter* sp. has been shown through various reactions, such as the asymmetric sulfoxidation of alkyl aryl sulfides (Colonna et al., 1996), 1,3-dithioacetals (Colonna et al., 1995) and dialkyl sulfides (Colonna et al., 1997).

The first epoxidation of an alkene by CHMO was reported by Colonna et al. (2002). CHMO from strain 9871 was overexpressed in *Escherichia coli*, purified, and the enzymatic reaction was conducted in Tris-HCl buffer (pH 8.6) containing NADPH, glucose-6-phosphate and glucose-6-phosphate dehydrogenase for NADPH regeneration.

The enzyme was tested on dimethylvinylphosphonate, an olefein that resembles fosfomycin (Figure 2.2a). In another enzymatic assay study, CHMO from *Xanthobacter* sp. ZL5 catalyzed the epoxidation of a bicyclic ketone, instead of the usual conversion into its corresponding lactone (Figure 2.2b) (Rial et al., 2008). BLASTP results for the CHMO from strain JS666 give 62% and 61% identity to CHMOs of *Acinetobacter* sp. and *Xanthobacter* sp., respectively.

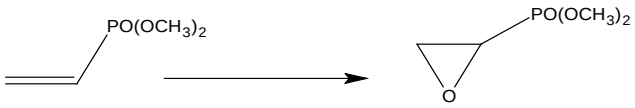

(a)

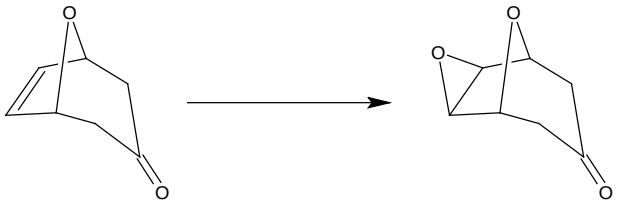

(b)

Figure 2.2. (a) Epoxidation of dimethylvinylphosphonate by CHMO from strain 9871 (Colonna et al., 2002) and (b) a mesobridge bicyclic ketone by recombinant *E. coli* cells expressing a BVMO from *Xanthobacter* sp. ZL5 (Rial et al., 2008).

The amino acid sequence of CHMO from strain JS666 is shown in Figure 2.3. Classification as a Baeyer-Villiger monooxygenase can be recognized by the FxGxxxHxxxWP motif sequence, located at the start of NADP-binding sequence. Studies of protein structure and conformational changes enable researchers to understand CHMO's ability to accept various substrates (Mirza et al., 2009). CHMOs share conserved substrate binding pocket residues and the differences in the amino acid sequence around the binding pocket may account for the flexibility of CHMOs in accommodating various types of compounds. Tryptophan W479 (at the mobile loop region, residues 474 – 491) is a conserved residue common to CHMOs, and mutation on that residue to alanine (of a CHMO from *Rhodococcus* strain) decreased by 86% the activity on CYHX (Mirza et al., 2009). Strain JS666 has three glycine residues in the mobile loop while other CHMOs have resides with larger side groups, such as glutamate, asparagine and alanine, which better allows movement of substrates (Alexander, 2010). Because of similarities among these enzymes and the structure of the protein, it is possible that CHMO from strain JS666 could serve an identical role of alkene epoxidation.

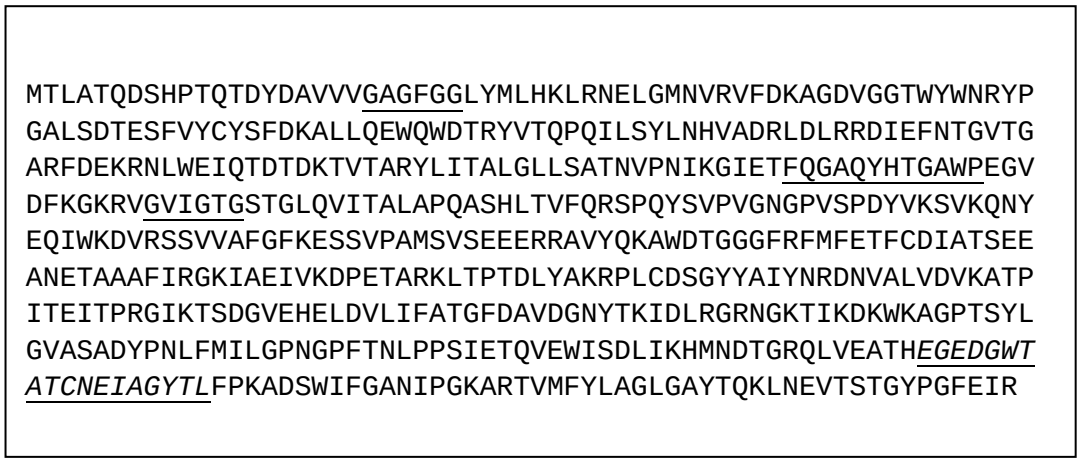

Figure 2.3. The protein sequence of CHMO from strain JS666. The motif FxGxxxHxxxWP identifies it as Baeyer-Villiger Monooxygenase Type I (Fraaije et al., 2002). Binding motif for adenosine moiety of FAD is GxGxxG at the beginning of the sequence (Hasegawa et al., 2000; Fraaije et al., 2002). $NADP^+$ co-factor binds at a GxxGxG motif site (Mirza et al., 2009). A conserved peptide sequence that is common to FAD- and NADPH-binding proteins (385-ATGFDA-390) is also found in CHMO (Vallon, 2000). Underlined and italicized is the mobile loop region (Alexander, 2010).

2.3.2 Overexpression of CHMO.

In the original study, CHMO from strain 9871 was expressed in its native state (Donoghue et al., 1976). Chen et al. (1988) continued the work by identifying the nucleotide sequence of the *chmo* gene and subsequently overproducing the enzyme in *E. coli*. Study of CHMO continued with resequencing and identification of several enzymes associated with CHMO in the cyclohexanol catabolic pathway (Iwaki et al., 1999). Cheesman and coworkers (2001) successfully purified and characterized a hexahistidine-tagged CHMO in both *E. coli* and *Saccharomyces cerevisiae*. Since the initial work, several studies have been conducted on other bacterial CHMOs, namely from *Acinetobacter* sp. SE19 (Cheng et al., 2000), *Arthrobacter* sp. BP2, *Rhodococcus* sp. PH1, *Rhodococcus* sp. PH2 (Brzostowicz et al., 2003) and *Xanthobacter* sp. ZL5 (Van Beilen et al., 2003).

Heterologous gene expression in *E. coli* has been routinely used to produce a high-amount of protein, although it tends to yield insoluble and inactive protein. To minimize the production of inclusion bodies, CHMO from strain 9871 was co-expressed with molecular chaperones or foldases in *E. coli* and has displayed an improvement of up-to 38-fold in the enzyme's activity (Lee et al., 2004). Another solution is to conduct enzymatic assays in whole-cell *E. coli.* Iwaki et al. (2002b) conducted whole-cell experiments on overexpression of cyclopentanone 1,2-monooxygenase from *Comamonas* sp. NCIMB 9872 in LB broth, supplemented with 2% glucose at 30°C. Substrates were added directly to the media after induction with isopropyl β-D-1-thiogalactopyranoside (IPTG). The other genes in the cyclopentanol operon were assayed in cell-free extracts.

Using a low amount of inducer leads to more production of soluble protein. Lee and coworkers (2005) found that the yield of CHMO can be increased by inducing the overexpression with a low concentration of IPTG (0.01 mM) at 30°C. The dissociation value for flavin adenine dinucleotide (FAD) binding of CHMO from *Acinetobacter* sp. is 40 nM, suggesting that flavin dissociation would likely occur and destabilize the flavin-containing enzyme (Donoghue et al., 1976). The addition of riboflavin, a precursor of FAD, to the media ensures enough supply of FAD for the flavoprotein as conducted in the overexpression study of CHMOs from *Brevibacterium* isolate (Brzostowicz et al., 2000). An improvement was also observed in NADPH-dependent CHMO activity by non-growing *E. coli* cells when riboflavin was added at the start of the reactions (Walton and Stewart, 2004).

Alexander (2010) studied the overexpression of CHMO from strain JS666. Whole-cell experiments were conducted, and when *E. coli* cells were actively growing,

the inducer and the substrates were supplied to the cells. Yet, no activity of CHMO was observed on cDCE or ethene.

2.3.3 Oxidation mechanism of CHMO.

The CHMO-catalyzed oxidation has been shown to proceed in the same manner as a chemical Baeyer-Villiger reaction (Figure 2.4). In CHMO-catalyzed CYHX oxidation, the FAD molecule (molecule 2.4.1) undergoes reduction by NADPH before reacting with molecular oxygen to form a C4a-peroxyflavin intermediate (molecule 2.4.2). This peroxyflavin intermediate serves as a nucleophile, attacking the carbonyl carbon of the CYHX. This step forms the Criegee intermediate (molecule 2.4.3) that successively produces C4a-hydroxyflavin and CAP. Subsequently, the hydroxyflavin intermediate is transformed into an oxidized FAD by eliminating a water molecule.

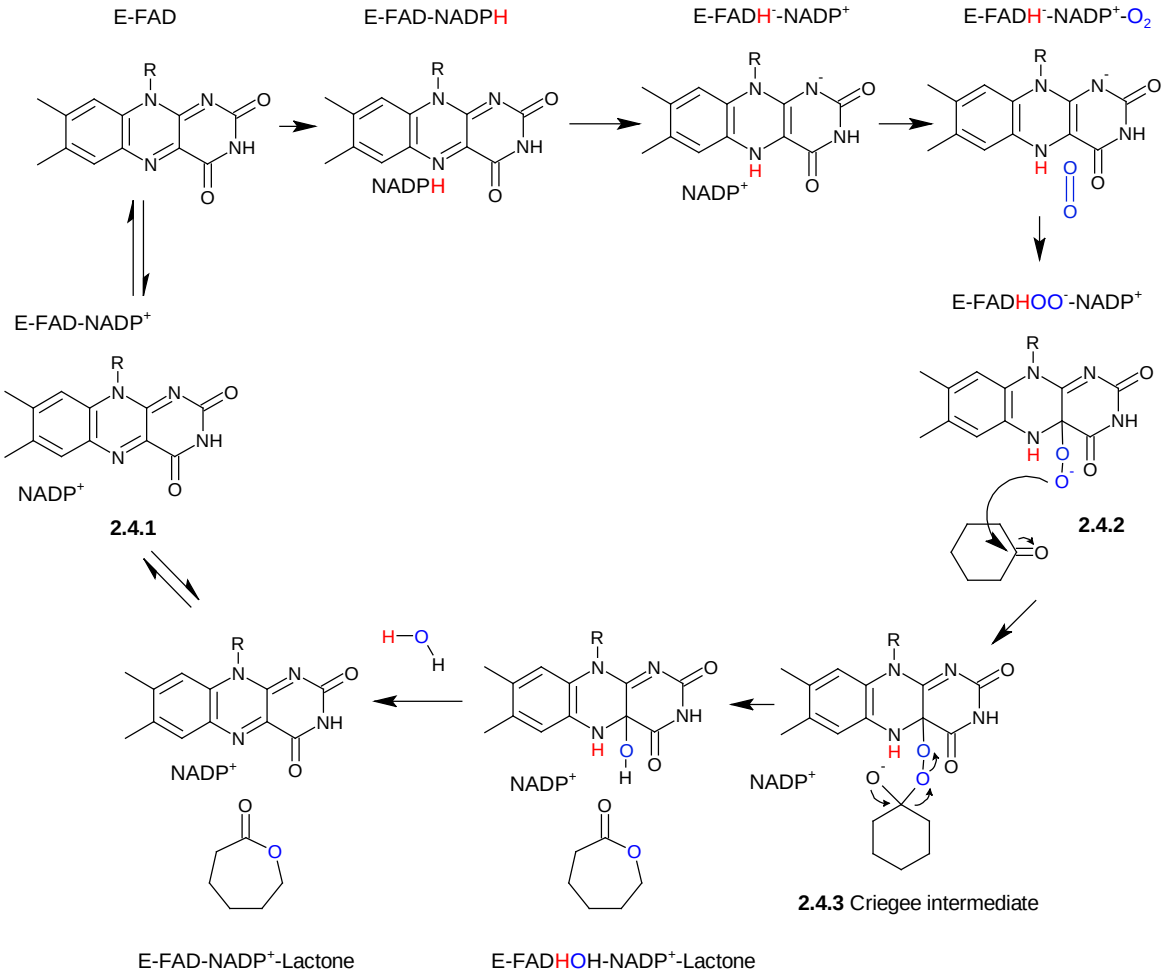

Figure 2.4. Proposed mechanism for CYHX-lactonization with CHMO of *Acinetobacter* sp. Adapted from Mirza et al. (2009).

The mechanism for reaction of CYHX with mCPBA to yield CAP is proposed in Figure 2.5. The reaction is an adaptation of the lactonization of substituted CYHX by peracid, such as methylcyclohexanone (Corma et al., 2001) and silyl ketones (Hudrlik et al., 1980). The hydroperoxyl group of mCPBA acts in a manner analogous to that of a peroxyflavin intermediate. Chemically synthesized 4a-hydroperoxy-5-ethyl-3-methyllumiflavin produced an epoxide when reacted with 2,3-dimethyl-2-butene in

chloroform, though the reaction with ethene was not tested (Bruice et al., 1983). This supports the evidence of possible epoxidation capability by the hydroperoxyflavin group of flavin-containing monooxygenases.

Peracid epoxidation of chlorinated ethenes has been commonly utilized in many studies to prepare authentic materials for use in confirming peak identities in gas chromatography. TCE and DCEs have been reacted with mCPBA to produce their corresponding epoxides (Liebler and Guengerich, 1983; Cai and Guengerich, 1999). 1,1-DCE-epoxide was chemically synthesized by reacting its parent compound with mCPBA at 60°C for 3 hours (Liebler and Guengerich, 1983). A similar approach was used to synthesize tDCE-epoxide (Janssen et al., 1988) and cDCE-epoxide (Verce et al., 2002). Epoxides can also be synthesized at low temperature, such as the synthesis of octene-1,2-oxide at 0°C (Guengerich and Mason, 1980).

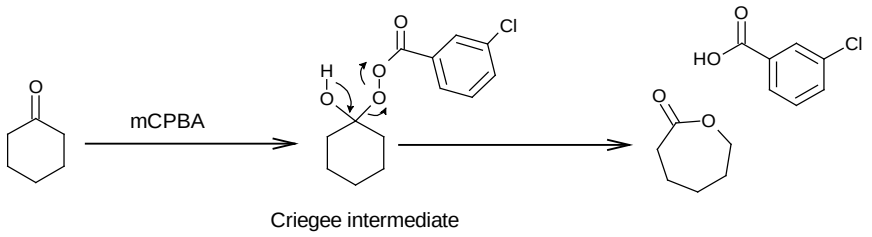

Figure 2.5. Theoretical lactonization of CYHX by peracid (mCPBA), resulting in CAP and chlorobenzoic acid. Adapted from Corma et al. (2001).

2.3.4 Cytochrome P450.

In strain JS666, a cytochrome P450 system exists which consists of P450 itself, an iron-sulfur electron carrier (ferredoxin), and an FAD-containing reductase (ferredoxin reductase). Studies of similar P450 systems in other bacteria have shown them to be involved in reactions on a broad range of substrates, viz. alkanes, alkenes and alcohols (Wackett et al., 1989; Fulco, 1991). Scheps and coworkers (2011) cloned and overexpressed P450 (Bpro_5301) in *E. coli* and supplemented the growth of whole cells with $FeSO_4$. The purified enzyme catalyzes reactions with alkanes and alcohols, which oxidize to alcohols and diols, respectively. Shin (2010) has successfully overexpressed the P450 system (P450, its adjacent genes and its promoter region, Bpro_5299 – Bpro_5301) from strain JS666 in *E. coli* and tested the whole cells with cDCE. During P450 reaction with cDCE, a percentage of loss in the mass balance was reported that may be due to the production of a suicidal complex (a dead-end product due to an irreversible porphyrin *N*-alkylation with one carbon atom of the ethenes (de Visser et al., 2004)), in addition to the cDCE-epoxide and 2,2-dichloroacetaldehyde (DCAL) produced (Shin, 2010). Another possible outcome from P450 catalysis is the production of chloroacetylchloride, which will be rapidly decomposed into chloroacetate and hydrogen chloride. Abiotic breakdown of cDCE-epoxide has been shown to release chloride ions. The activities of TOM-Green on chlorinated ethenes were calculated by measuring the chloride concentrations 24 hours after the enzymatic reactions were stopped (Canada et al., 2002a). However, cDCE-epoxide is relatively stable, with a half-life of about 72 hours (Janssen et al., 1988), as opposed to the half-lives of VC-epoxide and TCE-epoxide, which are 78 and 21 seconds, respectively (van Hylckama Vlieg et al., 1996).

The relationships between FMO and P450 have been studied in eukaryotes. Both enzymes catalyze transformation of various xenobiotic compounds, and their substrate specificities may overlap (McManus et al., 1987; Williams et al., 1990; Morgan et al., 2001; Attar et al., 2003). There are several key differences between the enzymes, namely: (i) substrate metabolism; (ii) catalytic mechanism and protein structure; and (iii) regulation (Cashman, 2005). During substrate metabolism, both enzymatic activities can be distinguished *in vitro* by difference in their optimal pHs — i.e. P450 is active at pH 7.4, while FMO at pH 9. The use of inhibitors, such as metyrapone and methimazole, selectively inhibit the activity of P450 and FMO, respectively (Williams et al., 1990). The catalytic nature of both enzymes is also different. As previously discussed, in FMO, molecular oxygen is added to the reduced FAD, forming a C4a-hydroperoxyflavin, which initiates a nucleophilic attack on the substrates, whereas P450 forms a ferrous-O_2 complex that eventually generates hydrogen peroxide. While P450 and FMO may catalyze similar compounds, the result may be different products.

2.4 Possible roles of other genes in the cyclohexanol operon

Several bacteria capable of biodegrading cyclic alcohols and their associating ketones have been isolated (Griffin and Trudgill, 1972; Donoghue and Trudgill, 1975; Davey and Trudgill, 1977), and researchers have been interested in characterizing the gene clusters involved in their metabolism (Donoghue et al., 1976; Cheng et al., 2000; Kostichka et al., 2001; Iwaki et al., 2002b). Biodegradation of cyclohexanol and its byproducts by strain 9871 has been extensively studied (Donoghue et al., 1976; Iwaki et al., 1999). Most researchers focus on identifying and characterizing CHMO due to its

mechanism of enzymatic Baeyer-Villiger oxidation. Nevertheless, genes downstream of this step have been characterized (Iwaki et al., 1999) and most, if not all, enzymes in cyclic alcohol metabolism can be used for the purpose of biocatalysis.

The biochemical steps of cyclohexanol degradation by *Acinetobacter* sp. NCIMB 9871 are illustrated in Figure 2.6 (Donoghue and Trudgill, 1975). Cyclohexanol is transformed into its dicarboxylic acid through a five-step conversion: cyclohexanol is oxidized to CYHX by a dehydrogenase (ChnA). CYHX is then oxidized to CAP via Baeyer-Villiger oxidation by a flavin-containing monooxygenase (ChnB). The cyclic lactone is then hydrolyzed by an α/β hydrolase-fold coding sequence homolog of CAP lactonase (hydrolase, ChnC) into 6-hydroxyhexanoic acid (6-HHA), before being converted into 6-oxohexanoic acid by a dehydrogenase (ChnD). 6-oxohexanoate dehydrogenase (ChnE) converts 6-oxohexanoic acid into adipic acid, which is further oxidized to acetyl-CoA and succinyl-CoA through a β-oxidation pathway.

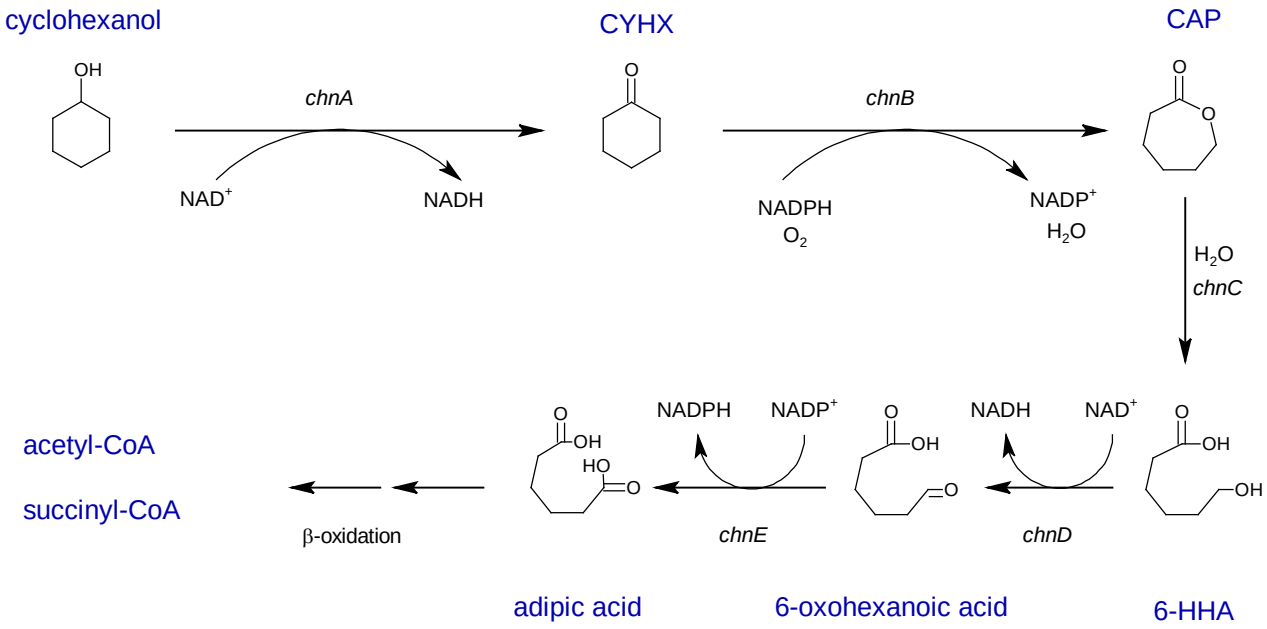

Figure 2.6. Biodegradation of cyclohexanol in *Acinetobacter* sp. NCIMB 9871. Adapted from Donoghue and Trudgill (1975). CYHX = cyclohexanone; CAP = ε-caprolactone; 6-HHA = 6-hydroxyhexanoic acid.

2.4.1 Genetic organization

After the isolation of strain JS666 and the sequencing of its genome (Coleman et al., 2002a), all genes necessary for cyclohexanol metabolism were found to be represented (Mattes et al., 2008). In *Acinetobacter* spp. NCIMB 9871 and SE19, the organization of *chnBER* is identical, while the organization of *chnACD* (Iwaki et al., 2002a) is slightly different. In strain JS666, the genes are organized in a single operon, where *chnCBAD* genes are clustered together in one of its two megaplasmids while *chnE* is in its chromosome (Mattes et al., 2008) (Figure 2.7). *Brevibacterium epidermidis* HCU contains two gene clusters involved in cyclohexanol degradation and neither cluster contains a homolog of *chnE* (Brzostowicz et al., 2002). There is only one copy of *chnB* (*chmo*) gene in strain JS666. The transcription termination sequence (i.e. palindromic sequence) for the operon is in a position 30 bp after the stop codon sequence of the *chnD* gene.

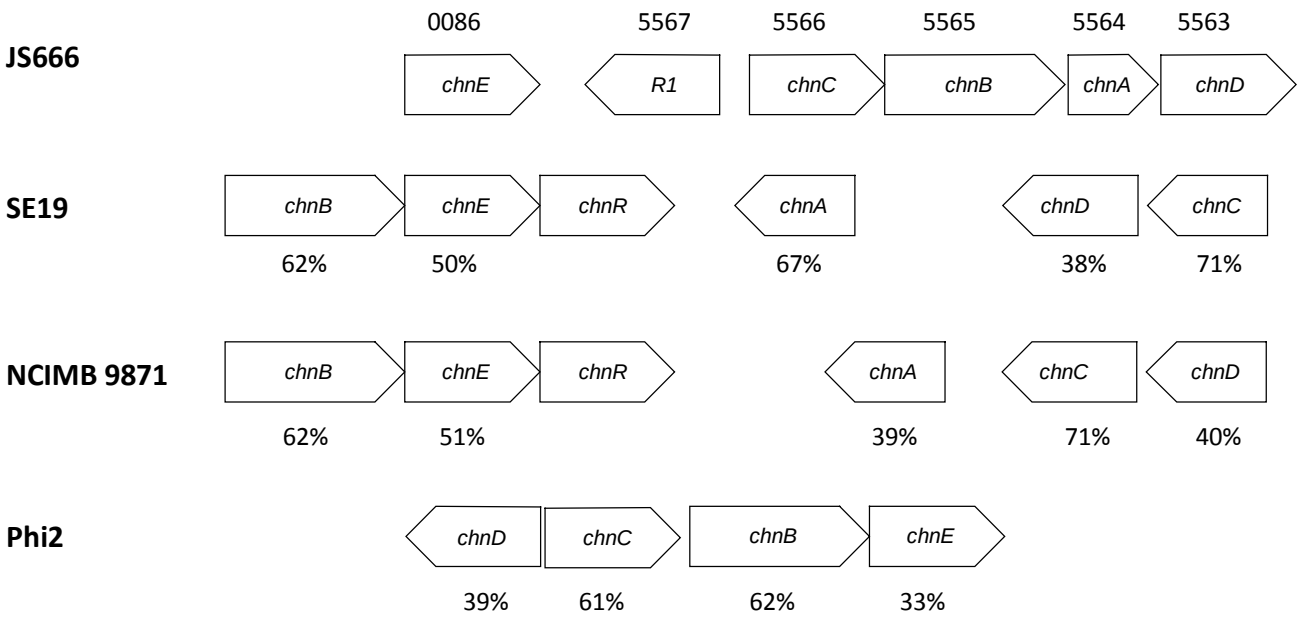

Figure 2.7. Genetic organization of the genes that catalyze cyclohexanol biodegradation in *Polaromonas* sp. JS666, *Acinetobacter* spp. SE19, NCIMB 9871 and *Rhodococcus* sp. Phi2. JS666 gene numbers (Bpro) are shown above the genes and percentage amino acid identities are shown under other bacterial genes (Iwaki et al., 2002a; Brzostowicz et al., 2003; Mattes et al., 2008). *chnR* encodes the transcriptional activator. *R1* is the Fis-family transcriptional regulator. Adapted from Mattes et al. (2008).

2.4.2 Hydrolase

Hydrolase catalyzes the addition of a water molecule to its substrate. Strain JS666 contains 111 hydrolases. Transcriptomic analysis revealed that putative *chnC* gene (Bpro_5566) was upregulated 7.5-fold by cDCE. This enzyme shares 71% amino acid sequence identity with a CAP-hydrolase from strain 9871 and catalyzes the hydrolysis of CAP to 6-HHA, cleaving the C-O bond. It is possible that this enzyme possesses similar function akin to an epoxide hydrolase, cleaving the C-O bond and transforming the epoxide into a corresponding diol (Figure 2.8).

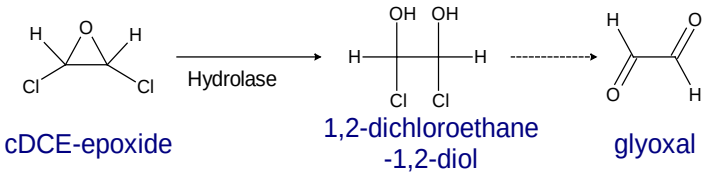

Figure 2.8. cDCE-epoxide transformation into its corresponding diol by an epoxide hydrolase as proposed by van Hylckama Vlieg and Janssen (2001). The formation to glyoxal is a spontaneous reaction.

An epoxide hydrolase from *A. radiobacter* AD1 (EchA) is capable of metabolizing epoxides (Rui et al., 2004a). The overexpressed EchA transformed cDCE-epoxide to its corresponding diol (1,2-dichloroethane-1,2-diol), which is proposed to be rapidly transformed into glyoxal (van Hylckama Vlieg and Janssen, 2001). The accumulation of chloride ions served as an indication of cDCE-epoxide mineralization, even though the formation of glyoxal was not reported. BLASTP search of EchA against strain JS666's genome resulted a match with an α/β hydrolase-fold coding sequence

homolog of haloacetate dehalogenase (Bpro_4478) with 29% amino acid identity (Figure 2.9). This hydrolase has been screened, overexpressed, purified and tested, and found capable of dehalogenation of haloacetates (Chan et al., 2010), thus sharing similar function to haloacid dehalogenases (Bpro_0530 and Bpro_5186).

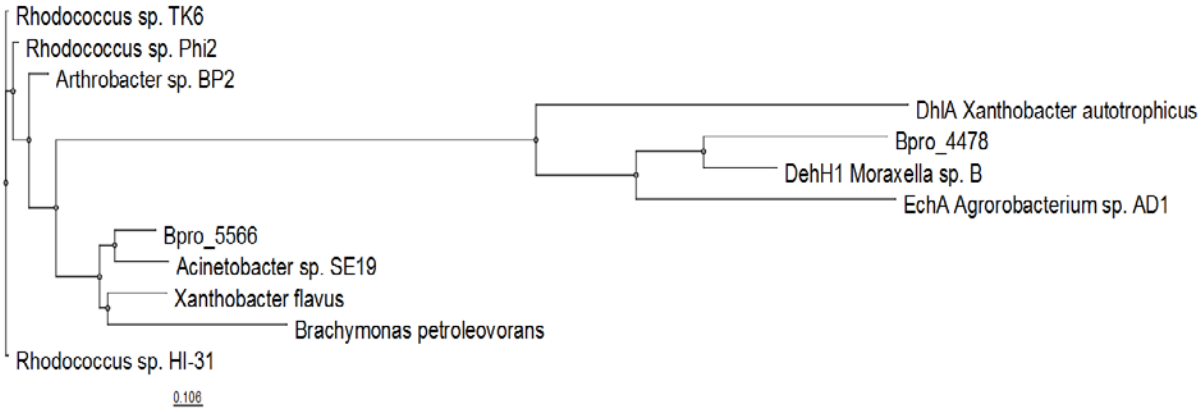

Figure 2.9. Phylogenetic relationships of amino acid sequences of bacterial CAP-hydrolases and other hydrolases. Sequences were aligned based on 324 amino acid sequences using ClustalX 2.1 and the phylogenetic tree was drawn using Ugene, where the length of branch is proportional to the evolutionary distance. Both Bpro_5566 (300 a.a) and Bpro_4478 (317 a.a) are hydrolase proteins from strain JS666. DhlA is haloalkane dehalogenase, DehH1 is haloacetate dehalogenase and EchA is epoxide hydrolase.

2.4.3 Alcohol dehydrogenases

Dehydrogenases are enzymes that facilitate the transfer of hydrogen from electron donor to electron acceptor, such as NAD^+. Alcohol dehydrogenases catalyze the interconversion between alcohols and aldehydes or ketones. The resulting aldehydes can be further oxidized by dehydrogenases into carboxylic acids. Jennings et al. (2009) reported elevated expression levels of putative alcohol dehydrogenase (encoded by *chnA*,

Bpro_5564), which was upregulated 6-fold by cDCE. It is a putative alcohol dehydrogenase related to the short-chain dehydrogenase/reductase (SDR family). This protein shares 70% amino-acid identity with a cyclohexanol dehydrogenase of *Xanthobacter flavus* and 69% amino acid identity with a cyclopentanol dehydrogenase of *Comamonas testosteroni*.

An adjacent gene, downstream of Bpro_5564, is another putative alcohol dehydrogenase (Bpro_5563 or ChnD). It is a zinc-binding alcohol dehydrogenase that attacks the hydroxyl group of 6-HHA and converts it to an aldehyde group. This enzyme shares 40% amino acid identity with 6-HHA dehydrogenase from strain 9871. 6-HHA is an ω-hydroxy acid, which is a carboxylic acid substituted with a hydroxyl group at the far carbon.

Alcohol dehydrogenases are also capable of reducing an alkanal (or aldehyde) to an alcohol, which is seemingly counterproductive to bacterial growth. The upregulation of alcohol dehydrogenases in the omic studies may be due to the presence of chlorinated ethanal, which normally exists in hydrate (acetal) form. The production of 2,2-dichloroethanol (DCET) was observed in hepatic microsomal P450 assay with DCE isomers (*cis* and *trans*) (Costa and Ivanetich, 1982). P450 produced DCAL and its transformation to DCET may be catalyzed by alcohol dehydrogenase in hepatic microsomes. In the preliminary work with the isolated perfused rat liver with cDCE, up to 10% DCAL transformation to DCET was observed compared to 1 – 3% transformation to dichloroacetic acid (DCAA) (Bonse et al., 1975). The metabolism of cDCE in rat hepatocytes resulted in production of DCET and smaller amount of DCAL and DCAA (Costa and Ivanetich, 1984). DCET was also detected when hepatocytes were incubated

with 1,1-DCE and tDCE. In similar study, the researchers observed that when the rate of DCAL production was low (from tDCE and 1,1-DCE metabolism), DCAA was the major metabolite. On the contrary, DCET was the major dichlorinated metabolite when the DCAL rate production was high (from cDCE metabolism). This was supported by the relatively lower K_m and V_{max} values of DCE transformation to DCAA than that of DCE transformation to DCET (Costa and Ivanetich, 1984). The haloalcohol formation is estimated to be favored by the cellular redox potential (Dolfing and Janssen, 1994; Bull et al., 2006).

In another example, one of the primary byproducts of TCE metabolism by mammalian P450 is 2,2,2-trichloroacetaldehyde (TCAL), which is rapidly converted into chloral hydrate in water. The hydrate can be readily reduced by alcohol dehydrogenase into 2,2,2-trichloroethanol (TCET, Figure 2.10) (Forkert et al., 2005). During the degradation of TCE by *Methylosinus trichosporium* OB3b cells, low levels of TCAL and TCET were identified (Oldenhuis et al., 1989). The cells also partially converted TCAL to TCET and vice versa. In mammals, DCET and TCET may be rapidly glucuronidated by glucuronidase and excreted in urine (Hutson et al., 1971; Miller and Guengerich, 1983). The addition of ethanol (EtOH) could alter the NAD^+/NADH ratio in bacterial cells, resulting the shifting of metabolism pathways. When EtOH was co-administered with TCE in hepatocytes, the trichloroacetic acid levels in blood was decreased and the ratio of TCET to trichloroacetic acid in urine was increased (Larson and Bull, 1989).

One of many applications of dehydrogenases is to generate NADPH or NADH, which has been used up extensively during monooxidation of xenobiotic compounds. It has been observed that, if the supply of NADPH for the initial metabolic step is lower

than the demand, biodegradation is stalled (Johnson et al., 2006). In strain JS666, NADPH or NADH can be generated by dehydrogenation of 6-phosphogluconate into ribulose-5-phosphate or by a putative alcohol dehydrogenase (such as Bpro_5563), respectively. The genome of strain JS666 also contains a pentose phosphate pathway system which enables the strain to recycle cofactors (Mattes et al., 2008).

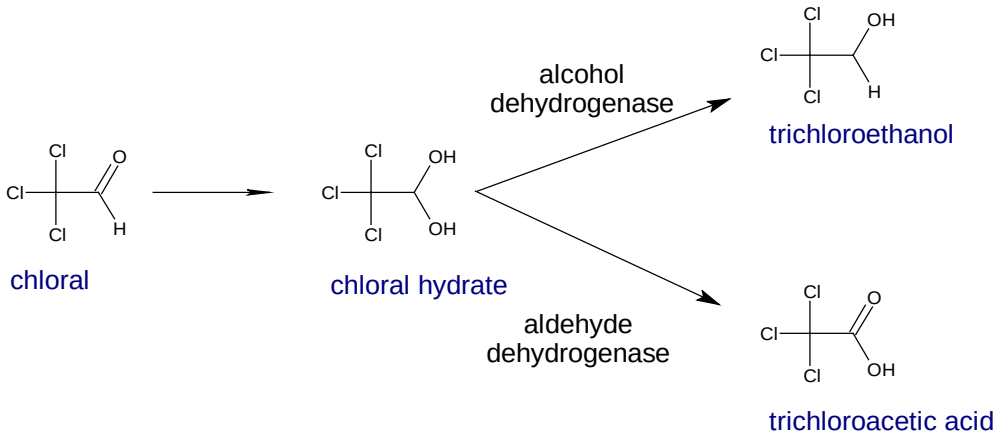

Figure 2.10. The fate of chloral during TCE metabolism. Chloral (or TCAL) is reduced to TCET and oxidized to trichloroacetic acid (Newman and Wackett, 1991; Forkert et al., 2005).

2.5 Gene inactivation using a suicide vector

Suicide vectors have been utilized to disrupt genes of interest by integrating an entire vector through homologous Campbell-type recombination at a specific targeted site. The vector contains the vegetative replication origin of plasmid R6K but lacks its *pir* gene, and therefore replicates only in strains that contain *pir* on a separate replicon. The plasmid also contains the origin of conjugal transfer of plasmid RP4 and therefore can be

mobilized by the transfer system of that plasmid. Translational fusions are created as a consequence of integration of the entire plasmid into the target gene. It is important to ensure that the fragment of the target gene that is fused to the reporter does not retain any of the functions of the wild-type gene. The presence of an antibiotic resistance gene in the vector is useful for colony selection. As a result, recipient cells will only maintain the plasmid when it is integrated into the chromosome and grown on media containing antibiotic (Kalogeraki and Winans, 1997).

Cyclopentanol metabolism in *Comamonas* sp. strain NCIMB 9872 was studied by inactivating its cyclopentanol 1,2-monooxygenase gene (*cpnB*) via insertion of a cassette containing a promoterless *lacZ* gene and a kanamycin resistance gene (Iwaki et al., 2002b). Furthermore, overexpressed CpnB in *E. coli* demonstrated its capability to transform various ketones, including cyclopentanol and CYHX. The knockout mutant strain failed to transform cyclopentanol, cyclopentanone, cyclohexanol or CYHX. Genetic organization showed that cyclopentanol dehydrogenase is located directly downstream of the *cpnB* gene; knocking out *cpnB* disrupted both genes (Iwaki et al., 2002b).

In *Polaromonas* sp. strain CJ2, the method of knocking out genes using suicide vectors was utilized to investigate the roles of the naphthalene catabolic genes. Researchers found two gene clusters, a large and a small gene cluster controlled by LysR-type (*nagR*) and MarR-type (*nagR2*) regulators, respectively. A mutant strain was constructed to create a polar knock-out of *nagR2*. The suicide plasmid also contained the *lacZ* gene that could be utilized as a transcriptional assay. A strain with a *nagR2*::*lacZ* fusion was constructed, and lacZ reporter assays concluded that *nagR2* is a negative

regulator (Jeon et al., 2006). An initial BLAST homology search indicated that a gene in the small gene cluster (of strain CJ2) encodes a putative salicylate 5-hydroxylase, and further investigation concluded that it encodes 3-hydroxybenzoate 6-hydroxylase. In that work, a suicide plasmid containing a kanamycin-resistance gene and a *sacB* gene was used to inactivate the targeted gene, *nagX* (Park et al., 2007). *sacB* encodes levansucrase from *Bacillus subtilis*, catalyzing the hydrolysis of sucrose and producing considerable amounts of levan that may be lethal to the cells (Gay et al., 1983). *nagX* was inactivated by plasmid insertion, producing a mutant strain resistant to kanamycin. Its deletion was acquired by further growing the kanamycin-resistant strain in media containing sucrose. One colony with truncated *nagX* gene (with a 2-bp deletion) was obtained and three colonies reverted to the wild-type *nagX* (Park et al., 2007). Recently, three copies of the *nagI* gene, which encodes gentisate dioxygenase, were successfully inactivated using a similar approach (Lee et al., 2011).

2.6 Starvation studies in other monooxygenase-expressing bacteria

Carbon deficiency in the subsurface is common and can significantly affect rates of biodegradation of targeted contaminants. In the past, the effects of carbon starvation have been studied in several oxygenase-expressing bacteria. The degradation rates of these bacteria were reduced exponentially as carbon starvation time increased (Johnson et al., 2006; Mattes et al., 2007; Park et al., 2008). Lag-phase for VC degradation has been observed in VC-degrading bacteria. In *Nocardioides* sp. strain JS614, a lag period exceeding 40 days was reported after carbon starvation for one day (Coleman et al.,

2002b). Singh et al. reported a decreasing degradation rate after the mixed cultures were starved for 150 days (Singh et al., 2004). Nevertheless, another VC-degrader, *Mycobacterium rhodesiae* strain JS60, did not suffer any lag period after 7-days of carbon starvation (Verce et al., 2000). Schmidt et al. (2010) conducted a study where an enrichment culture, which was obtained from a groundwater microcosm, was subjected to cDCE-starvation up to 250 days. The culture started to degrade 3 mg/L (0.03 mM) cDCE after 15 days.

The oxidation of chlorinated ethenes yields reactive epoxides that could be damaging to the bacteria that produce them. A starvation period could possibly disrupt regulation of the cell's epoxide-detoxification mechanism, leading to an imbalance between epoxide formation and epoxide degradation, resulting in their accumulation when previously starved cells are resupplied with the chlorinated-ethene substrate. In *Mycobacterium aurum* L1, short interruption of vinyl chloride feed led to accumulation of VC-epoxide. The reactive epoxide was not observed when the culture was continuously fed (Hartmans and De Bont, 1992).

In strain JS614, decreased lag periods for VC- or ethene-degradation were observed when co-administered with small concentrations of other carbon sources such as acetate and glucose after starvation. However, acetate addition gave mixed results, depending upon previous culture conditions. Small concentrations of acetate (provided along with VC or ethene) improved VC- or ethene-degradation after a period of starvation, if cells had been grown on VC or ethene, but not if they had been grown on acetate. This suggests that these small amounts of acetate provide ATP and/or NADH used to initiate oxidation (i.e., "prime the pump"), but there is also a need to induce

expression of genes that are required for VC- or ethene-degradation, such as monooxygenase and epoxyalkane:coenzyme M transferase (Mattes et al., 2007).

2.7 Multiple aerobic cDCE-degradation pathway(s).

Consistent with the proteomic and transcriptomic studies of JS666 — and with the two phenotypical cDCE-degradation behaviors observed — there are several possible cDCE-degradation pathways that may be operating in JS666. These include: (i) cDCE-dehalogenation catalyzed by GST, followed by dehydrogenase- and dehalogenase-catalyzed formation of glycolate; and (ii) cDCE-epoxidation catalyzed by monooxygenase(s), followed by formation of glyoxylate (Jennings et al., 2009). The levels of expression of enzymes predicted to be involved in the GST-catalyzed dehalogenation pathway were higher than of the enzymes predicted to be involved in the monooxygenase-catalyzed epoxidation pathway. Initial results thus suggested that the former is the primary cDCE-degradation pathway in JS666, and the latter is a less important transformation pathway, which also agrees with compound specific isotope analysis (CSIA) (Jennings et al., 2009). The change in ratio of heavy to light isotopes ($^{13}C/^{12}C$) that occurs during biological degradation can suggest the type of bond that is initially broken. Fractionation values associated with VC epoxidation (cleavage of C=C bond) are between -8.2 ± 0.1 ‰ to -7.0 ± 0.3 ‰ (Chu et al., 2004; Chartrand et al., 2005), whereas reductive dehalogenation of VC (cleavage of the C-Cl bond) is much lower, between -31.1 ‰ and -21.5 ‰ (Bloom et al., 2000; Hunkeler et al., 2002).

The reported fractionation value from aerobic enrichment cultures that co-metabolize cDCE is -9.8 ± 1.7 ‰ (Tiehm et al., 2008) and values for anaerobic reductive dehalogenation of cDCE range between -29.7 to -14.1 ‰, which akin to VC dechlorination (Bloom et al., 2000; Lee et al., 2007). cDCE-degradation in monooxygenase-containing *M. trichosporium* OB3b cultures yielded a value of -0.4 ± 0.5 ‰ (Chu et al., 2004). In one study with JS666, a fractionation value of -8.5 ± 0.1 ‰ was reported for cDCE-oxidation, suggesting that epoxidation is the initial step (Abe et al., 2009). Opposing this, another study with JS666 found much lower fractionation values for cDCE degradation (-17.4 to -22.4 ‰), suggesting anaerobic dechlorination or C-Cl bond breakage as the initial step (Jennings et al., 2009). Reports of two quite different extents of fractionation support the hypothesis of two distinctly different cDCE metabolic pathways within JS666. A study with groundwater microcosms during aerobic cDCE biodegradation reported an average stable carbon isotope enrichment factor of -15.2 ± 0.5 ‰, which agrees with Jennings et al. (Schmidt et al., 2010). Figure 2.11 depicts the proposed cDCE-biodegradation pathways. The conversion of chloroacetaldehyde to chloroacetate was confirmed in cDCE-grown JS666 crude extracts, but the identity of the specific chloroacetaldehyde dehydrogenase gene is still not known (Jennings, 2009).

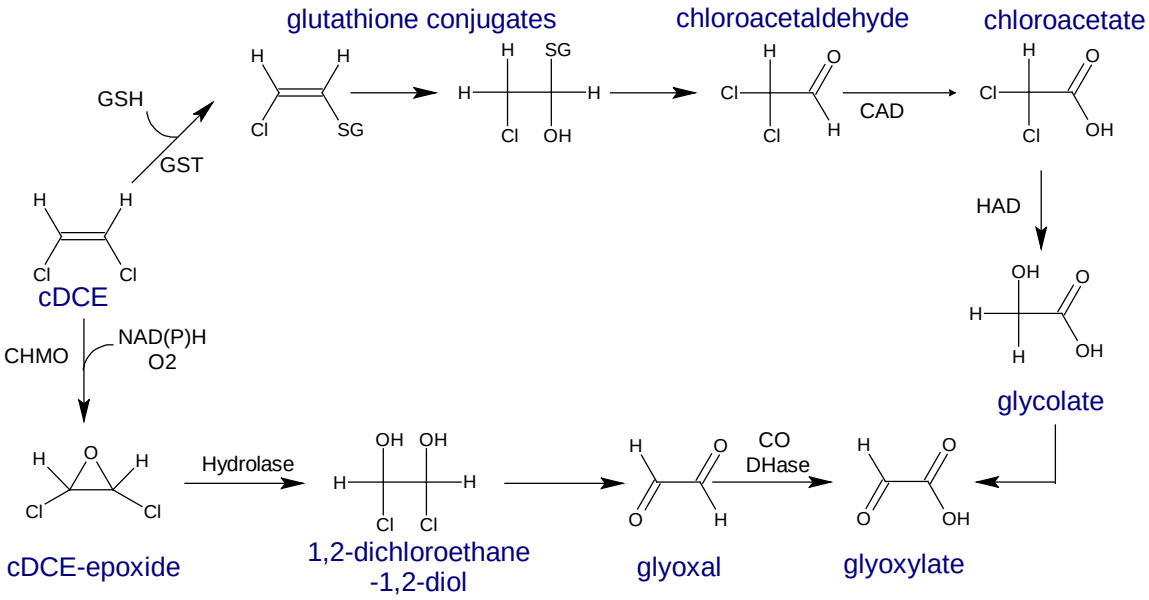

Figure 2.11. GST-catalyzed dehalogenation and monooxygenase-catalyzed epoxidation pathways of cDCE by strain JS666. CAD: chloroacetaldehyde dehydrogenase; HAD: haloacid dehalogenase; CO DHase: Carbon monoxide dehydrogenase. Adapted from Jennings et al. (2009).

Recent studies demonstrating activity of P450 on cDCE, on the other hand, might favor the importance of a monooxygenase-catalyzed pathway followed by dehydrogenase- and dehalogenase-catalyzed formation of chloroglycolate and formation of glyoxylate (Shin, 2010). These findings did not rule out oxygenation roles for other monooxygenases, such as FMOs. In cDCE- and DCA-degradation pathways of strain JS666, multiple enzymes possess similar catalytic specificity, such as HADs and hydrolase (Bpro_4478). Both types of enzymes have shown activities on haloacetates, cleaving one or more halogens (Chan et al., 2010). The conversion of cDCE by P450 revealed the formation of DCAL, apart from cDCE-epoxide. P450-cDCE suicide

complex formation was proposed to counter the missing mass balance from the transformation (Shin, 2010). Figure 2.12 shows the updated cDCE-biodegradation pathways.

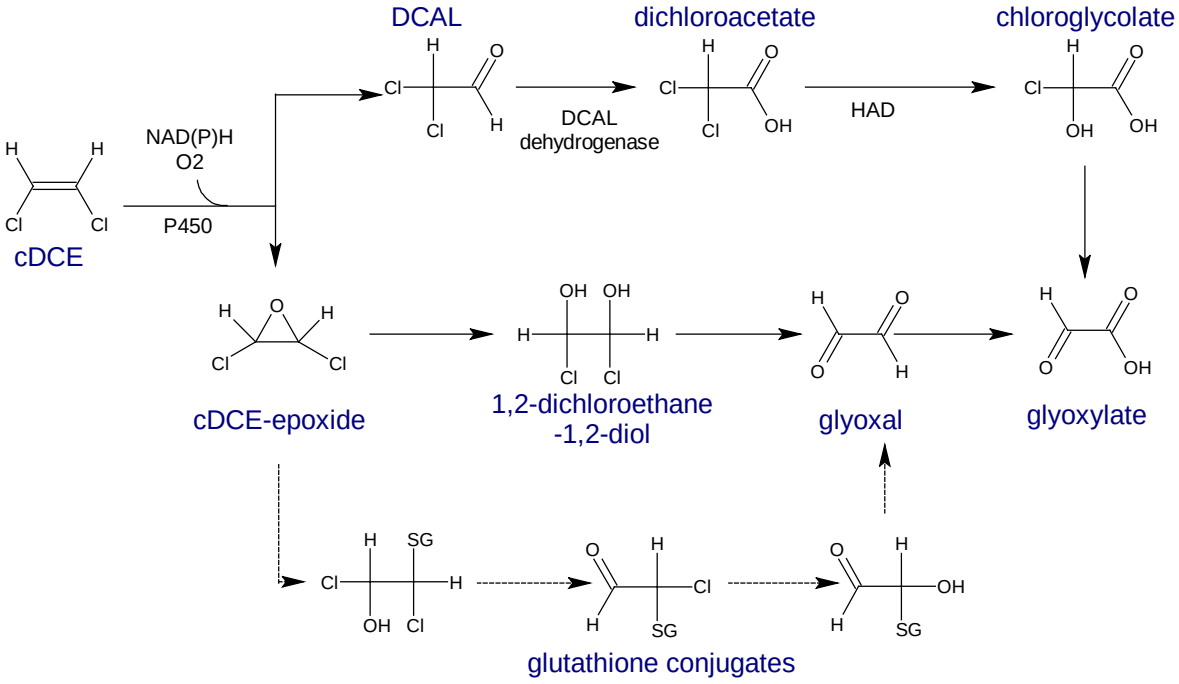

Figure 2.12. Proposed cDCE-degradation pathways updated by Shin (2010). DCAL is dichloroacetaldehyde.

2.8 Summary

The formation of epoxides during bacterial growth on cDCE and ethene is linked to the activity of monooxygenases, such as P450 and CHMO. Proteomic and transcriptomic analyses revealed the induction of these enzymes by cDCE. P450 has been demonstrated to catalyze the epoxidation of cDCE, nevertheless there are several examples where the functions of P450 and FMO may overlap. Production of epoxide by chemically-synthesized methyllumiflavin supports the possibility of epoxidation by hydroperoxyflavin group of FMOs. Akin to this reaction, peracid has also shown ability to epoxidize several chlorinated ethenes.

Genes in the same operon with *chmo*, namely hydrolase and dehydrogenases, may serve important roles, especially in detoxification of byproducts from cDCE-degradation. Hydrolase is postulated to catalyze the hydrolysis of epoxide, and dehydrogenases may react with chlorinated alcohols or aldehydes.

In this study, we will look at the involvement of the *chmo* gene and the roles of other genes in the cyclohexanol operon of strain JS666 during aerobic cDCE-degradation. Results from this study will be used to update the cDCE-degradation pathways and understand the detoxification mechanism during degradation.

CHAPTER 3

3. MATERIALS AND METHODS

3.1 Chemicals

cDCE (99%, stabilized with hydroquinone monomethyl ether (MEHQ)) and DCA (99.5%) were obtained from TCI America. Cyclohexanol (98%, Fisher), CYHX (99.8%, Acros), and CAP (99%, Acros) were reagent grade. TCE (100%, Fisher), VC (99.5%, Sigma-Aldrich), 1,1-DCE (99%, Aldrich), tDCE (99.7%, stabilized with MEHQ, Acros), ethene (99.999%, Matheson, inc.) and epoxyethane (99.5%, Aldrich) were used in various experiments. Other chemicals used include ethanol (EtOH, 99.5+%, Acros), acetaldehyde (99.5%, Acros), succinate (disodium salt, 99%, Fisher), acetate (sodium salt, anhydrous, 100%, Fisher), sodium chloride (99.57%, Fisher), glycolic acid (70% in water, TCI America), 6-HHA (95%, Acros), DCET (99%, Aldrich), DCAL hydrate (90%, TCI America), DCAA (99%, Sigma-Aldrich), chloroacetic acid (99%, Acros), styrene (99.5%, Acros) and styrene oxide (97+% Acros). Ethyl acetate (EtOAc, 99.9%), diethyl ether (Et_2O, 95%) and acetonitrile (99.9%) were obtained from Fisher scientific. 3-chloroperoxybenzoic acid (mCPBA, 70 – 75% in water) and *d*-chloroform (99.6+% deuterium atom) were obtained from Acros. Sodium hydroxide pellets (NaOH, 97%, Fisher) were dissolved in deionized distilled water, used as eluents in the ionic chromatography.

For maintenance and propagation of *E. coli* in molecular biology procedures, Lysogeny Broth, Miller (LB, 10 g/L tryptone, 5g/L yeast extract, 10 g/L NaCl) was used

and obtained from Fisher. D-glucose (99%, Fisher) or riboflavin (98%, Acros) were supplemented when needed. A 1M stock solution of isopropyl β-D-1-thiogalactopyranoside (IPTG, dioxane-free, 95%, Fisher) was used in the enzymatic assays as the inducer when required. A list of antibiotics used in our study: ampicillin (sodium salt, 95%, Fisher), rifampicin (95%, Fisher), kanamycin sulfate (95%, Acros), streptomycin sulfate (95%, Acros), chloramphenicol (98 – 102%, Acros) and tetracycline (98%, Fluka).

cDCE- and tDCE-epoxides were chemically synthesized by reacting 0.86 mL of cDCE or tDCE with 1.6 g mCPBA dissolved in 6 mL of an organic solvent, such as *d*-chloroform or acetonitrile, and heating at 50°C – 60°C for 8 – 12 hours. The cDCE-epoxide peak was identified by gas chromatography-mass spectrometry (GC-MS; HP6890) using a DB-5ms column (30 m × 0.25 mm, 0.25-μm film thickness; J&W scientific). See Appendix B for detailed discussion of the issues with epoxide identification. For enzymatic assay purposes, cDCE-epoxide synthesized in acetonitrile was used.

DCAL monomer is not commercially available. Our colleague (Shirley Nishino) at Georgia Institute of Technology (Atlanta, GA) prepared DCAL monomer from DCAL-hydrate by reacting the hydrate with series of sulfuric acid treatments (Wakasugi et al., 1993). DCAL and its hydrate turned out to be indistinguishable by GC-MS (Nishino, 2011). Therefore, when DCAL was required in our studies, its hydrate was dissolved in water creating a 100-mM stock solution.

3.2 Bacterial strains, plasmids and culturing techniques.

All bacterial strains, vectors, plasmids and primer sets used in the present study are listed in Table 3.1. The culture techniques for strain JS666 which best ensure sustained cDCE-degradation were previously described by Jennings et al. (2009). In brief, strain JS666 cultures were grown in 160-mL serum bottles sealed with Teflon®-coated butyl rubber septa containing 100 mL of minimal salts medium (MSM, containing among other constituents 20 mM phosphate, 10 mM ammonium, trace metals, and 0.02 mM chloride) as previously described (Coleman et al., 2002a). 4 μL of cDCE was injected to obtain a nominal concentration of 520 μM, and the bottle was left in inverted position on an orbital shaker at 23°C. After 2.5 – 3.5 additions of cDCE were degraded, 5% of the culture volume was transferred into fresh MSM. JS666 was streaked on ¼-strength trypticase soy agar (¼-TSA) plates for purity check (i.e., to look for anomalous colony morphologies on this rich medium). JS666 wild-type (WT), *chmo*-knockout (KO), and *chmo*-complement strains were also grown in ¼-strength trypticase soy broth (¼-TSB) and streaked on ¼-TSA plates with appropriate antibiotics. All *E. coli* strains were grown in LB broth at appropriate temperature (depending on the enzymatic studies, but usually 30°C) in a rotary-shaking incubator, and appropriate antibiotics were provided when required to maintain plasmids.

Table 3.1. The bacterial strains, vectors and primers used in this study.

Name of strain, plasmid, or primer	**Relevant characteristics or sequence**	**Source or reference(s)**
Strains		
Polaromonas sp.		
JS666	cDCE aerobic degrader (WT)	This study
JS666 Δ*chmo::kan*	*chmo*-knockout strain (KO)	This study
JS666 Δ*chmo::kan*, *chmo*	*chmo*-complement strain	This study
E. coli		
SY327 λ*pir*	Host for pVIK110, contain λ*pir* for *pir* plasmids	Madsen, E.
S17-1 λ*pir*	Contains λ*pir* for *pir*-dependent plasmids, conjugal donor;	Madsen, E.
Rosetta 2 (DE3)	Host for gene expression	Novagen
BL21 Star™ (DE3)	Host for gene expression	Invitrogen
Plasmids or vector		
pVIK110	*lacZY* for translational fusions, R6K oriV, suicide vector; kan^R	Madsen, E.
pVcmo	Suicide vector construct containing fragment of *chmo* gene	This study
pET101/D-TOPO®	Expression vector, amp^R	Invitrogen
pCOLADuet™-1	Expression vector, kan^R	Novagen
pET21(a)+	Expression vector, amp^R	Novagen
pJB866	Expression vector, tet^R	NBRP-*E.coli* at NIG, Japan
pJcmo	Expression vector (pJB866) with Bpro_5565, tet^R	This study
p15TV-L	Expression vector with Bpro_4478, amp^R	Chan et al. (2010)
pJS597	Expression vector with Bpro_5299 – Bpro_5301, amp^R	Shin (2010)
p66H	Expression vector (pET101D) with Bpro_5566, amp^R, His_6-tagged	This study

[a] nucleotide sequences for restriction enzyme sites are underlined
[b] bp: resulting amplicon sizes in base-pairs.
amp = ampicillin; kan = kanamycin; tet = tetracycline

Table 3.1 (continued)

Name of strain, plasmid, or primer	Relevant characteristics or sequence		Source or reference(s)
p65R	Expression vector (pET101D) with Bpro_5565, amp^R		This study
p63R	Expression vector (pET101D) with Bpro_5563, amp^R		This study
p6566	Expression vector (pET21a) with Bpro_5566 and Bpro_5565, amp^R		This study
p6364	Expression vector (pCOLADuet) with Bpro_5564 and Bpro_5563, kan^R		This study
PCR primers [a]		bp [b]	
VcmoF (SalI)	5'-CCCTCTAGACAACATCAAGGGCATCGAG-3'	427	This study
VcmoR (XbaI)	5'-CCCGTGGACTTCTTCGCTGGTGGCAATG-3'		This study
ocmoF	5'-GAAATCCAGACCGATACCGA-3'	823	This study
vxR	5'-TTGACCGTAATGGGATAGGT-3'		This study
isoF	5'-TGCCGCTGACAACAACAC-3'	139	Jennings (2005)
isoR	5'-ATCAATGCCTTTGGAGTGC-3'		Jennings (2005)
Protein overexpression			
66F	5'-CACCATGAAACCTTCAACCGAGGC-3'		This study
66H	5'-AGCAGCCTTAAACCATTGGG-3'		This study
65F	5'-CACCATGACCCTGGCAACACAAGA-3'		This study
65R	5'-TTAGCGGATCTCAAAACCTGG-3'		This study
63F	5'-CACCATGAATTACCGCTGCGCCCA-3'		This study
63R	5'-TCAAGGCTGCAGCACCACG-3'		This study
E6566F (BamHI)	5'-CCCGGATCCATGACCCTGGCAACACAAGA-3'		This study
E6566R (XhoI)	5'-CCCCTCGAGTCAAGCAGCCTTAAACCATT-3'		This study
C6364F (EcoRI)	5'-CCCGAATTCATGAAACGCGTACAAGA-3'		This study
C6364R (HindIII)	5'-CCCAAGCTTTCTTCAAGGCTGCAGCA-3'		This study

[a] nucleotide sequences for restriction enzyme sites are underlined
[b] bp: resulting amplicon sizes in base-pairs.
amp = ampicillin; kan = kanamycin; tet = tetracycline

Table 3.1 (continued)

Name of strain, plasmid, or primer	Relevant characteristics or sequence		Source or reference(s)
Reverse transcription PCR		bp [b]	
RT-RpoF	5'-GCCTATTCCTATACCGAACGC-3'	387	This study
RT-RpoR	5'-GTAGACTTCCTGCTCCTTGAC-3'		This study
RT-ISOF	5'-GAAATTCAGCACTCCAAAGGC-3'	397	This study
RT-ISOR	5'-TCTTGTAGAAACCTTCGGCG-3'		This study
RT-p450F	5'-ACCCCGTGCATTACTGTAAG-3'	370	This study
RT-p450R	5'-CAAGGGAAATCAAACAGCGTC-3'		This study
RT-GSTF	5'-TTGAACGGGTGGAGATTGAC-3'	411	This study
RT-GSTR	5'-AGCTGTAGTTGGCAATATCGG-3'		This study
RT-CMOF	5'-GAAATCCAGACCGATACCGA-3'	572	This study
RT-CMOR	5'-TCCGGGTCTTTGACAATCTC-3'		This study
RT-HYDF	5'-GCAAACAACATCACCACCAG-3'	330	This study
RT-HYDR	5'-AGGAACGGGAACACATGCT-3'		This study
RT-ALDF	5'-AATCTCGGCATCCAGTTACC-3'	419	This study
RT-ALDR	5'-GGCTTCATTCGGGTCAAAAG-3'		This study
RT-HADF	5'-AGATGGTCAGCAAGATGTGG-3'	322	This study
RT-HADR	5'-AAGTGATCGAAGGAGTTGGTC-3'		This study

[a] nucleotide sequences for restriction enzyme sites are underlined
[b] bp: resulting amplicon sizes in base-pairs.
amp = ampicillin; kan = kanamycin; tet = tetracycline

3.3 Analytical methods.

TCE, cDCE, VC, DCA, ethene and epoxyethane were analyzed by 0.1-mL headspace samples injected (using a locking gas-tight syringe [VICI Pressure-Lok® Series A]) into a gas chromatograph (GC, Perkin-Elmer Autosystem) equipped with a flame-ionization detector (FID) and a 8-ft x 1/8-inch stainless-steel column packed with 1% SP-1000 on 60/80 Carbopack B (Supelco) that was operated isothermally at 160°C. For detecting cDCE-epoxide, headspace samples up to 2 mL were injected. Oxygen and carbon dioxide levels were measured with a Perkin-Elmer GC equipped with a thermal-conductivity detector and a 80-inch × 1/8-inch column packed with 60/80-mesh 13X molecular sieve (Supelco), operated at 90˚C. Substrate levels were quantified by comparison to standards prepared using known-amount additions in serum bottles containing phosphate buffer.

Cyclohexanol, CYHX and CAP were analyzed by GC after extraction of aqueous samples with EtOAc (1:1 = sample: EtOAc), and 2 μL of the organic layer was injected into a GC (Hewlett Parkard HP5890 Series II) equipped with an FID and a SPB™-5 column (15 m × 0.53 mm × 1.5 μm; Supelco). The column temperature was maintained at 50°C for 2 min, then ramped 15°C/min to 215°C. The injector and detector temperatures were both 250°C. Standards for these substrates were made gravimetrically and extracted using EtOAc for GC measurements.

DCAL, DCET, styrene and styrene oxide concentrations were analyzed by GC after extraction of aqueous samples with Et_2O (2:1 = sample:Et_2O), and 3 μL of organic extract was injected into a GC (Hewlett Parkard HP5890) equipped with an FID and a

DB-5ms column (30 m × 0.53 mm × 1.0 μm; Agilent Technologies) that was operated with column at 40°C for 4 min, then ramped 40°C/min to 200°C until all had been eluted. The injector and detector temperatures were 200°C and 250°C, respectively. Standards for these substrates were made gravimetrically and extracted using Et_2O for GC measurements.

For EtOH and acetaldehyde measurements, direct aqueous injection (3 μL) was made to the GC (HP5890) with FID and DB-5ms column, operated with similar program conditions described above with a longer final temperature (200°C) to remove excess water. Prior to analyses, samples were centrifuged to remove cell debris and kept on ice between measurements to ensure stability of EtOH and acetaldehyde. Standards for both EtOH and acetaldehyde were made by adding 45.2 μL and 42.7 μL of substrates into 9.54 mL and 9.95 mL of distilled water, respectively.

The concentrations of acetate, succinate, chloride, 6-HHA and glycolate, were measured using a Dionex Ion Chromatograph (AS50) equipped with Dionex AS14A analytical and guard ion-exchange columns with suppressed conductivity detection in an isocratic CO_2-free, 40-mM NaOH eluent at 1 ml/min for 15 minutes. NaOH eluent was primed with high-purity helium before use. Samples were centrifuged to remove cell debris prior to analyses. Standards for chloride concentrations were prepared gravimetrically through known amount of additions into volumetric flasks.

3.4 Disruption of *chmo* by homologous recombination.

As an aid to selecting for successful recombinants after mating, the inserts contain (among other genes) an antibiotic-resistance gene that confers resistance upon the recombinant to an antibiotic to which the wild-type is not natively resistant. Thus, preliminary to attempting homologous recombination with JS666, we needed to ascertain its native resistance to various antibiotics. To determine the antibiotic resistance of strain JS666, WT cells were grown on ¼-TSA plates containing selected antibiotic gradients (maximum concentration of antibiotics tested, μg/mL): rifampicin (100), kanamycin (50), streptomycin (100), ampicillin (100), chloramphenicol (20), and tetracycline (20).

Strain JS666 was plated on ¼-TSA plates containing a rifampicin gradient (up to 100 μg/mL) and showed resistance to it, but sensitivity to kanamycin, ampicillin, chloramphenicol, streptomycin and tetracycline, even though some genes that are known to be involved in chloramphenicol resistance exist in strain JS666 (Bpro_0389 and Bpro_3811). We tested *E. coli* strains used in this study for their sensitivity to different antibiotics (maximum concentrations tested: rifampicin, 50 μg/mL; kanamycin, 50 μg/mL; ampicillin, 100 μg/mL; chloramphenicol, 20 μg/mL; tetracycline, 20 μg/mL), and all *E. coli* strains with the broad-host range vectors were resistant to kanamycin but sensitive to the other antibiotics tested.

To prepare the suicide vector, pVIK110 was extracted from *E. coli* SY327 pVIK110 using the PureYield plasmid purification kit (Promega). An internal fragment of *chmo* was PCR-amplified from JS666 genomic DNA using the VcmoF and VcmoR primer pair (T_m = 60°C) with a Mastercycler Gradient (Eppendorf). The resulting

amplicons and pVIK110 were cut using *Xba*I and *Sal*I restriction enzymes (Fermentas), ligated and transformed into chemical-competent *E. coli* S17-1 λ*pir* cells using heat-shock treatment. Chemical-competent *E. coli* S17-1 λ*pir* cells were prepared using a rubidium chloride method (Douglas, 1983).

JS666 cells were harvested by centrifugation, suspended in ¼-TSB and left to grow unshaken 24-48 hours before mating was conducted. The conjugation frequency of a suicide plasmid in strain CJ2 was reported to be low, which may be caused by unsuitable growth temperature for the donor strain (mating temperature = 25°C) or extracellular polysaccharide production (Park et al., 2007). To improve vector transfer to the recipient strain, the donor strain was grown at 30°C and the mating was conducted in ¼-TSB for more than 24 hours. *E. coli* S17-1 λ*pir* pVcmo cells were grown in LB broth at 30°C overnight before the cells were harvested and suspended in ¼-TSB. Suicide vector containing the internal *chmo* fragment, pVcmo, was transferred into rifampicin-resistant JS666 by conjugational mating with *E. coli* S17-1 λ*pir* pVcmo cells on ¼-TSB at 23°C for another 24-48 hours. 100-µL aliquots of the bacterial mixtures were subsequently spread on ¼-TSA plates containing 60 µg/mL rifampicin and 30 µg/mL kanamycin (TRK plates) and were left to grow for 5-7 days at 23°C. The resulting colonies were carefully transferred to another fresh TRK plate. The transconjugants (KO) were confirmed by PCR with isoF-isoR, ocmoF- vxR and 65F-65R (or RT-CMOF and RT-CMOR) primer pairs (T_m = 60°C) and run on 1% TBE or TAE gel. The first primer set (isoF-isoR) is used to identify that the colonies are strain JS666. The second set (ocmoF-vxR) looks for the presence of the insert within the interrupted *chmo* gene –

thereby proving that the colony is KO. The third primer set hybridizes to the *chmo* sequences before and after the insert, resulting a 572-bp amplicon for WT and none for KO (because of an extra 9.3-kbp insert and short PCR extension time). The resulting amplicons were excised and purified for sequencing. See Appendix A for more details on sequencing results. KO colonies were then transferred into ¼-TSB containing 30 μg/mL kanamycin before transferring into a 160-mL bottle with 50-mL MSM containing 10 mM succinate, 26 μmol/bottle cDCE (or a nominal concentration of 520 μM) and 30 μg/mL kanamycin. Occasionally, KO cultures were checked for purity by streaking on a fresh ¼-TSA plate and several colonies were selected for PCR-testing using ocmoF-vxR and isoF-isoR primer sets, looking specifically for KO characteristics.

3.5 Complementation

The intent of these studies was to re-insert the *chmo* gene back onto the *chmo*-negative mutant strain and see what functions lost to the KO strain were thereby restored. *chmo*-knockout mutant strains were grown on MSM containing 10 mM succinate. The cells were then harvested and suspended in ¼-TSB and left to grow at 23°C for 24-48 hours without shaking. *E. coli* S17-1 λ*pir* cells containing pJcmo plasmid were grown in LB broth with 10 μg/mL tetracycline at 30°C. The conjugation technique was similar to the method of creating KO strains, except the bacterial mixtures were spread on ¼-TSA plates containing 60 μg/mL rifampicin and 5 μg/mL tetracycline (TRT plates). Colonies that grew on the plate were transferred onto a fresh TRK plate. Subsequently, the

colonies that grew on the TRK plate were streaked on a fresh TRT plate. The complement strain was confirmed by PCR with isoF-isoR, ocmoF-vxR and 65F-65R primer pairs (T_m = 60°C) and by sequencing the resulting amplicons.

3.6 Growth and substrate-utilization experiments.

Both WT and KO strains were first grown in 5 mL ¼-TSB with 1.3 μmol/bottle cDCE. Aliquots of 0.1 mL were transferred into 5 mL MSM containing 1.3 μmol/bottle cDCE with either 10 mM succinate, 10 mM acetate, 1 mM CYHX or 10 mM EtOH. This step was to ensure similar initial conditions for the subsequent experiments. Then, approximately 0.2-mL aliquots of WT cells from each substrate (10 mM succinate, 10 mM acetate, 1 mM CYHX or 10 mM EtOH) were transferred into fresh 100-mL MSM containing the respective substrates with added cDCE levels of of 132 μmol/bottle, 52 μmol/bottle or none. For KO cultures, approximately similar amounts of cells from acetate-grown (with 1.3 μmol/bottle cDCE) cultures were used as innocula. A similar experiment was conducted with CAP. WT and KO cultures were grown in 100-mL MSM with 1 mM CAP along with cDCE (106 μmol/bottle, 52 μmol/bottle or none). cDCE concentrations and optical densities of the cultures at 600 nm (OD_{600}) were monitored. All experiments were conducted with biological duplicates.

In a preliminary experiment, WT and KO cultures were also tested on their capabilities of growth on cyclohexanol. 5 mL of the succinate-grown cultures (with cDCE exposure) were transferred into 95-mL fresh MSM with 0.5 mM cyclohexanol in

160-mL serum bottles. Cyclohexanol concentrations were monitored with time and any production of cyclohexanone was noted.

To assay possible TCE, VC, DCA and ethene transformations, WT and KO cultures were grown in 1-L serum bottles containing 400-mL MSM plus 1 mM CAP and 208 μmol/bottle (nominal concentration of 520 μM) of cDCE. When the OD_{600} reached 0.3 – 0.5 or at mid-cDCE degradation, the cells were harvested by centrifugation, washed once with MSM, and resuspended into 160-mL serum bottles containing 50 mL MSM. TCE, DCA, VC and ethene were delivered accordingly, and the quantities of these hydrocarbon compounds were monitored (headspace sampling) with time. Any formation of epoxyethane was also noted. TCE- and VC-epoxides were short-lived and have not been synthesized for this study; therefore their formations were not monitored. DCA is transformed into 2-chloroethanol and its production was not monitored. The experiments were conducted with biological duplicates. Remaining substrate levels were estimated by comparison to standards prepared by addition of known amounts of TCE, DCA, VC and ethene to 160-mL serum bottles containing 50-mL MSM.

3.7 Overexpression of enzymes involved in cyclohexanol metabolism.

To overexpress genes in the cyclohexanol operon of JS666, each individual gene was cloned into the expression vector pET101/D-TOPO® (Invitrogen). Putative *chnB* (*chmo*, Bpro_5565) and *chnD* (Bpro_5563) genes were PCR-amplified from WT genomic DNA by using *Pfu*Ultra II Fusion HS DNA polymerase (Agilent Technologies, Inc.) and 65F-65R and 63F-63R primer pairs (T_m = 60°C), respectively. The resulting

amplicons were cloned into the expression vector pET101/D-TOPO and further transformed into *E. coli* BL21 Star™ (DE3). For a hexahistidine-tagged putative α/β hydrolase-fold (*chnC*, Bpro_5566), 66F forward primer was coupled with 66H reverse primer (T_m = 60°C) and *chnC* gene was PCR-amplified from WT genomic DNA by using *Pfu*Ultra II Fusion HS DNA polymerase. Similarly, the resulting amplicons were cloned into the pET101/D-TOPO vector and the construct was transformed into *E. coli* BL21 Star™ (DE3).

To overexpress the complete cyclohexanol operon, both *chnC* and *chnB* (*chmo*) genes were cloned in tandem into a cloning vector, pET21a(+) (Novagen), and both *chnA* and *chnD* genes were cloned in tandem into pCOLADuet™-1 (Novagen). The *chnC-chmo* gene pair was PCR-amplified by using the E6566F-E6566R primer pair (T_m = 60°C), which contains BamHI and XhoI restriction sites, respectively. The amplified PCR product obtained and pET21a(+) were then excised with FastDigest®, BamHI, and XhoI (Fermentas) and ligated, resulting in the recombinant plasmid designated p6566. The *chnA-chnD* gene pair was PCR-amplified by using C6463F-C6463R primer pair (T_m = 60°C), which contains EcoRI and HindIII restriction sites, respectively. The resulting amplicons were excised with FastDigest®, EcoRI and HindIII (Fermentas) and ligated into pCOLADuet™-1, resulting in pC6463. Initially, these two plasmid constructs were co-transformed into a single *E. coli* strain, however the strain grew well only at 37°C and all of our whole-cell studies were conducted at 30°C or room temperature. We have decided to transform and test them separately. All sequences were checked with the

NCBI database and any error was corrected using QuickChange Multi Site-Directed Mutagenesis Kit (Agilent Technologies).

3.8 Enzymatic assays.

3.8.1 CHMO enzymatic assays.

For assaying overexpression of the *chmo* gene in *E. coli*, whole-cell studies were adopted based on previous studies (Iwaki et al., 2002b; Alexander, 2010). *E. coli* Bl21 Star™ strains containing p65R or p6566 were grown in LB broth supplemented with 100 μg/mL ampicillin and 1 μg/mL riboflavin on a rotary shaker at 30°C. When the optical density reached 0.4 – 0.5, IPTG was added to the media (to yield a concentration of 0.1 mM), and the cultures were left shaken for 5 minutes before the substrates were added and subsequent incubation to assay growth was conducted at 23°C. The disappearance of the substrates and the appearance of products were monitored. Substrates tested were CYHX, cDCE, styrene and DCAL, and the expected products were CAP, cDCE-epoxide and DCAA, respectively. Cell cultures that were not induced and *E. coli* strains without the plasmids were used as controls.

3.8.2 Hydrolase enzymatic assays

For ChnC (hydrolase, Bpro_5566) overexpression, a method similar to that described above for CHMO assays was used. In another separate experiment, *E. coli* Bl21 Star™ strains containing p66H were grown in LB broth supplemented with 100 μg/mL

ampicillin at 30°C. When the optical density reached 0.4 – 0.5, 0.1 IPTG was added (yielding 0.1 mM) to the media, and the cultures were left shaken for 5 minutes before the substrate, such as 10 μL CAP, 0.5 mL epoxyethane or 5 μL chemically-synthesized cDCE-epoxide, was injected into 20-mL cultures in 160-mL serum bottles. For assay with styrene oxide, approximately 5 μL was injected into 50-mL cultures in 160-mL serum bottles. Subsequent incubation to assay growth was conducted at 23°C.

Another hydrolase from strain JS666 (Bpro_4478) was also tested with chemically-synthesized cDCE-epoxide (Chan et al., 2010). The gene was cloned in p15TV-L plasmid (containing ampicillin resistance gene), and the plasmid was transformed into *E. coli* BL21 Star™ cells. In a preliminary experiment, the cells were grown in LB broth containing 100 μg/mL ampicillin at 30°C. When OD_{600} reached 0.5 – 0.6, IPTG was introduced (yielding 0.5 mM), and they were left shaken at 23°C overnight. For control cells, IPTG was not added to the separate cultures. The cells were then harvested and washed once with phosphate buffer. The pellets were then resuspended into 20 mM phosphate buffer supplemented with 1 mM succinate. Chloride ions were measured after an hour of incubation and three hours after the first measurement. At 5-hour incubation, 1 mM succinate was added to both induced and uninduced cultures. Final readings were taken after the cultures were left shaken overnight.

The experiment was repeated by growing the cells in LB broth containing 0.5% glucose and 100 μg/mL ampicillin at 30°C. When OD_{600} reached 0.5 – 0.6, IPTG was

introduced (yielding 1 mM). After 4-hour induction at 30°C, the cells were harvested by washing them twice in phosphate buffer to remove traces of chloride ions (LB broth contains 10 g/L NaCl). The cells were resuspended in 20 mM phosphate buffer and chemically synthesized cDCE-epoxide (in acetonitrile) was introduced to the cultures. Uninduced cells were assayed for background activity and chloride release. Phosphate buffer with no cells was used as blank control.

3.8.3 Dehydrogenases enzymatic assays

E. coli BL21 Star™ (DE3) strains containing either p6364 or p63R were grown on LB broth with 0.5% glucose and 30 μg/mL kanamycin or 100 μg/mL ampicillin, respectively, at 30°C. An *E. coli* cell culture with no plasmid was used as negative control. When the culture's optical density (OD_{600}) reached 0.4 – 0.5, IPTG was supplied (yielding 1 mM) to induce the production of the proteins, and the cultures were left shaken overnight at 23°C. The cultures were then harvested by centrifugation and washed once with phosphate buffer. The pellets were resuspended in 20 mM phosphate buffer (pH 7.5) and aliquots (10-mL) of the culture (containing approximately 20 mg of cells) were transferred into 25-mL serum bottles, and substrates were subsequently added. Uninduced cells were used as control. Among substrates tested for ChnD (long-chain dehydrogenase) activity were cyclohexanol, 6-HHA, EtOH, acetaldehyde, glycolate and DCET. With the overexpressed tandem of ChnA (cyclohexanol dehydrogenase) with ChnD, cyclohexanol, 6-HHA, EtOH, and acetaldehyde were tested. To add acetaldehyde,

a stock solution was first created: 155 μL acetaldehyde was injected into 23.2 mL phosphate buffer using a cold syringe (kept at 4°C) to make a 5.25 g/L stock.

3.8.4 P450 enzymatic assays

P450 and its adjacent genes (ferredoxin and ferredoxin reductase) were cloned in IPTG-inducible pET101D-TOPO vector and transformed into *E. coli* Rosetta2 (DE3) (Shin, 2010). The strain was grown in LB broth containing 100 μg/mL ampicillin and 20 μg/mL chloramphenicol until OD_{600} reached 0.4 – 0.5 at 30°C. IPTG was subsequently added (yielding 0.5 mM) to the cultures, and they were left shaken at 23°C overnight. The cells were then harvested and washed twice with phosphate buffer to remove any remaining chloride ions. The pellets were then resuspended into 20 mM phosphate buffer supplemented with 5 mM succinate. Aliquots (20-mL) of the culture were transferred into 160-mL serum bottles and 0.5 μL of cDCE was then added. Uninduced cells and no-cDCE induced cells were used as background controls. Samples for cDCE measurement were taken twice by drawing out 2 mL of headspace and injecting to GC/FID with packed column. Samples of mixed culture (2-mL) were also removed at each time-point for chloride measurements. cDCE levels were calibrated gravimetrically through additions of known amounts (0.1098, 0.1172, 0.1145 mg of cDCE) into serum bottles containing known amounts of buffer (19.72, 20.27, 20.01 mg phosphate buffer).

3.9 Starvation studies

cDCE-grown, strain JS666 cultures were transferred into 50-mL MSM containing CYHX (1-2 mM) or succinate (10 mM) and grown to an OD_{600} of 0.4-0.5. Aliquots (20-mL) of the CYHX-grown or succinate-grown cultures were transferred into 580 mL MSM containing 1 mM of CYHX or 10 mM succinate, respectively, and the concentration of CYHX and OD_{600} of succinate-grown cultures were monitored.

When the actively degrading CYHX (at 0.3 – 0.5 mM), cells were harvested by centrifugation, washed and resuspended with fresh carbon-free MSM (5 mL). The cells were then injected into 160-mL serum bottles containing 45 mL MSM. The succinate-grown cells were harvested when OD_{600} reached approximately 0.5 – 0.7, and similarly the cells were washed, resuspended (in 5-mL fresh carbon-free MSM) and injected into 160-mL serum bottles containing 45 mL MSM. Substrates were either added immediately or after 24 hours of carbon starvation. CYHX-grown cells were fed with 1 mM CYHX as a control, cDCE only, or cDCE with 1 mM succinate. Approximately 2 μL of neat cDCE was injected into the 50-mL cultures that received cDCE.

A similar amount of cDCE was injected to two 160-mL serum bottles containing succinate-grown cells in 50 mL MSM. Then, 1 mM succinate was added to one of the bottles and none to the other. Concurrently, other aliquots of succinate-grown cells in 50 mL MSM were also fed with 0.2 mM CYHX and 26 μmol/bottle cDCE (520 μM nominal concentration). All experiments were conducted in duplicate. All culture bottles were shaken inverted at 160 rpm and incubated aerobically at 23°C.

3.10 iTRAQ

3.10.1 Protein extraction.

Both WT and KO strains were grown in 2 mM CAP, with or without cDCE (52 μmol/bottle = 520 μM nominal concentration) in 100-mL MSM. The utilization of the substrates by both strains was monitored using gas chromatography as previously described. The cultures were harvested when the cells were actively degrading cDCE and/or CAP. The cells were centrifuged and washed with phosphate buffer once. The pellets were then resuspended in 20 mM phosphate buffer (pH 7.5), and these cells were French-pressed at 20,000 psi. In between pressings, the French-press cell was rinsed with distilled water thrice, 70% ethanol once, and distilled water thrice. The French-press cell and the lysates were kept cold at 4°C. Small amounts of WT and KO pellets were kept at -80°C for later RNA extractions. Subsequent procedures (i.e. protein quantitation, digestion, iTRAQ labeling, fractionation, chromatography, spectrometry and data processing) were performed by James McCardle, Wei Chen and Sheng Zhang at The Proteomics and Mass Spectrometry Core Facility, Cornell University. Details of the procedures are included in Appendix C.

3.10.2 Reverse transcription polymerase chain reaction (RT-PCR)

10 mL of WT and KO cultures from the iTRAQ studies were harvested and total RNA was extracted using the Qiagen Allprep RNA/DNA Mini Kit and treated twice with RNase-free DNase I (Qiagen and Promega). Extracted total RNAs were measured and checked for DNA contamination using an Agilent RNA Nano chip analyzed in an Agilent 2100 Bioanalyzer.

100 ng of RNA was used as a template for the reverse transcription reaction. The first strand of complementary DNA (cDNA) was primed using a cocktail of gene-specific primers (2 pmol/primer, 8 primers total). A two-step RT-PCR protocol was used: a mixture of RNA template and primers was incubated at 65°C for 5 min and then chilled on ice. Reverse transcriptase and its provided buffer (Bio-rad iScript) were mixed into the previous contents and mixed, centrifuged and incubated at 42°C for 60 min. The reaction was terminated by incubation at 85°C for 5 min. The concentrations of synthesized cDNAs were measured and checked for purity using a NanoDrop 2000C (Thermo Scientific). For RT-PCR, 300 ng of cDNA was used as template with RT-PCR primers listed in Table 3.1. Melting temperature used for the PCR reaction was 60°C, and the reaction was conducted using 30 or 35 cycles.

CHAPTER 4

4. RESULTS

4.1 Disruption of the *chmo* gene in JS666

The role of CHMO in JS666 was studied through disruption of the *chmo* gene. Plasmid pVIK110 with an internal fragment of the *chmo* gene was used to create translational fusion as a consequence of integration of the entire plasmid into the target gene (Figure 4.1) (Kalogeraki and Winans, 1997). PCR was used to confirm that the transconjugants contained an insert at the designated location and the resulting amplicons were sequenced (Appendix A and Figure 4.2).

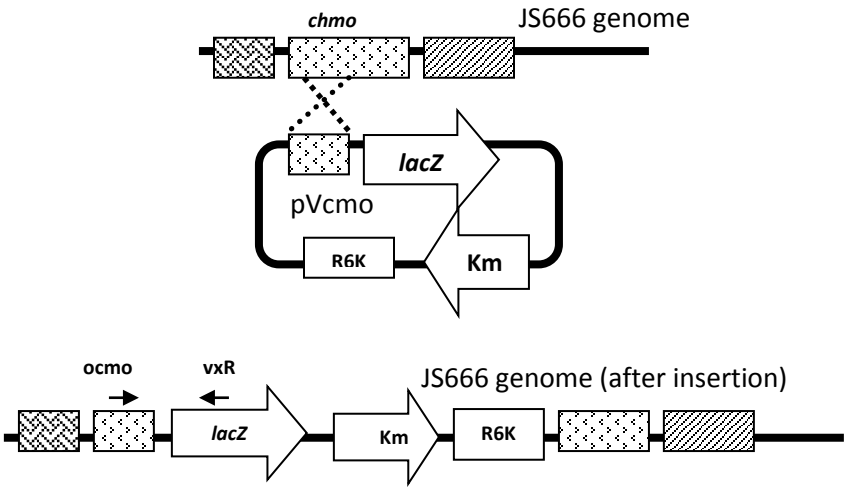

Figure 4.1. Suicide vector was integrated into the genome of JS666 through homologous recombination. Primers ocmo and vxR were used to confirm the integration of the plasmid into the genome at the designated location. Km is kanamycin resistance gene. R6K is the origin of replication. The resulting protein is a CHMO-LacZ fusion.

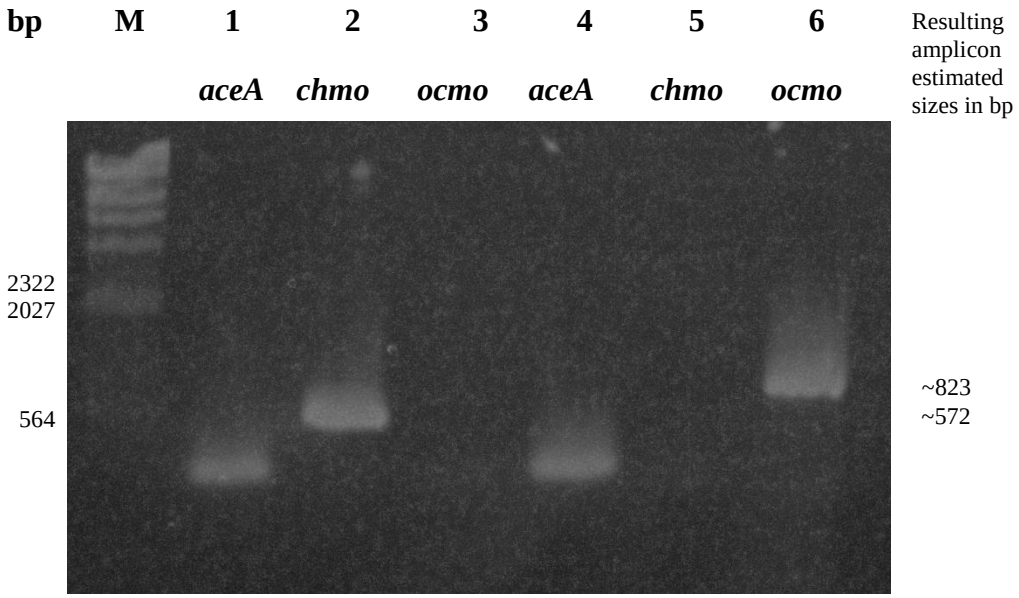

Figure 4.2. Example of PCR on WT and KO strains using three different primer pairs: isoF-isoR pair, which targets a JS666-specific sequence in the gene encoding isocitrate lyase (*aceA*); RTcmoF-RTcmoR pair, which targets sequences upstream and downstream of the location of the insert within the *chmo* gene; and ocmoF-vxR pair, which targets a part of *chmo* gene (upstream from sequence of VcmoF) and *lacZ* gene of the suicide vector. M: Lambda DNA/HindIII marker; Lane 1-3: WT; and Lane 4-6: KO; bp: base-pairs.

Preliminary results indicated that a portion of the *chmo* gene downstream of the insertion point was transcribed in the KO strain (Giddings, 2010) (primers for the *chmo* gene were initially designed to target a sequence that is downstream from the insert; cDNA corresponding to transcripts from this downstream region were detected with these primers). Then, the KO cultures were plated on ¼-TSA plates and several colonies were randomly chosen and PCR-assayed using the ocmoF-vxR primer pair. The results were positive (results not shown).

An attempt to produce a *chmo*-complementary strain from the KO strain was also successful (results not shown). A complete *chmo* gene was cloned into a high-copy number vector (pJB866) containing a tetracycline-resistance gene. The construct was transformed into the KO strain using a conjugation method similar to that used to produce the KO strain. Colony PCR was used to confirm the transformation. Transfers from these colonies, however, were capable only of growing on TSB; several attempts to culture them on MSM with succinate were unsuccessful. Overproduction of CHMO, usage of multiple antibiotics (kanamycin and tetracycline), and additional high-copy number of the large plasmid (9 kbp) may have affected the fitness of the complementary strain (Smith and Bidochka, 1998).

4.2 The growth of WT and KO strains on different substrates.

The primary purpose of this set of experiments was to ascertain what metabolic capabilities – if any – had been lost in the KO strain, versus the WT strain. Additionally, we hoped: (i) to determine which growth co-substrates might best induce cDCE-degradation; (ii) to investigate the inhibitory effects of cDCE on bacterial growth; and (iii) to determine the extent to which cDCE *degradation* (producing potentially toxic metabolites) matters to observed cDCE toxicity, versus the mere *presence* of cDCE.

Both WT and KO cells were first grown in TSB with cDCE (1.3 μmol/bottle) before transferring into MSM with succinate, acetate, CYHX or EtOH – each with or without co-presence of cDCE. The WT cultures grew on all four substrates, and the KO cultures grew only on succinate or acetate. When WT and KO cultures were grown on

acetate, the presence of cDCE had virtually no effect. It did not impact bacterial growth by either strain, nor was cDCE degraded by either (Figure 4.3). While final cell densities were apparently highest in WT cultures at the higher cDCE level, the size of the error bars on those particular values makes impossible the drawing of any conclusion to that effect. In essence, both strain types behaved as though cDCE were irrelevant, when both were provided with – and growing on – acetate.

On the other hand, when cultures were growing on succinate, high concentrations of cDCE slowed down growth of both strains. At the higher concentration of cDCE (132 μmol/bottle), minimal growth was observed in WT or KO cultures provided with succinate (Figure 4.4). Unlike what was observed with acetate, the WT cultures provided with succinate did exhibit cDCE degradation at the lower cDCE level; however, it was not sustained with additional, added cDCE. This bottle exhibited the "bad behavior" with respect to cDCE degradation so often observed with JS666. The observation with succinate-grown WT cultures indicates that high concentrations of cDCE (and/or possibly the presence of cDCE metabolites produced from cDCE oxidation) inhibit growth, although succinate was supplemented in excess (10 mM). We currently have no sure explanation for the lack of cDCE toxicity in acetate-fed cultures, versus the obvious toxicity observed in succinate-fed cultures. Since cDCE was transformed in succinate-fed WT cultures at the lower cDCE level, it might also have been partially transformed in them at the higher cDCE level – at least to an extent that toxic metabolites resulted. However, we have never seen any evidence of cDCE transformation by the KO strain, although it is possible that the KO strain partially metabolizes cDCE to a highly inhibitory intermediate (e.g., an epoxide) that accumulates, yet does not represent a

significant loss of the fed level of cDCE. This could occur, for example, if genes involved in steps other than the initial step of cDCE degradation were adversely affected in the KO strain. It is also possible that the explanation lies in some physiological difference between acetate and succinate metabolisms — possibly differences in their transmembrane transport mechanisms that could account for the observations, since high levels of cDCE would likely disrupt membrane function.

Neither CYHX nor EtOH could support growth by the KO strain (Figure 4.5 and Figure 4.6); nor was cDCE apparently degraded by the KO strain in these bottles. On the other hand, when WT cultures were provided with CYHX and EtOH as co-substrates, the cells relatively quickly exhibited cDCE degradation – and sustained it through multiple additions, even at the higher cDCE level (Figure 4.5 and Figure 4.6). (The apparent decrease in cDCE degradation rate in the EtOH-fed cultures with the lower cDCE level at later time-points is explainable by oxygen depletion).

WT cultures grown with co-presence of CAP started degrading cDCE after 6-8 days of incubation (Figure 4.7), whereas WT cultures that co-utilized EtOH or CYHX began using cDCE after only 1-2 days of incubation. The densities of the WT cultures grown on CAP were higher than those of EtOH or CYHX cultures when cDCE-degradation started. The WT cultures grown on CAP and cDCE showed higher final culture density than cultures grown on CAP only, suggesting that cDCE was utilized for bacterial growth (Figure 4.7). In KO cultures fed CAP, there was no cDCE degradation. Final densities in bottles fed CAP-only were similar in KO and WT cultures, but final densities were lower in the KO cultures in presence of cDCE than in absence of cDCE, suggesting conditions impeding bacterial growth. The final density for KO culture

amended with highest amount of cDCE was the lowest among the three, suggesting that high concentrations of cDCE may cause high stress to the cells. Again, since there was no evidence of cDCE transformation in the KO cultures, the observed inhibition of growth caused by cDCE is presumed not the result of inhibitory metabolites. However, it is difficult to rule such out, because enzymes other than CHMO might be capable of producing inhibitory levels of cDCE metabolites without resulting in a detectable fractional loss of the high, initial cDCE level. Still, there is no basis from these data to support such a hypothesis.

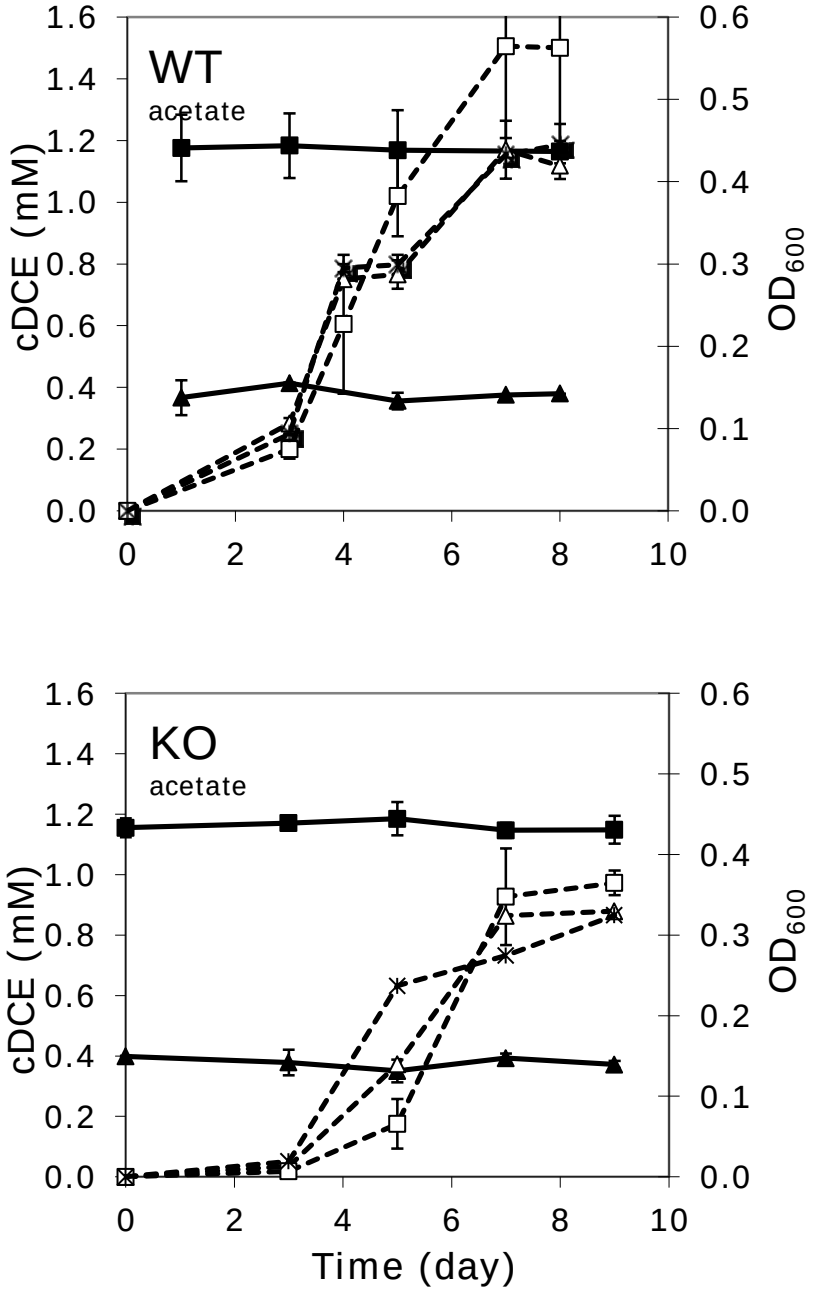

Figure 4.3. Growth of WT and KO strains on MSM and 10 mM acetate supplied with or without cDCE. Bars depict standard errors of experimental biological duplicates. Solid lines with closed markers are cDCE, and dotted lines with opened markers are OD_{600}. Cultures were supplied with 132 μmol/bottle cDCE (square markers), 52 μmol/bottle cDCE (triangle markers) or no cDCE (star markers).

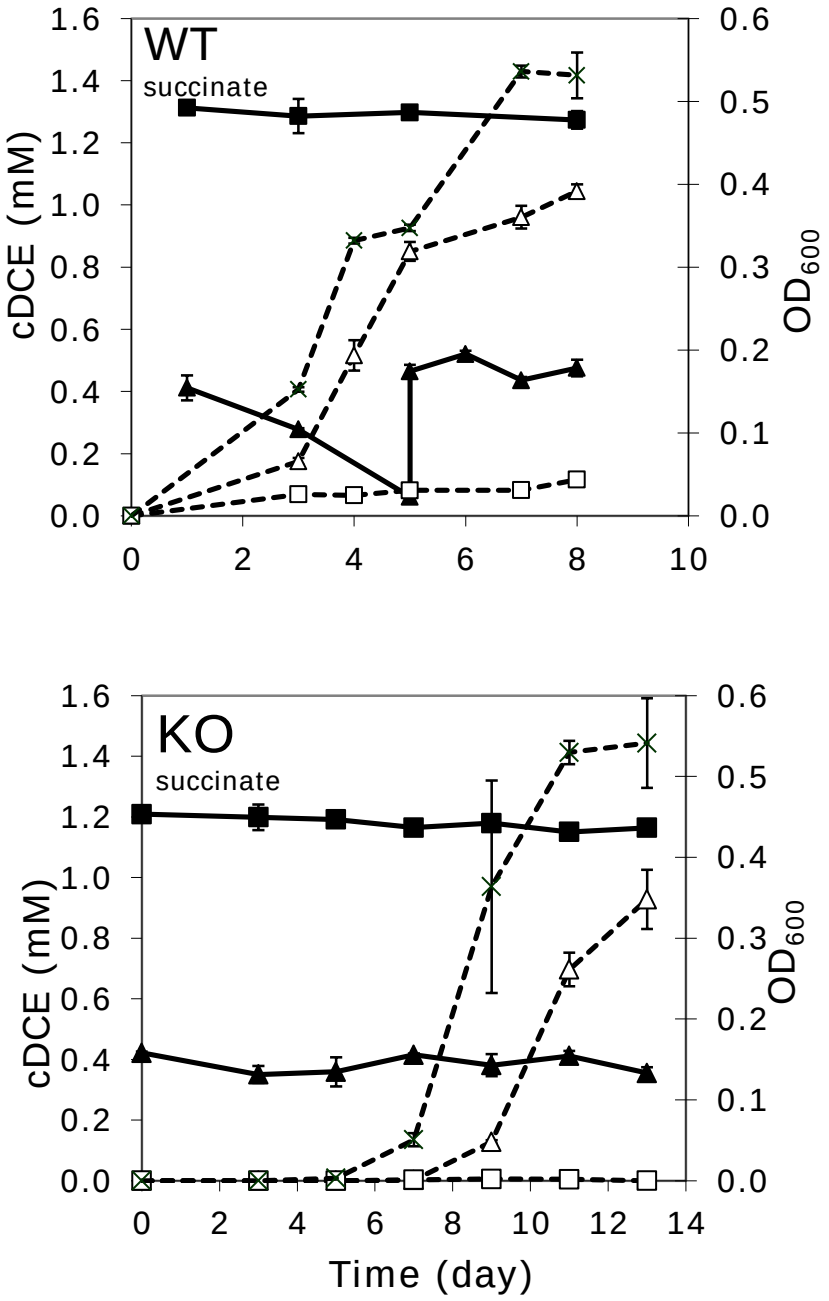

Figure 4.4. Growth of WT and KO strains on MSM and 10 mM succinate supplied with or without cDCE. Bars depict standard errors of experimental biological duplicates. Solid lines with closed markers are cDCE, and dotted lines with opened markers are OD_{600}. Cultures were supplied with 132 μmol/bottle cDCE (square markers), 52 μmol/bottle cDCE (triangle markers) or no cDCE (star markers).

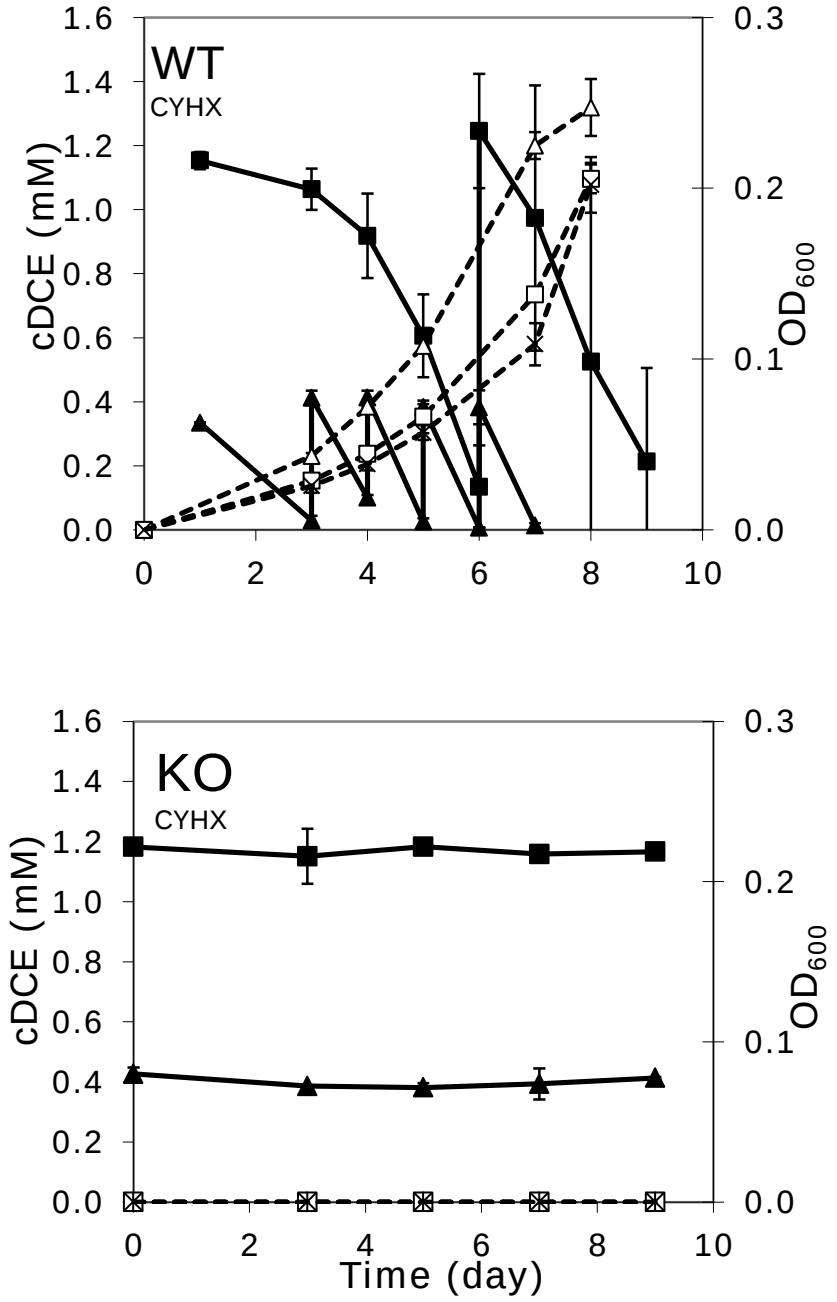

Figure 4.5. Growth of WT and KO strains on MSM and 1 mM CYHX supplied with or without cDCE. Bars depict standard errors of experimental biological duplicates. Solid lines with closed markers are cDCE, and dotted lines with opened markers are OD_{600}. Cultures were supplied with 132 μmol/bottle cDCE (square markers), 52 μmol/bottle cDCE (triangle markers) or no cDCE (star markers).

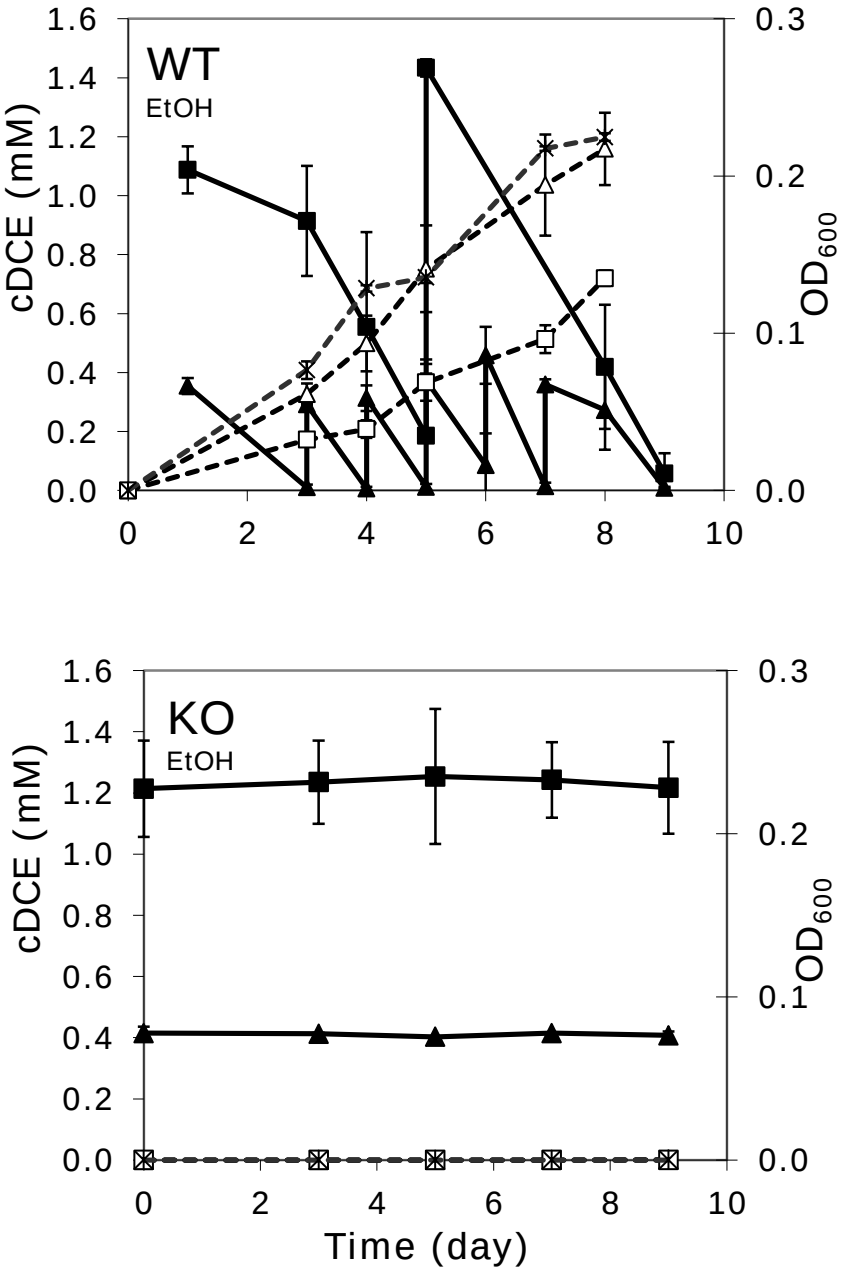

Figure 4.6. Growth of WT and KO strains on MSM and 10 mM EtOH supplied with or without cDCE. Bars depict standard errors of experimental biological duplicates. Solid lines with closed markers are cDCE, and dotted lines with opened markers are OD_{600}. Cultures were supplied with 132 μmol/bottle cDCE (square markers), 52 μmol/bottle cDCE (triangle markers) or no cDCE (star markers).

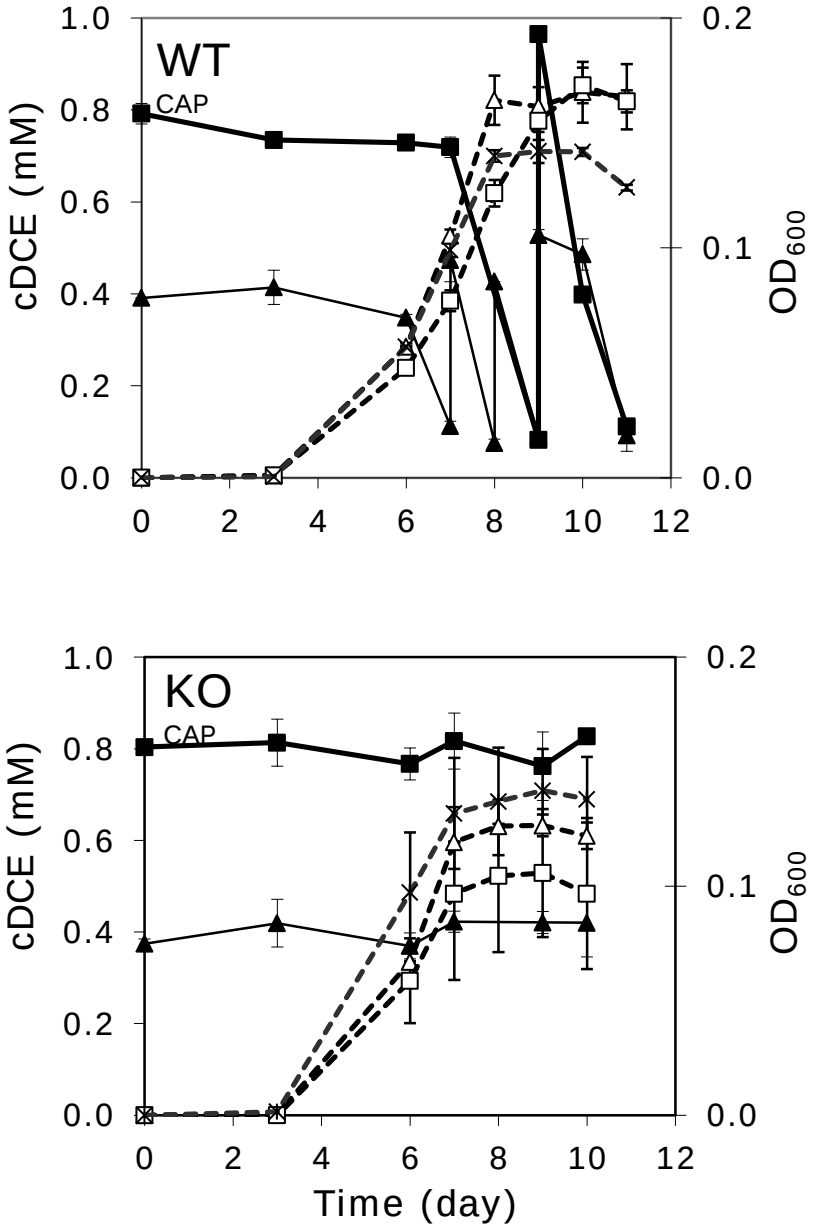

Figure 4.7. Growth of WT and KO strains on MSM and 1 mM CAP supplied with or without cDCE. Bars depict standard errors of experimental biological duplicates. Solid lines with closed markers are cDCE, and dotted lines with opened markers are OD_{600}. Cultures were supplied with 106 μmol/bottle cDCE (square markers), 52 μmol/bottle cDCE (triangle markers) or no cDCE (star markers).

WT and KO cultures were tested on their capabilities of growth on cyclohexanol (Figure 4.8). After a few days of incubation, the first measurements were taken, and the WT culture had produced 0.04 mM CYHX. After 10 days of further incubation, the production of CYHX by WT culture was almost doubled from the first reading and no formation of CYHX was observed in the KO bottle. The production of CAP in WT culture was not observed in the time frame of the experiment.

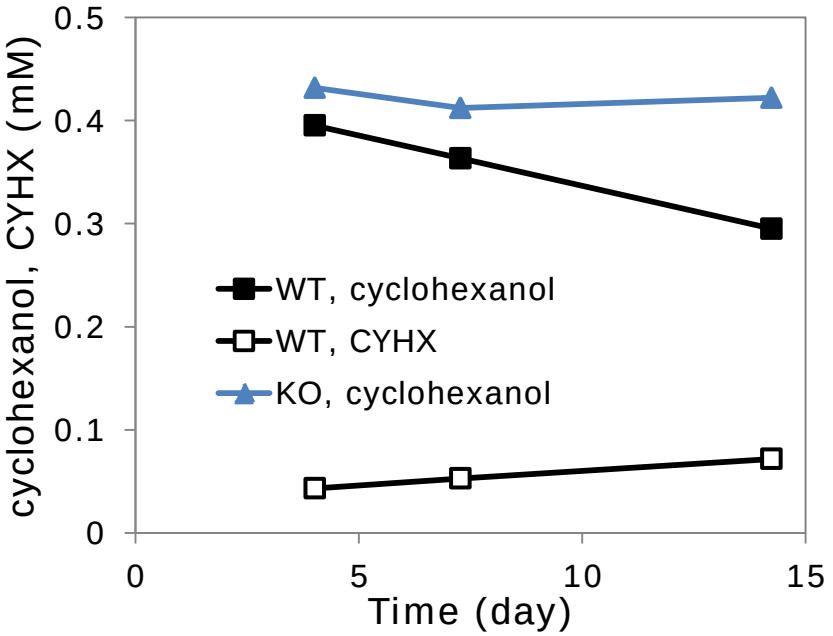

Figure 4.8. Preliminary results for WT and KO cultures tested with 0.5 mM cyclohexanol. Formation of CYHX was detected only in WT culture.

4.3 Transformation of other ethenes and of 1,2-dichloroethane.

One of many purposes of the knockout study was to determine whether inactivation of the *chmo* gene would affect the transformation of other ethenes and of DCA by strain JS666. Figure 4.9 shows the transformation of other substrates by WT culture that was previously grown on CAP (with cDCE present), then harvested, washed, and resuspended in MSM with the individual test substrates. At the beginning of the experiment, DCA was supplied at a nominal concentration of 160 μM, and the WT culture immediately transformed DCA. After two DCA supplements, a higher amount of DCA than the initial concentration was applied to the WT cultures. WT cells degrading DCA showed co-metabolic-like (slowed) phenotypical behavior after a total addition of approximately 75 μmol of DCA. VC was also readily degraded by WT cells. Almost 98.9% of VC supplied was transformed by WT cells in approximately 21 hours. With a second addition of VC, the VC-transforming rate steadily decreased (Figure 4.9).

Similar phenomena were observed in WT cultures transforming TCE or ethene. These 50-mL WT cultures reached their maximum transformation capacity after transforming 0.05 μmol of TCE and 2.4 μmol of ethene. The formation of epoxyethane was observed in ethene-fed bottles. The plateau may be due to formation of reactive metabolites, such as epoxides, chlorinated aldehydes and chlorinated acetates that may slow the degradation rates. KO cultures, in contrast, showed no ability to transform these compounds (Figure 4.9).

In previous studies in our laboratory, strain JS666 administered TCE or VC as sole substrates exhibited slow, declining rates of transformation, and the later addition of

cDCE improved their degradation (Liu, 2009). At low concentration levels of TCE, JS666 cultures provided with both TCE and cDCE demonstrated a competitive inhibition between the two substrates, but high levels of TCE have proven to be quite inhibitory. It is possible that the oxidation of TCE or VC can cause detrimental effects to the cells, and by adding a growth co-substrate (e.g. cDCE), cells are able to repair the damage, synthesize new cells, provide an energy source and supply a source of reducing agents. Providing JS666 with both DCA and cDCE also affects cDCE's maximum degradation rate, but only slightly affects degradation of DCA (Liu, 2009).

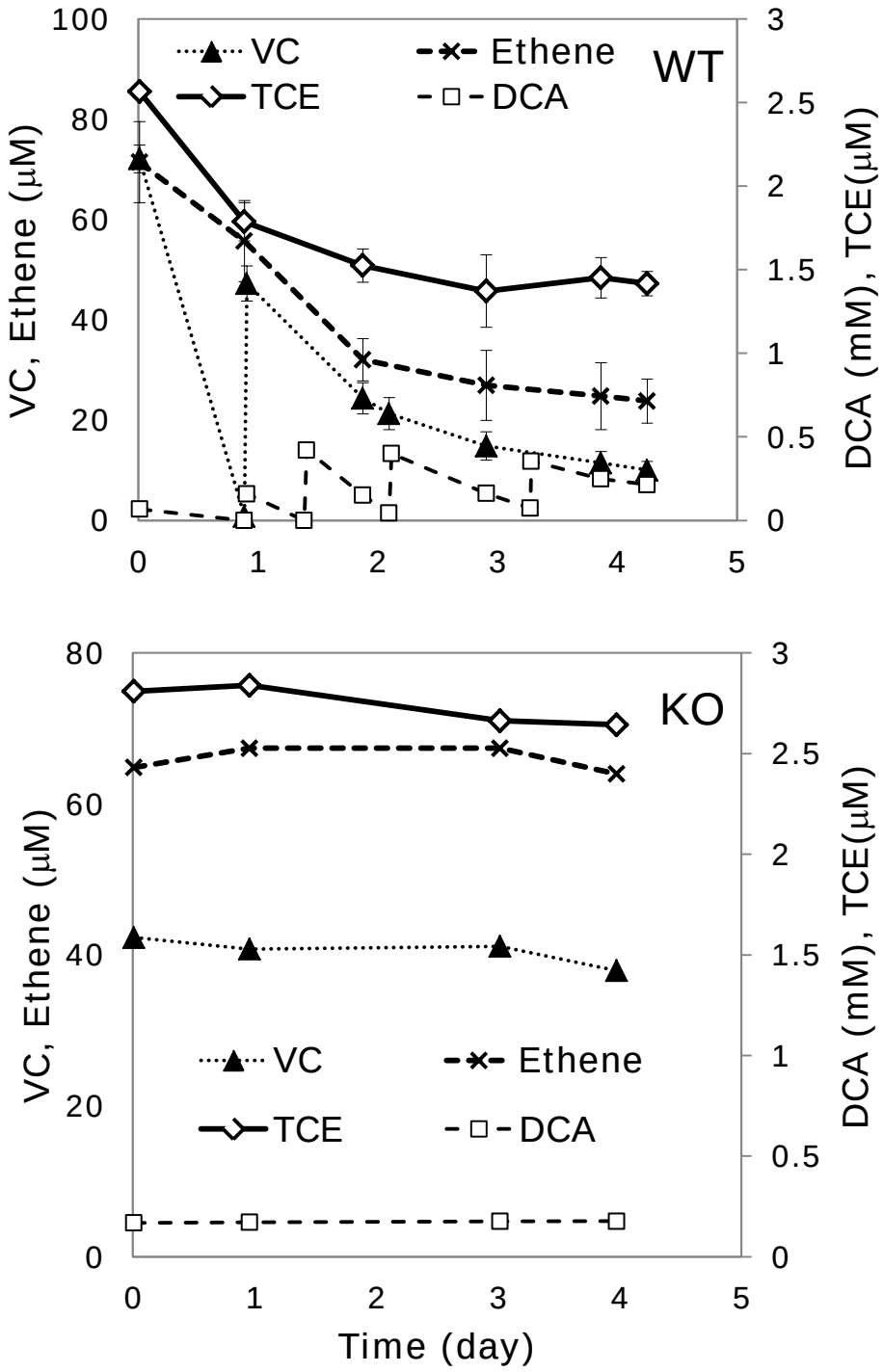

Figure 4.9. Transformation of other ethenes and of DCA by WT and KO cultures. Bars depict standard errors of experimental biological duplicates.

4.4 Cloning and characterization of the operon involved in cyclohexanol metabolism.

Four genes in the operon involved in cyclohexanol metabolism were cloned in IPTG-inducible plasmids as individual genes or in tandem. [Note: see earlier Figures 2.6 and 2.7 for relative positions of the genes in the operon.] The constructed plasmids in *E. coli* BL21 Star™ (DE3) cells contained *chnB* (p65, the monooxygenase), *chnC* (p66, the hydrolase), *chnD* (p63, a long-chain dehydrogenase), *chnCB* (p6566, the hydrolase and monooxygenase in tandem), or *chnAD* (p6364, the short- and long-chain dehydrogenases in tandem). Attempts to amplify the whole operon (approximately 5.0 kbp, including 414 bp upstream of *chnC*) at once using *Pfu* DNA polymerase were unsuccessful. This may be due to the uneven length and GC distribution of forward and reverse primers. Enzyme activities were all conducted in whole-cell *E. coli*. A summary of results from enzymatic assays is presented in Table 4.1, with detailed results following.

Table 4.1. Summary of substrates tested on different overexpressed enzymes. The study was conducted in whole-cell *E. coli.* (+) indicates an activity was observed, (++) indicates high activity was observed, (-) indicates no activity was observed and (0) both induced and uninduced cells transformed the substrate. N.T means not tested.

Clones [a]	p63R	p6364	p65R	p66H	p6566	P450 [b]	4478
cDCE	N.T.	N.T.	-	N.T.	-	++	N.T.
cDCE-epoxide	N.T.	N.T.	N.T.	-	-	N.T.	-
epoxyethane	N.T.	N.T.	N.T.	-	-	N.T.	-
cyclohexanol	+	+	N.T.	N.T.	N.T.	N.T.	N.T.
CYHX	N.T.	N.T	++	N.T	++	-	N.T.
CAP	N.T.	N.T.	N.T.	++	++	N.T.	N.T.
6-HHA	++	++	N.T.	N.T.	N.T.	N.T.	N.T.
glycolate	-	N.T	N.T.	N.T.	N.T.	N.T.	N.T.
styrene	N.T.	N.T.	-	N.T.	-	N.T.	N.T.
styrene oxide	N.T.	N.T.	N.T.	-	-	N.T.	N.T.
DCET	-	N.T	-	N.T	N.T	N.T	N.T
EtOH	+	+	N.T.	N.T.	N.T.	N.T.	N.T.
acetaldehyde	0	0	N.T.	N.T.	N.T.	N.T.	N.T.
DCAL	+	N.T.	0	N.T.	N.T.	N.T.	N.T.

[a] p63R = alcohol dehydrogenase (Bpro_5563); p6364 = alcohol and short-chain dehydrogenases (Bpro_5563 and Bpro_5564); p65R = CHMO (Bpro_5565); p6566 = CHMO and hydrolase (Bpro_5565 and Bpro_5566); P450 = cytochrome P450 and its adjacent genes (Bpro_5299 – Bpro_5301); 4478 = hydrolase (Bpro_4478, another hydrolase outside the cyclohexanol operon). Position of genes in the cyclohexanol operon in the direction of transcription: hydrolase, CHMO, short-chain dehydrogenase and alcohol dehydrogenase (Figure 2.7).

[b] All of these constructs were transformed into *E. coli* BL21 Star (DE3), except P450, which is transformed into *E. coli* Rosetta2 (DE3)

4.4.1 CHMO enzymatic assay

In this experiment, CHMO (or ChnB) utilized CYHX after 12 hours with production of CAP (Figure 4.10). In *E. coli* p6566, CYHX was completely transformed, and the lack of CAP accumulation suggests it was immediately hydrolyzed by hydrolase (ChnC). In a separate experiment, CAP was delivered to *E. coli* p6566 and was completely utilized (presumably by ChnC) within several hours (Figure 4.10). There was no activity on cDCE in strains containing ChnB (p65) or ChnC-ChnB (p6566), confirming the study by another research group (Alexander, 2010). CHMO was also tested on styrene (data not shown), and no production of styrene oxide was observed. Thus, while we successfully demonstrated that we had cloned a functional CHMO, it simply did not show activity on cDCE.

An aldehyde is another possible substrate for CHMO, and perhaps this explains the upregulation of *chmo* by cDCE in JS666. DCAL was reported as one of the major oxidation products of P450 (Shin, 2010), and it is possible that DCAL could be converted into DCAA by CHMO. A whole-cell assay was conducted to test this hypothesis; however, interpretation of results was complicated by the transformation of DCAL to DCET by *E. coli* controls, whereas the goal of this assay was to see the formation of DCAA from DCAL. In a separate assay (data not shown), *E. coli* p65R cells were tested with CYHX and DCAL. In induced *E. coli* p65R cells, the conversion of DCAL to DCET was rapid (up to 70% conversion after 7 hours when CYHX conversion to CAP was only 25%. Formation of DCAA from DCAL in the *E. coli* cells harboring CHMO was not observed.

In the usual whole-cell enzymatic assays, the test substrate is added after the cells

(induced or uninduced) are harvested, washed and suspended in buffer solution. However, in this *chmo* assay, the test substrate was added immediately after IPTG-induction in rich media. Attempts to obtain active CHMO through the usual enzymatic assay were unsuccessful.

4.4.2 Hydrolases

Lactone hydrolase catalyzes breakage of the C-O bond, forming hydroxyl acid. A putative hydrolase (Bpro_5566 or ChnC) was postulated to break the C-O bond of CAP, forming 6-HHA. In a separate experiment to that described above, hydrolase activities were assayed by conducting whole-cell experiments. *E. coli* cells harboring p66h (hydrolase) were assayed with 2 mM of CAP, and the disappearance of the substrate was recorded (Figure 4.11). The induced cells completely utilized CAP within 16 hours of incubation (and perhaps even much earlier, as the CAP was completely depleted by the time of first measurement after the experiment was initiated). The slight reduction of CAP in uninduced cells may due to the leaky T7-promoter of the *E. coli* (DE3) cells after incubating the cells to stationary phase. The pET vector system (Novagen, Inc.), which is used in numerous protein expression studies, including our study, is a powerful expression tool. Even in the absence of IPTG, detectable levels of targeted protein production were observed due to leaky T7-promoter (Novy and Morris, 2001). Novagen has recommended the addition of 0.5 – 1.0 % glucose to the growth medium for host strains containing pET plasmid constructs to reduce basal expression of the proteins (Novy and Morris, 2001).

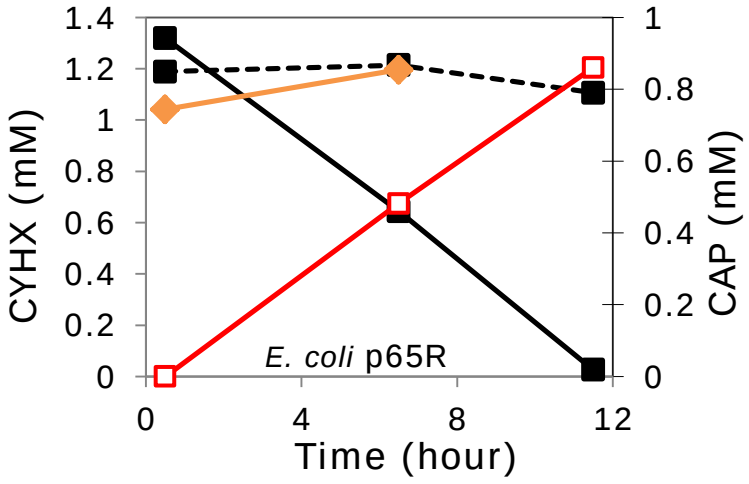

(a)

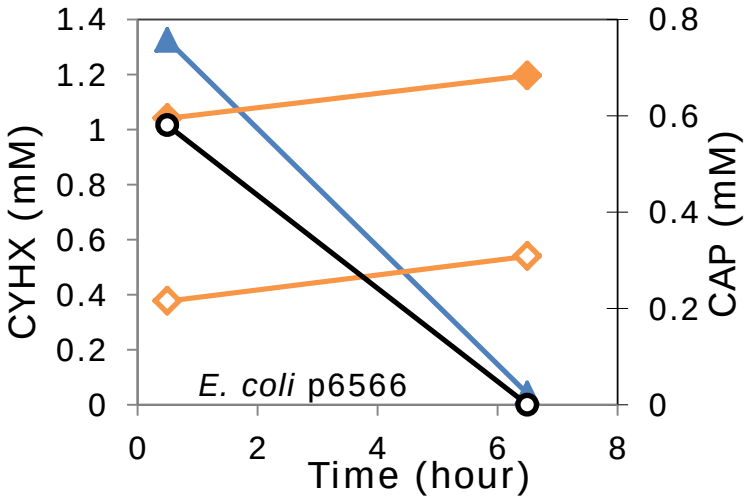

(b)

Figure 4.10. Transformation of CYHX and CAP by whole-cell *E. coli* p65R (CHMO) or p6566 (hydrolase and CHMO in tandem). (a) The induced *E. coli* p65 cells were given CYHX (—■—) and formation of CAP (—□—) was monitored. Uninduced *E. coli* p65 cells tested with CYHX were used as control (- -■- -). (b) The induced *E. coli* p6566 cells were given CYHX (—▲—) or CAP (—○—). Induced *E. coli* BL21 cells containing no plasmid were given CYHX (—◆—) or CAP (—◇—) as negative control.

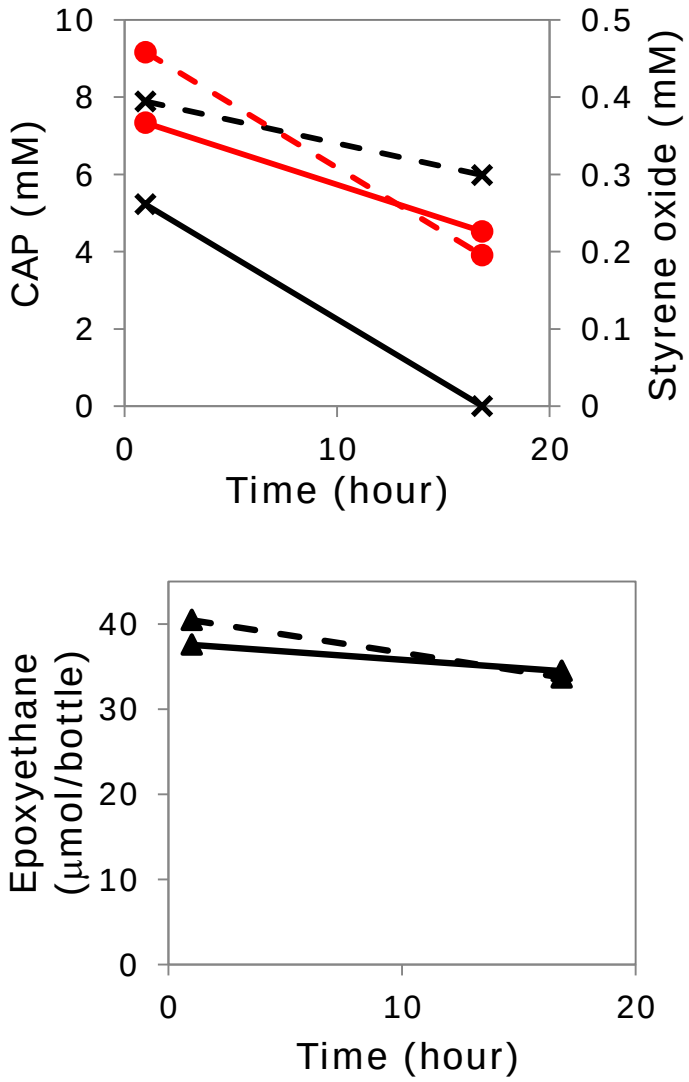

Figure 4.11. *E. coli* p66h (hydrolase) cells subjected to different substrates and conditions: CAP, induced (—×—) and not induced (- -×- -); styrene oxide, induced (—●—) and not induced (- -●- -); epoxyethane, induced (—▲—) and not induced (- -▲- -).

Other substrates tested on *E. coli* expressing the hydrolase (p66H) were epoxyethane and styrene oxide (Figure 4.11), and chemically-synthesized cDCE-epoxide (Figure 4.12). Both cDCE-epoxide and epoxyethane were monitored by GC-FID

(headspace injection on packed column) and styrene oxide was monitored by GC-FID (Et_2O extract on megabore capillary column). In all of these cases, slight disappearances of all substrates were observed in both induced and uninduced *E. coli* cells (Figure 4.11 and Figure 4.12). Results from whole-cell assays of *E. coli* containing p6566 (hydrolase and monooxygenase, in tandem) with and without 0.1 mM IPTG-induction agreed with the results with that of hydrolase only. The significant disappearance of cDCE-epoxide in both cell cultures suggests an abiotic transformation of epoxides (Appendix B).

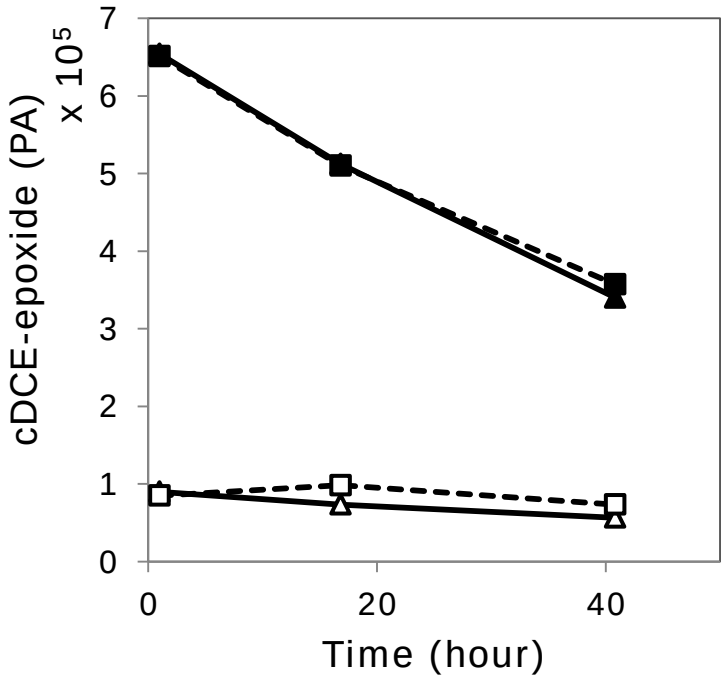

Figure 4.12. *E. coli* p66h (hydrolase) cells subjected to different conditions: cDCE-epoxide, induced (solid lines, triangle marker) and not induced (dotted lines, square marker). Closed symbols represent peaks at 2.8 min and opened symbols represent peaks at 3.5 min in raw peak-area (PA) units.

Another hydrolase from strain JS666 (Bpro_4478) has been reported to show dehalogenase activity on haloacetates (Chan et al., 2010) and was tested with chemically synthesized cDCE-epoxide. Preliminary results indicated that chloride was released in all of the cultures – whether this hydrolase was induced or not (Figure 4.13). High initial chloride background apparently resulted from the previous growth media (LB contains 10 g/L NaCl), even though the cells were washed once with phosphate buffer.

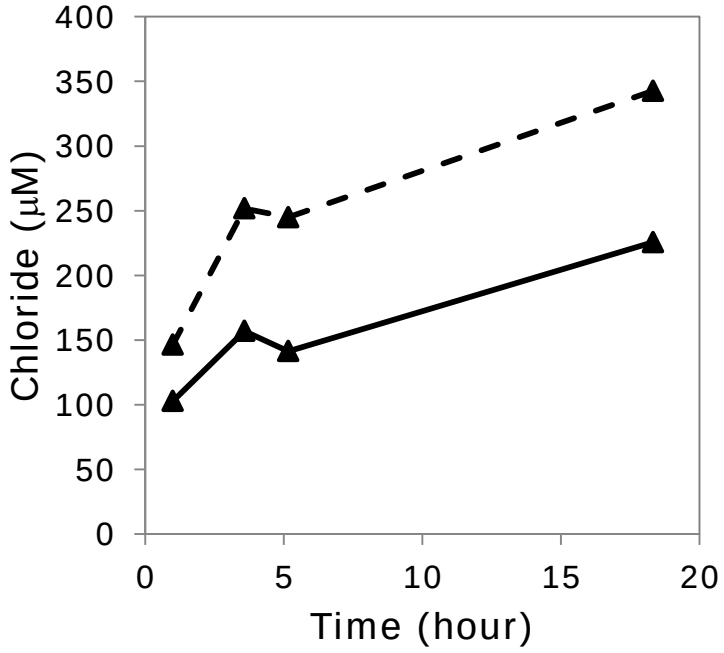

Figure 4.13. Preliminary results for whole-cell *E. coli* (containing Bpro_4478 gene, hydrolase) assay with chemically-synthesized cDCE-epoxide. Chloride ions were released in both IPTG-induced (—▲—) and uninduced cultures (- -▲- -). 1 mM (final concentration) succinate was added at 5-hour mark.

Further investigation showed no significant drop in the epoxide peaks even after 15 hours of incubation (Figure 4.14). The release of chloride from chemically-

synthesized cDCE-epoxide in phosphate buffer (pH 7.5) suggests that there was a significant, abiotic dechlorination of epoxide (Appendix B). Furthermore, the release of chloride cannot be proven to be from cDCE-epoxide alone. The resulting synthesis of epoxide by peracid may contain other chlorinated-organic byproducts other than chlorobenzoate that may interfere with the results (Ray et al., 2008). This work would have to be further explored with a purified, biologically synthesized epoxide (e.g., by *E. coli* containing p450 and its adjacent genes) and purified hydrolase (Shin, 2010).

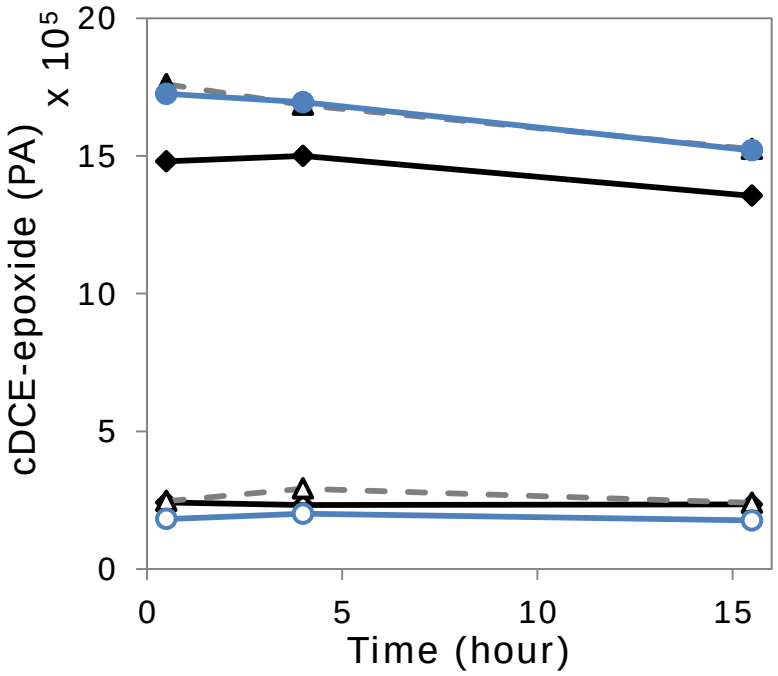

Figure 4.14. cDCE-epoxide GC peak areas at 2.8 min (closed symbols) and 3.5 min (opened symbols) versus time in raw peak-area (PA) units. *E. coli* cells overexpressing Bpro_4478 (hydrolase) were grown with induction with IPTG (diamond symbol, solid lines) and without induction (triangle symbols, dashed lines). A bottle with no cells was used as blank control (circle symbols, blue lines).

4.4.3 Dehydrogenases

Two dehydrogenases are located downstream of *chmo* transcription: a short-chain dehydrogenase (*chnA*, Bpro_5564) and a long-chain, putative alcohol dehydrogenase (*chnD*, Bpro_5563). ChnA shares 39% amino acid identity with cyclohexanol dehydrogenase, encoded by a *chnA* gene from *Acinetobacter* sp., which has been shown to catalyze the transformation of cyclohexanol to CYHX. ChnD shares 40% amino acid identity with 6-HHA dehydrogenase from strain 9871.

The dehydrogenase assays were conducted in *E. coli* whole-cells containing p6364 (the tandem of the two JS666 dehydrogenases) or p63R (the putative alcohol dehydrogenase) at 23°C. Test substrates included cyclohexanol, EtOH, acetaldehyde, 6-HHA, glycolate, DCAL and DCET. Cyclohexanol was degraded in *E. coli* cells containing either p6364 or p63R, with both strains transforming approximately 30% of cyclohexanol to CYHX after 2 days (Figure 4.15). No formation of CYHX was observed in uninduced cells and negative controls (induced and uninduced *E. coli* cells with no plasmids). The putative alcohol dehydrogenase gene (Bpro_5563) and the tandem of the two dehydrogenases genes (Bpro_5564 and Bpro_5563) were cloned into two different vectors (pET101D and pCOLADuet, respectively). It is probable that each clone produced a different amount of Bpro_5563 (ChnD). The activities of these two clones were the same, but the alcohol transformation rates between ChnA and ChnD may be different. The cloning of *chnA* (encodes ChnA, Bpro_5564), by itself, into pET vector was unsuccessful, so we do not have the opportunity to compare these enzymes individually. Thus, we cannot rule out the possibility that ChnA also contributed to transformation of the alcohols by the tandem clone.

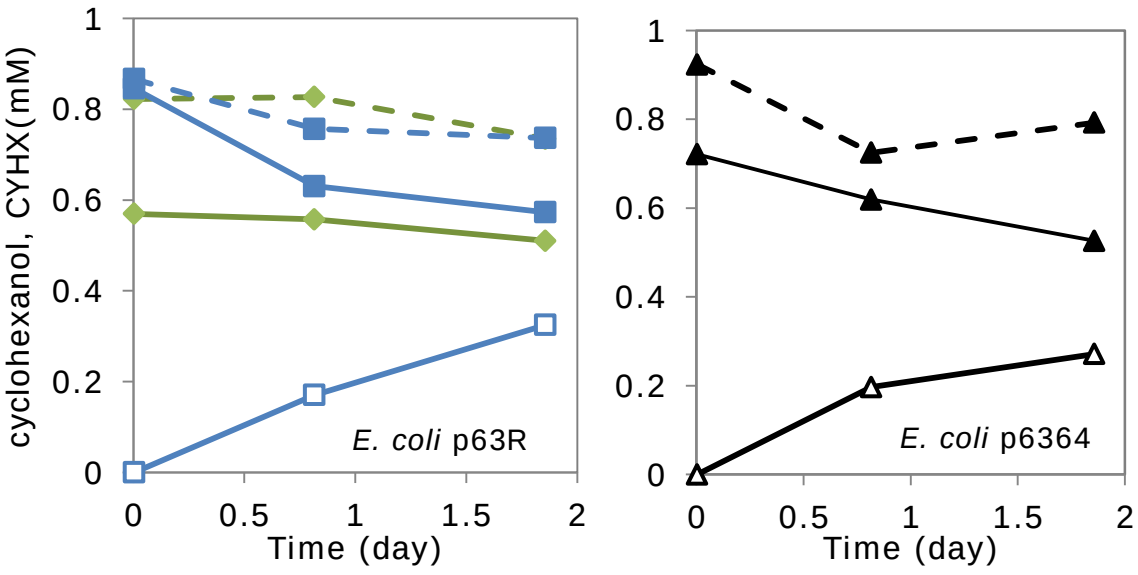

(a) (b)

Figure 4.15. Transformation of cyclohexanol to CYHX by *E. coli* strains containing either p63R (alcohol dehydrogenase) or p6364 (short-chain and alcohol dehydrogenases in tandem). (a) The induced (—■—) and uninduced (- -■- -) *E. coli* p63R cells were given cyclohexanol and the formation of CYHX by induced cells (—□—) was monitored. The induced (—◆—) and uninduced (- -◆- -) *E. coli* cells with no plasmid tested with cyclohexanol were used as negative control. (b) The induced *E. coli* p6364 cells were given cyclohexanol (—▲—) and formation of CYHX by induced cells (—△—) was monitored. Uninduced *E. coli* p6364 cells were used as control (- -▲- -).

6-HHA was also degraded by the induced *E. coli* cells containing either p63R or p6364 (Figure 4.16). After 20-hour incubation, only 12% and 8% of 6-HHA initial concentration remained in the *E. coli* cells cultures containing p63R and p6364, respectively. No degradation was observed in the uninduced cells and negative controls (*E. coli* with no plasmids). The product (i.e. 6-oxohexanoate) is not commercially available for chromatography peak identification and according to Brzostowicz and

coworkers (2002), 6-oxohexanoate was spontaneously oxidized to adipate. When all *E. coli* cultures were tested with glycolate (a hydroxy acid), no apparent degradation was observed (Figure 4.16).

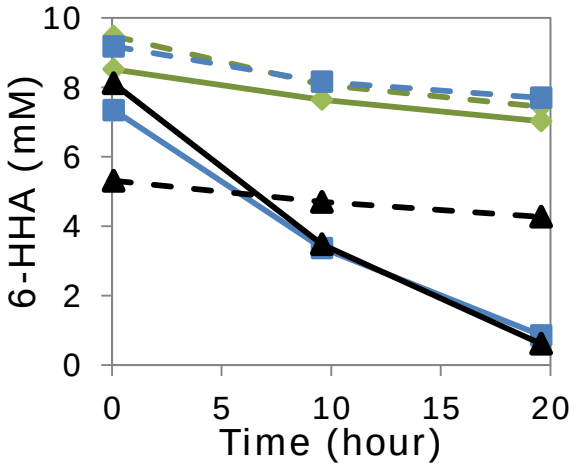

(a)

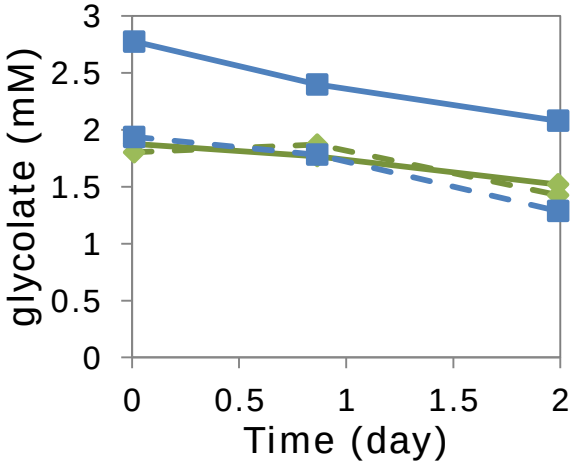

(b)

Figure 4.16. Enzymatic assays by whole-cell *E. coli* containing p63R (alcohol dehydrogenase) or p6364 (short-chain and alcohol dehydrogenases in tandem), tested with (a) 6-HHA and (b) glycolate. Blue lines and square symbols (■) represents *E. coli* p63R cells and black lines and triangle symbols (▲) represents *E. coli* p6364 cells. The IPTG-induced cells are represented by solid lines, and uninduced cells by dashed lines. IPTG-induced (—◆—) and uninduced (- -◆- -) *E. coli* BL21 cells were used as negative controls.

Alcohol dehydrogenases catalyze the interconversion of alcohol and aldehyde. *E. coli* cells containing p63R or p6364 were tested with EtOH or acetaldehyde. EtOH (approximately 10 mM) was assayed with these two dehydrogenases, with the production of acetaldehyde monitored. The cells were incubated with EtOH for approximately 10 hours and acetaldehyde was detected in all cultures (Figure 4.17). The induced cells containing p63R or p6364 produced higher amounts of acetaldehyde than the rest of the cell cultures. These induced *E. coli* p63R and p6364 cells produced 1.5 mM and 1.6 mM acetaldehyde, respectively, after 3 hours of incubation. The cultures were then left for an additional 6.5 hours, and the final concentration of acetaldehyde produced by *E. coli* p63R cells was 3.2 mM while with *E. coli* p6364, the production remained constant.

In acetaldehyde assays (approximately 10 mM), all *E. coli* cultures immediately reduced it to EtOH with no distinction between induced and uninduced cell cultures or the negative controls (Figure 4.18). Our results suggested that the enzymatic reaction has shifted more towards formation of EtOH until the equilibrium between EtOH and acetaldehyde has been reached. The addition of succinate may indirectly consume the NAD^+ pool in the cells causing the shift.

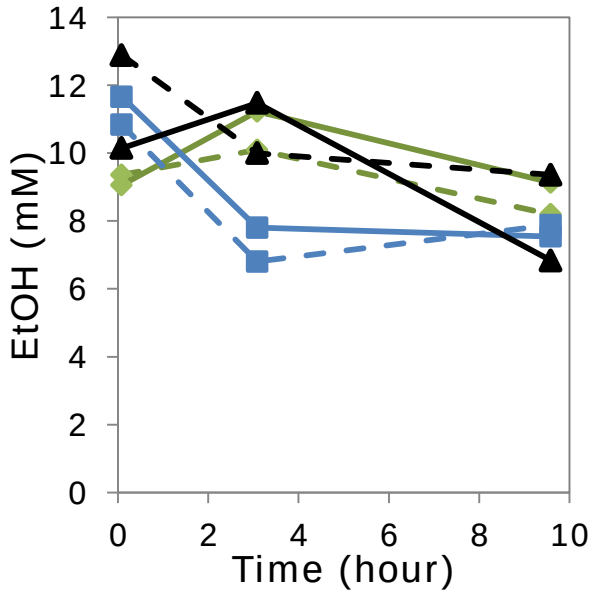

(a)

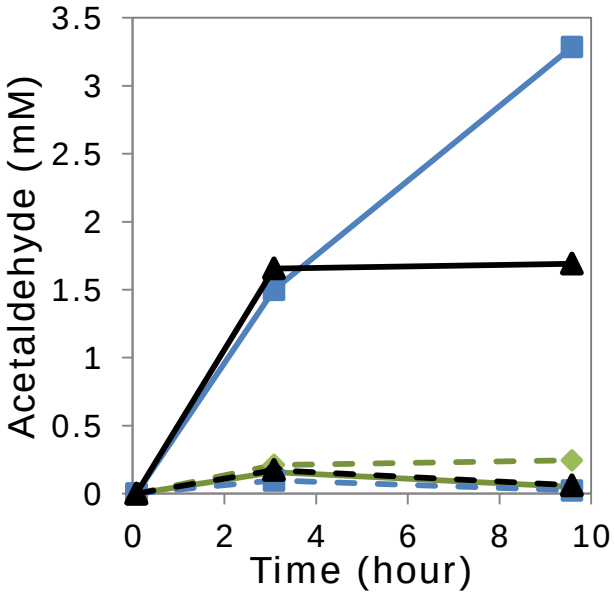

(b)

Figure 4.17. Production of acetaldehyde (b) in whole-cell *E. coli cultures* containing p63R (alcohol dehydrogenase) or p6364 (short-chain and alcohol dehydrogenases in tandem) that were assayed with EtOH (a). Blue lines and square symbols (■) represents *E. coli* p63R cells and black lines and triangle symbols (▲) represents *E. coli* p6364 cells. The IPTG-induced cells are represented by solid lines, and uninduced cells by dashed lines. IPTG-induced (—◆—) and uninduced (- -◆- -) *E. coli* BL21 cells were used as negative controls.

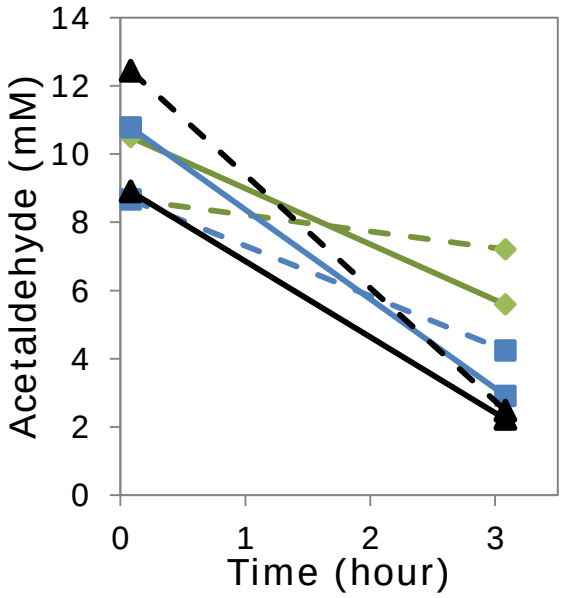

(a)

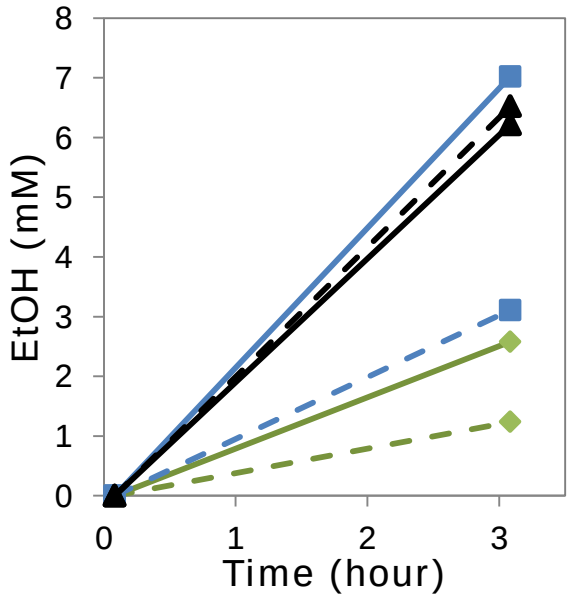

(b)

Figure 4.18. Production of EtOH (b) in whole-cell *E. coli cultures* containing p63R (alcohol dehydrogenase) or p6364 (short-chain and alcohol dehydrogenases in tandem) that were assayed with acetaldehyde (a). Blue lines and square symbols (■) represents *E. coli* p63R cells and black lines and triangle symbols (▲) represents *E. coli* p6364 cells. The IPTG-induced cells are represented by solid lines, and uninduced cells by dashed lines. IPTG-induced (—◆—) and uninduced (- -◆- -) *E. coli* BL21 cells were used as negative controls.

Transformation of DCAL to DCET was noticed in all cultures tested (Figure 4.19). *E. coli* p6364 cells were not tested with DCAL and DCET. Initial concentration of DCAL supplied to the induced *E. coli* p63R cells was 5.3 mM, and approximately 4.2 mM of DCET was measured after 20 hours of incubation. The loss of mass balance may be due to the inconsistent Et_2O extractions and different sensitivities of DCAL vs. DCET GC peaks. DCET gives a higher peak area than from the equivalent concentration of DCAL, thus making DCET easier to quantify at lower concentration. When the cells were assayed with DCET, the formation of DCAL was not observed. It could be that the kinetic equilibrium of the reversible dehydrogenase strongly favors the alcohol over the aldehyde, as was the case with acetaldehyde assays.

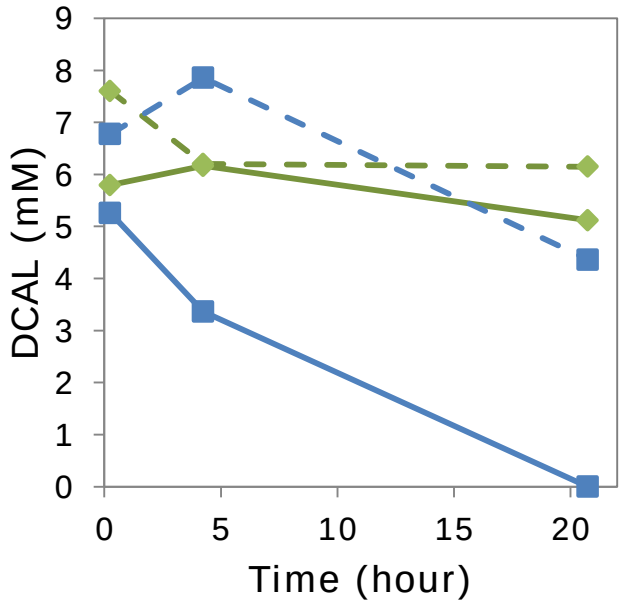

(a)

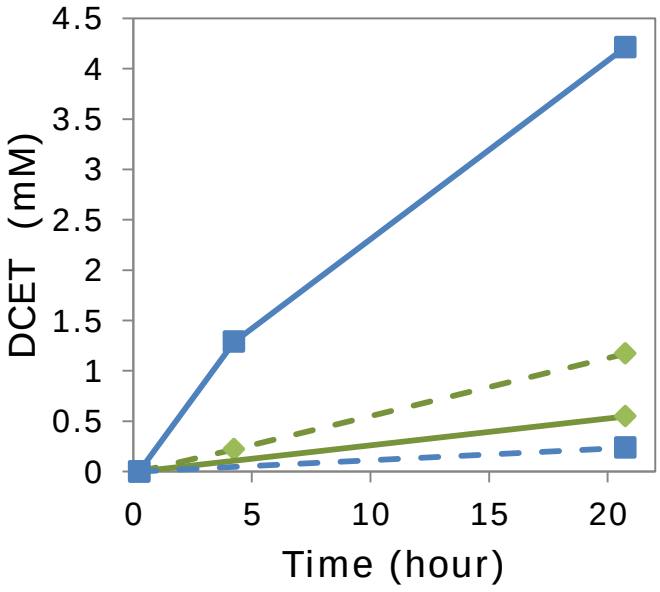

(b)

Figure 4.19. Transformation of DCAL (a) to DCET (b) in whole-cell *E. coli* containing p63R (alcohol dehydrogenase) that have been IPTG-induced (—■—) and not induced (- -■- -). IPTG-induced (—◆—) and uninduced (- -◆- -) *E. coli* BL21 cells were used as negative controls.

4.4.4 Cytochrome P450

P450 and its associated enzymes (ferredoxin and ferredoxin reductase) have been successfully cloned into *E. coli* and overexpressed (Shin, 2010). In our study, we monitored the concentration of chloride produced during P450 reaction with cDCE by the clone in whole-cell assays. A brownish phenotype was observed in induced cells as a result of excess formation of iron by ferredoxin (Bpro_5299) and ferredoxin reductase (Bpro_5300). 2-mL of headspace was drawn for cDCE measurement. The initial data-point for cDCE was calculated from known addition (its concentration was otherwise "over-range" with respect to the detector). Induced cells degraded 4.5 μmol of cDCE after 2 days and only 2.2 μmol of chloride was produced, when theoretically 9.0 μmol chloride should be produced from complete mineralization (Figure 4.20). The remaining balance was postulated to reside in accumulated, chlorine-containing intermediates (including the possible suicide complex postulated by Shin). When the same culture was incubated for 10 days, 2.6 μmol of chloride was measured after 4.6 μmol of cDCE degraded, still representing only 28% of the chlorine in the cDCE that had been degraded.

Formation of two DCE-epoxide peaks was observed early-on, with the first peak (at 2.8 min) smaller than the second peak (3.5 min). This is contrary to what was seen from the chemically-synthesized DCE-epoxide, which gave a much higher former peak than latter peak (Appendix B). Over more extended incubation, cDCE-epoxide was depleted, possibly accounting for most of the extra yield of chloride between Day 2 and Day 10. We do not have a suitable calibration for cDCE epoxide to determine the magnitude of the peak epoxide value accumulated early-on. However, if we assume that

the extra chloride observed between Days 2 and 10 all resulted from the epoxide that remained at the cessation of cDCE degradation (Day 2), then a rough estimation is that the peak epoxide level corresponded to a maximum of about 4% of the cumulative cDCE degraded. Of course, it is highly possible that other, non-epoxide involved pathways contributed to this latent chloride release.

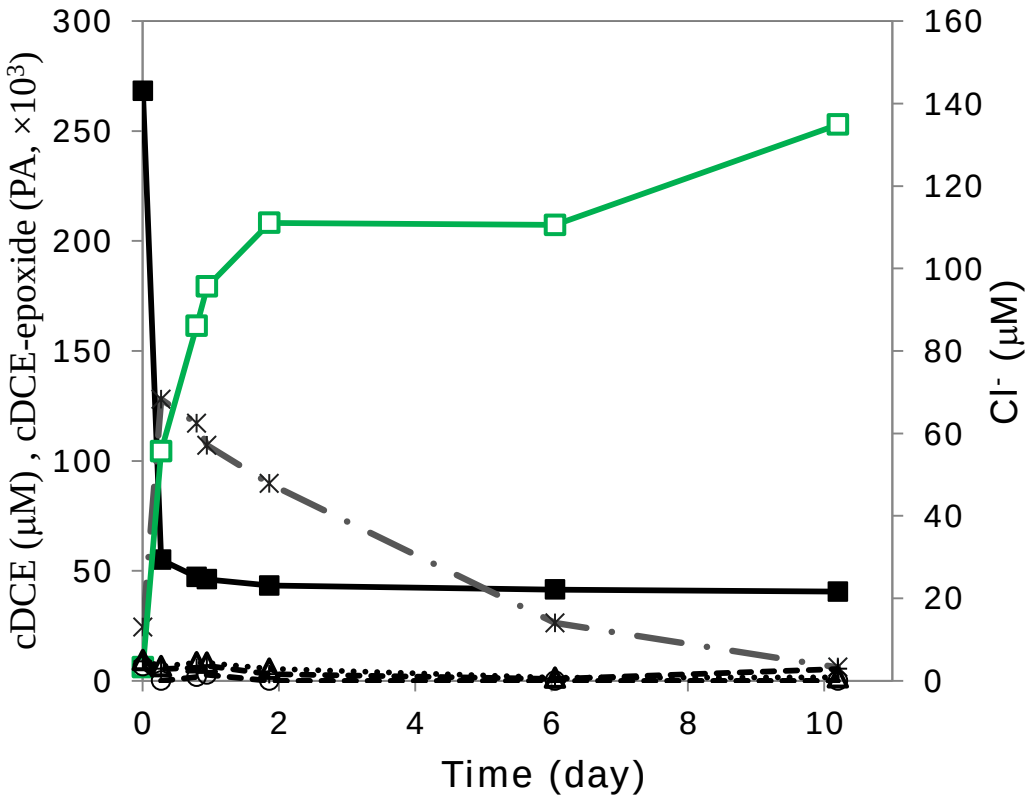

Figure 4.20. Epoxidation of cDCE by *E. coli* Rosetta2 (DE3) strain containing pJS597 (*p450*, ferredoxin and ferredoxin reductase). cDCE degradation (—■—) and chloride formation (—□—) were monitored in IPTG-induced cultures. Production of epoxide (3.5-min peak) is indicated by (· —✳— ·) in raw peak-area (PA) units and production of epoxide at 2.8 min is below the y-axis range. Chloride formation in uninduced cells was also monitored (—△—), as well as induced cells with no cDCE for background chloride release (—○—) and uninduced cells with no cDCE (—+—).

The formation of chloroacetate was monitored, but not detected (i.e. another postulated cDCE-degradation byproduct, from abiotic transformation of chloroacetyl chloride in water). Some of the missing mass of chloride may be due to formation of stable DCAL, which was not monitored in the experiment. The abiotic release of chloride was slow, considering that the cDCE conversion had essentially stopped within 2 days and chloride ions were still released for many days thereafter.

4.5 cDCE degradation by strain JS666 after a carbon-starvation period.

A lag period before cDCE degradation by strain JS666 has been observed previously when cultures have been grown to a high density on a non-cDCE substrate or after a period of cDCE starvation when previously grown on cDCE (Jennings et al., 2009; Giddings, 2012). In this study, the responses of strain JS666 to various environmental conditions were investigated. These included observations of the following: (i) lag in cDCE degradation after previous growth on various non-cDCE substrates; (ii) lag in cDCE degradation after previous growth on various non-cDCE substrates followed by 24-h starvation; and (iii) the possible benefits of co-presence of alternative substrate during subsequent exposure to cDCE after a period of starvation.

CYHX-grown cultures were harvested when the cells were actively degrading CYHX (at a concentration of 0.3 mM). After the cells were resuspended without starvation in 50 mL MSM and fed cDCE-only (26 μmol/bottle), they exhibited a variable lag period of 4-8 days before cDCE degradation commenced (Figure 4.21). CYHX in the control bottles was degraded immediately, which indicates that the cells were healthy –

i.e., the centrifugation, washing and resuspension steps did not interfere with the outcomes. Cultures that had been grown on CYHX, washed, resuspended, starved for 24 h, then given cDCE and 1 mM succinate also did not exhibit any significant lag leading to cDCE degradation (Figure 4.21).

Succinate-grown JS666 cells were harvested, washed and resuspended in 50 mL MSM (OD_{600} = 0.66). Without any intended starvation, cDCE (2 µL) was injected into the serum bottles under three different conditions of co-substrate (0.2 mM CYHX, 1 mM succinate, or none), and the degradation of cDCE was monitored. All cell cultures started to utilize cDCE after 15 days. Cultures that were given 0.2 mM CYHX degraded cDCE first, followed by cultures that were supplemented with succinate, and then by cultures that were given cDCE-only (Figure 4.22). Similar observations were made with succinate-grown cultures subjected to 24-hour carbon starvation. cDCE was degraded after 15 days in the cell cultures supplemented with CYHX or succinate, and required somewhat longer for cDCE degradation to begin when fed cDCE-only (Figure 4.22). Similar lag before cDCE-degradation was also observed in previously glycolate-grown cultures (Giddings, 2012).

These results, coupled with the observations of others (Jennings et al., 2009; Giddings, 2012), suggest that lag to cDCE degradation depends foremost upon what substrate the cells were grown in (cDCE or CYHX, versus succinate or glycolate), but also upon whether some readily degradable co-substrate is present during the lag period (perhaps to provide NADPH and/or energy and carbon for enzyme synthesis and repair). The 24-h starvation period was less important than was previous growth substrate or identity/presence of co-substrate during the subsequent lag period.

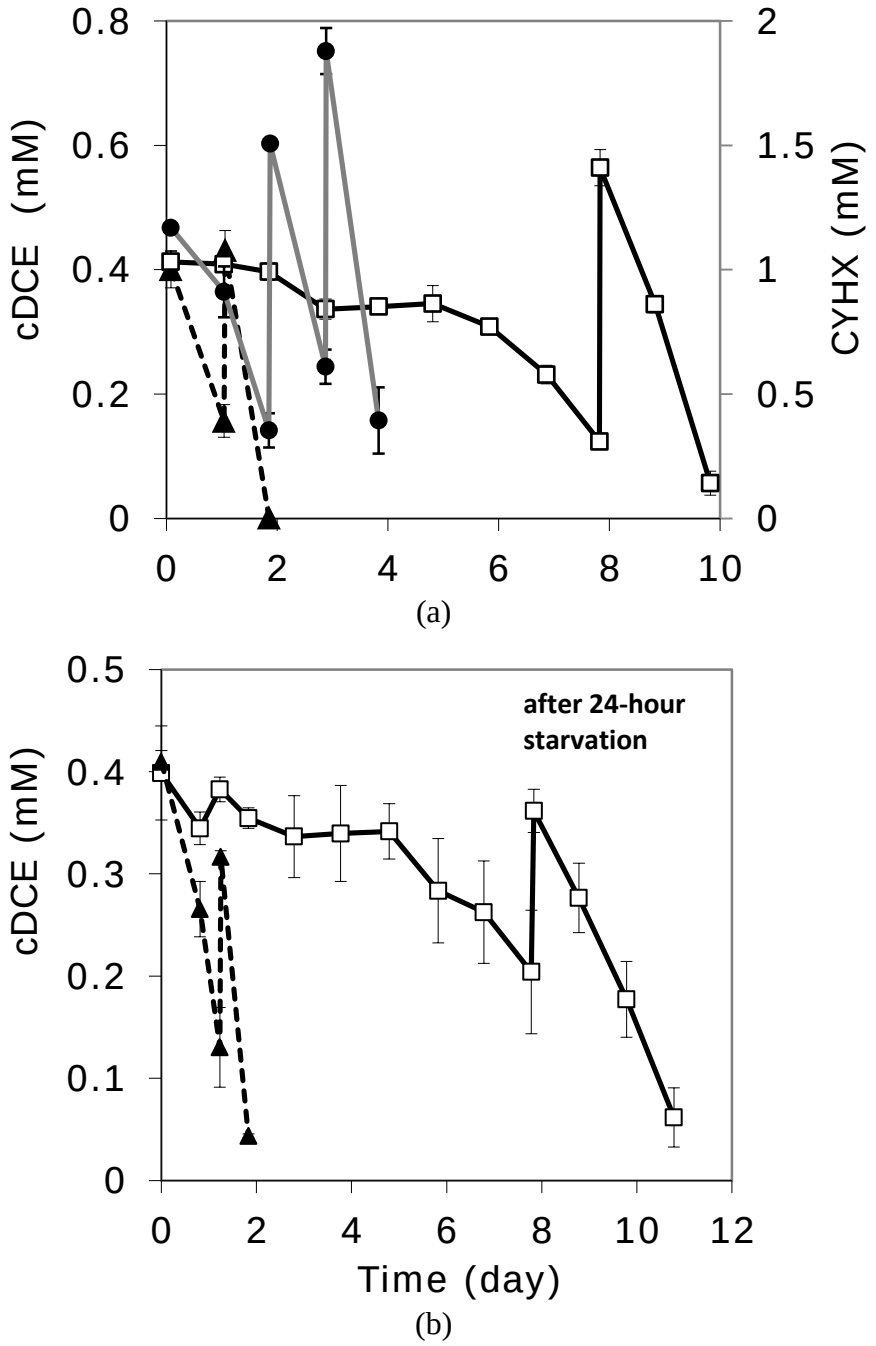

Figure 4.21. (a) The cDCE degradation by CYHX-grown JS666 cultures without carbon-source starvation and (b) after being subjected to 24-hour starvation. The resuspended cells were given 1 mM CYHX (—●—) as control, cDCE with 1 mM succinate (- -▲- -) or cDCE only (—□—). Bars indicate standard errors for biological duplicates.

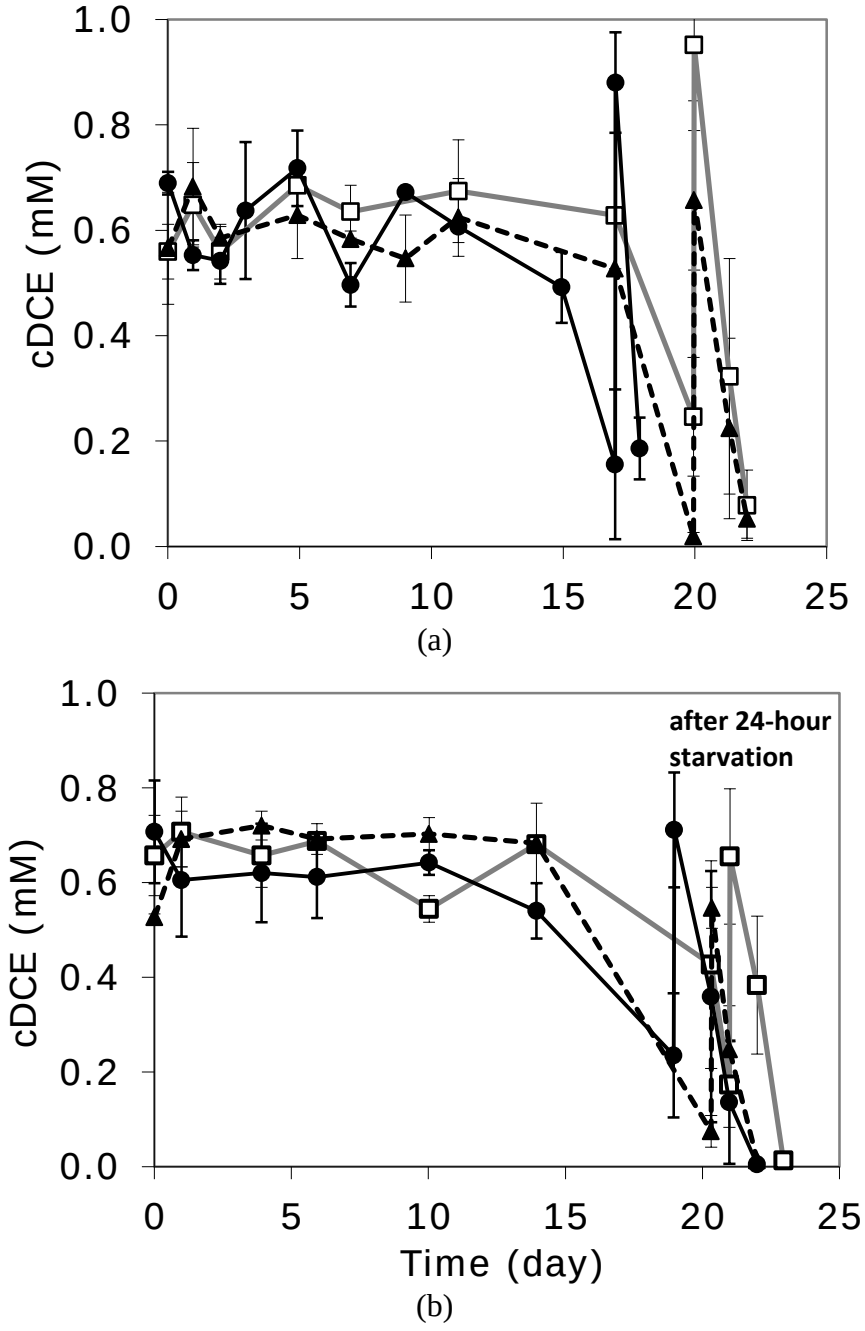

Figure 4.22. (a) The cDCE degradation by succinate-grown JS666 cultures without carbon-source starvation and (b) after being subjected to 24-hour starvation. The cells were given cDCE only (—□—), cDCE with 1 mM succinate (- -▲- -) or cDCE with 0.2 mM CYHX (—●—). Bars depict standard errors of experimental biological duplicates.

4.6 Proteome changes in both WT and KO cultures as assessed using iTRAQ

Both WT and KO cultures were grown in 2 mM CAP with the presence or absence of 52 μmol/bottle cDCE (520 μM nominal concentration). The concentrations of these compounds were monitored, and the cells were harvested when both of the cultures were actively degrading CAP and/or cDCE. CAP was chosen as secondary carbon source because both WT and KO strains can utilize it while allowing WT cells to sustain the "good" cDCE-degradation phenotypical behavior (Figure 4.7). KO cultures grown on CAP-only were highly active and immediately degraded CAP when it was supplied. During protein extraction, in order to minimize protein cross-contamination from WT to KO samples, WT cultures grown on CAP-only were French-pressed first, followed by WT on CAP and cDCE, KO on CAP-only, and KO on CAP and cDCE.

The samples were digested with trypsin, labeled individually with iTRAQ reagents, and analyzed simultaneously by LC-MS/MS. The peptides from the four culture-types were labeled with reporter groups as follows:

- 114.1 (WT on cDCE + CAP);
- 115.1 (WT on CAP only);
- 116.1 (KO on cDCE + CAP);
- 117.1 (KO on CAP only).

There were 1302 proteins identified based on 5627 peptides using the Mascot program for all four samples. More than 60% of the total proteome identified consisted of acidic proteins. Intensities of the reporter ions from iTRAQ tags upon fragmentation were used for quantification, and the relative quantitation ratios were normalized to the median ratio for the 4-plex in each set of experiments. The amounts of RNA polymerase (β subunit) were around the same throughout the four samples, inferring that the levels of housekeeping proteins, involved in the basic functioning of the cells, were similar (Table 4.2). 515 protein entries in the WT system were identified by only one peptide. These peptides were checked by Mascot software and were found not to have any immediate association with other proteins within the same proteome. Each protein ratio is assigned an error factor (EF), which allows calculation of its 95% confidence interval (CI). The lower limit of the 95% CI = protein ratio/EF; the upper limit of 95% CI = protein ratio*EF. In this iTRAQ report, a ratio of 115/114 that is less than one (WT cultures grown in CAP vs. grown in cDCE+CAP) implies protein whose presence is correlated to cDCE-degradation (or at least to its presence). Alternatively, one can examine the ratio of 116/114 (KO grown on cDCE+CAP vs. WT grown on cDCE+CAP) to attempt separation of the effects of mere presence of cDCE (in KO) from the effects of actual cDCE degradation (in WT).

The principal objective of the iTRAQ study was to determine whether the process of knocking out the *chmo* of JS666 had affected translation of adjacent genes. Can we assume that insertion of the vector sequence within *chmo* has affected only the production of CHMO protein? Results show that detectable levels of peptides from all

genes of the cyclohexanol operon were detected in both WT and KO strains, with the exception of the short-chain dehydrogenase (ChnA), which was not detected in any of the four culture samples (WT or KO). Five peptides associated with CHMO that are upstream and downstream of the plasmid insertion point were identified in KO cultures, and two of them yielded weak spectra or negative intensities. CHMO peptide fragments in the KO culture are not unexpected, since there is no stop codon at that point in the region to prevent transcription, though a functional CHMO should not result.

If we examine the genes adjacent to *chmo*, we see that abundances of peptides from the upstream hydrolase (Bpro_5566, ChnC) were reduced in KO cultures to 28% and 25% of abundances in corresponding WT cultures (i.e., iTRAQ ratios from labels 116/114 and 117/115). On the other hand, abundances of peptides encoded by *chmo* (Bpro_5565) were reduced in KO cultures to only 14% and 5% of abundances in corresponding WT cultures. Five peptides in KO samples were attributed the downstream alcohol dehydrogenase (Bpro_5563, ChnD). Abundances of peptides from ChnD were reduced in KO cultures to 10% and 18% of abundances in corresponding WT cultures. These relative levels suggest that translation of genes in the operon downstream of the insert were more affected than was translation of the adjacent, upstream hydrolase. While we do not have proteome data corresponding to the short-chain dehydrogenase (ChnA), its intermediate position between *chmo* and *chnD* would predict similar reduced abundance levels.

Table 4.2. Ratios of selected proteins identified in iTRAQ study.

Locus Tag	Protein Description	115/114	p[a]	EF[a]	116/114	p[a]	EF[a]	117/114	p[a]	EF[a]
Bpro_5301	P450	1.587	7	1.193*	0.180	7	1.524*	0.370	7	1.180*
Bpro_5566	hydrolase, ChnC	10.493	3	1.819*	0.282	3	1.653*	0.485	3	1.283*
Bpro_5565	CHMO, ChnB	2.994	9	[1.182]	0.140	6	[2.421]	0.148	7	1.371*
Bpro_5563	zinc-binding alcohol dehydrogenase, ChnD	0.770	5	1.104*	0.100	5	1.535*	0.139	5	1.319*
Bpro_5186	HAD, type II	0.155	12	[1.212]	0.142	12	1.160*	0.150	12	1.142*
Bpro_0056	HAD, type II	0.804	2	1.023*	0.651	2	1.007*	0.828	2	1.030
Bpro_2101	isocitrate lyase	2.494	9	[1.088]	2.114	9	1.075*	2.177	9	[1.102]
Bpro_0645	GST [b,c]	0.724	1	---	0.017	1	---	0.024	1	---
Bpro_0646	PNPox [b]	1.165	1	---	0.450	1	---	0.401	1	---
Bpro_4442	RNA polymerase subunit beta, RpoB	1.088	22	1.077*	0.949	22	1.090*	0.909	22	[1.088]
Bpro_0086	2,5-dioxopentanoate dehydrogenase NAD^+	0.738	3	1.022*	0.702	3	1.059*	0.654	3	1.234
Bpro_4478	hydrolase [b]	0.507	1	---	0.806	1	---	1.033	1	---
Bpro_4561	glyoxylate carboligase [b]	0.293	1	---	0.335	1	---	0.335	1	---
Bpro_4563	2-hydroxy-3-oxopropionate reductase	0.239	2	1.094*	0.051	5	3.652*	0.060	4	3.210*

[a] p = number of peptides associated with the protein; EF = error factor
[b] manual checking done with BLASTP
[c] MS/MS intensity peaks $\geq 10^4$
(*) indicates ratio that is significantly different from 1 at a 95% confidence level. Error factors with brackets [ ] indicate that the peptide match ratios do not appear to come from a sample with a normal distribution.

Since the KO strain is quite capable of growth on CAP, the approximately 70-75% reduction in abundance of the hydrolase (Bpro_5566, ChnC), which was shown in enzyme assays to be active on CAP, is either insufficient to cause deleterious effect on growth, or else there are other hydrolases in JS666 that serve this same purpose. On the other hand, the approximately 80-90% reduction in abundance of the alcohol dehydrogenase (Bpro_5563, ChnD) in the KO strain appears to exert a much greater effect, since the KO strain cannot grow on EtOH. Of course, peptide abundance does not tell the whole story; protein conformation matters, and the proteomics results do not address this potentially important factor. In the end, what we know for sure is that *chmo* was knocked out, and downstream translation of the alcohol dehydrogenase (and by deduction, the short-chain dehydrogenase also) was reduced.

Jennings et al. (2009) identified proteins elevated by cDCE (listed in Table 2.1), including GST-like protein (Bpro_0645), Type II HAD (Bpro_5186), 2-hydroxy 3-oxopropionate reductase (Bpro_4563) and glyoxylate carboligase (Bpro_4561). The authors also reported cDCE-induced transcripts, such as CHMO (Bpro_5565), hydrolase (Bpro_5566), P450 (Bpro_5301), ABC transporters and several hypothetical proteins (Table 2.2). Most noteworthy is the much higher abundance (i.e., low ratios 115/114, 116/114, and 117/114) of HAD (Bpro_5186) protein in WT cultures degrading cDCE than in any of the other cultures. HAD expression appears to correlate well with cDCE degradation and has been proposed as a marker for it in JS666 (Giddings, 2012).

Hydrolase (ChnC), which was demonstrated to have activity with CAP in our study, was highly reduced in WT cells degrading CAP+cDCE vs. WT cells degrading

CAP only. The WT cells supplied with both substrates utilized them concurrently while the WT cells supplied with CAP only, solely rely on CAP as the growth substrate. The reduction in hydrolase abundances in both KO cultures implies that the insert impacted the expressions of neighboring genes in the cyclohexanol operon. Alcohol dehydrogenase (ChnD) was also reported in lower abundances in KO strains than in both WT strains. There were higher levels of P450 peptides in cDCE-degrading WT cells than in both KO strains; however, levels were 60% higher in CAP-grown WT cultures. The lower abundance of P450 in cDCE-degrading cells, versus CAP-only WT cells may be due to inactivation of the protein as a result of covalent-binding of the cDCE-intermediates to the heme-containing proteins (Costa and Ivanetich, 1982).

The presumed presence of chlorinated alcohols and alkanals (aldehydes) resulting from cDCE degradation might be expected to affect the abundances of several alcohol and aldehyde dehydrogenases (Table 4.3). When comparing cDCE-degrading WT cultures and cDCE-exposed KO cells (116/114), a ratio that is less than 1 may infer that the protein expression levels were elevated by the presence of cDCE-metabolites and not just by cDCE only. Aldehyde dehydrogenases may be involved in the conversion of DCAL to DCAA (Sharpe and Carter, 1993) and based on our iTRAQ data, Bpro_3952 with 23 associated peptides is the primary candidate. Bpro_2298, which was modestly elevated in WT culture degrading cDCE+CAP vs. the rest of the cultures tested, shares 24% amino acid identity with ChnE from strain NCIMB9871, while Bpro_0086 (ChnE homolog) shares 51% (Figure 2.7). An aldehyde dehydrogenase in JS666 (Bpro_4570) has 77% identity with chloroacetaldehyde dehydrogenase of *Xanthobacter autotrophicus* GJ10, however this enzyme was not reported in our iTRAQ results.

Table 4.3. Ratios of aldehyde and alcohol dehydrogenases during cDCE metabolism.

Locus Tag	Protein Description	115/114	p[a]	EF[a]	116/114	p[a]	EF[a]	117/114	p[a]	EF[a]
Bpro_3952	**aldehyde dehydrogenase**	**0.385**	**23**	**1.081***	**0.055**	**22**	**1.380***	**0.081**	**23**	**1.228***
Bpro_2290	aldehyde dehydrogenase	1.141	6	1.046*	1.057	6	1.038*	1.061	6	1.061
Bpro_3422	aldehyde dehydrogenase	1.379	2	1.178	1.038	3	1.136	1.014	2	1.081
Bpro_4691	aldehyde dehydrogenase [b]	0.849	1	---	1.334	1	---	1.329	1	---
Bpro_2298	aldehyde dehydrogenase	0.824	2	1.036	0.828	2	1.481	0.854	2	1.387
Bpro_4702	aldehyde dehydrogenase	0.934	2	1.064	1.377	2	1.482	1.655	2	1.057*
Bpro_3129	zinc-binding alcohol dehydrogenase [b,c]	0.387	1	---	0.906	1	---	0.757	1	---
Bpro_2526	iron-containing alcohol dehydrogenase	0.546	3	1.178*	0.834	3	1.070*	1.081	3	1.074
Bpro_0360	zinc-binding alcohol dehydrogenase [b]	0.735	1	---	1.176	1	---	1.132	1	---
Bpro_5563	**zinc-binding alcohol dehydrogenase ChnD**	**0.770**	**5**	**1.104***	**0.100**	**5**	**1.535***	**0.139**	**5**	**1.319***
Bpro_3853	zinc-binding alcohol dehydrogenase	0.800	7	1.055*	1.907	8	1.113*	1.987	8	1.120*
Bpro_3259	zinc-binding alcohol dehydrogenase	0.806	5	[1.053]	0.710	4	1.051*	0.789	5	1.060*
Bpro_2634	zinc-binding alcohol dehydrogenase	1.122	5	1.043*	5.900	5	1.201*	5.295	5	1.187*
Bpro_4700	iron-containing alcohol dehydrogenase	1.129	4	1.094	1.604	4	1.123*	1.857	4	1.114*
Bpro_2565	zinc-binding alcohol dehydrogenase	1.536	4	1.157*	1.400	4	1.126*	1.438	4	1.182*
Bpro_3062	zinc-containing alcohol dehydrogenase	2.949	2	1.173	1.519	2	1.230	1.545	2	1.170
Bpro_2135	zinc-binding alcohol dehydrogenase	3.422	4	1.170*	0.901	4	1.042*	0.859	4	[1.068]

[a] p = number of peptides associated with the protein; EF = error factor [b] manual checking done with BLASTP
[c] MS/MS intensity peaks $\geq 10^4$
(*) indicates ratio that is significantly different from 1 at a 95% confidence level. Error factors with brackets [ ] indicate that the peptide match ratios do not appear to come from a sample with a normal distribution.

The levels of several alcohol dehydrogenases were also elevated by cDCE-metabolites (Table 4.3). These enzymes may catalyze the interconversion of DCET and DCAL. The transformation of chloral hydrate to TCET by alcohol dehydrogenases has been reported in many studies (Friedman and Cooper, 1960; Newman and Wackett, 1991; Forkert et al., 2005); nevertheless the exact functions of the aldehyde reduction during degradation of chlorinated ethene compounds were not elaborated. Bpro_5563 (ChnD), an enzyme that has been a subject in our study, showed moderately-high elevated abundances (1.3-fold, EF = 1.104, 5 peptides) in WT cells degrading CAP+cDCE vs. WT cells degrading CAP, and up to 10-fold when compared to KO cells grown in CAP+cDCE. This enzyme has been demonstrated to transform DCAL to DCET in our enzymatic assay. An ortholog of an alcohol dehydrogenase (Bpro_3129) is S-(hydroxymethyl)glutathione dehydrogenase, which catalyzes the conversion of S-hydroxymethyl glutathione (GS-CH_2OH) to S-formyl glutathione (GS-CHO). Bpro_3129 was elevated in abundance in WT cells degrading CAP+cDCE, versus WT cells degrading CAP only (115/114); however, this finding is based on identification of only one peptide in the sample.

WT cultures degrading both cDCE and CAP had 2-hydroxy-3-oxopropionate reductase, and glyoxylate carboligase up-to 4-fold more than WT degrading CAP only (Table 4.4). These two enzymes catalyze the two-step conversion of glyoxylate to D-glycerate (Figure 4.23). The transformation of glyoxal into glycolate can be catalyzed by glyoxalase I (Bpro_3549, encoded by *gloA*) and hydroxyacyl glutathione hydrolase (Bpro_2055, encoded by *gloB*), which both were elevated in WT degrading cDCE and

CAP vs. WT degrading CAP only, however for each of these enzymes only one peptide was identified in the sample. The primary function of these two enzymes is the two-step transformation of methylglyoxal into D-lactate. In JS666, we can speculate that these enzymes may be beneficial for channeling glyoxal into the TCA cycle. The induction of genes involved in gloxylate conversion was observed in an *E. coli* strain overexpressing monooxygenase and hydrolase (Lee et al., 2010). This confirmed the hypothesis of cDCE-epoxide hydrolysis, which yields the formation of glyoxal (Rui et al., 2004a; Lee et al., 2010). One of the possible roles for an D-2-hydroxyacid dehydrogenase (Bpro_4156, EC: 1.1.1.81) is the conversion of D-glycerate to hydroxypyruvate and interconversion of glycolate and glyoxylate. This enzyme was 1.1-fold elevated in cDCE-degrading WT cultures vs. CAP-grown WT cultures; however, this finding is based on only one peptide identified in the sample. The MS/MS intensity peaks for the associated peptide were at least 10^4.

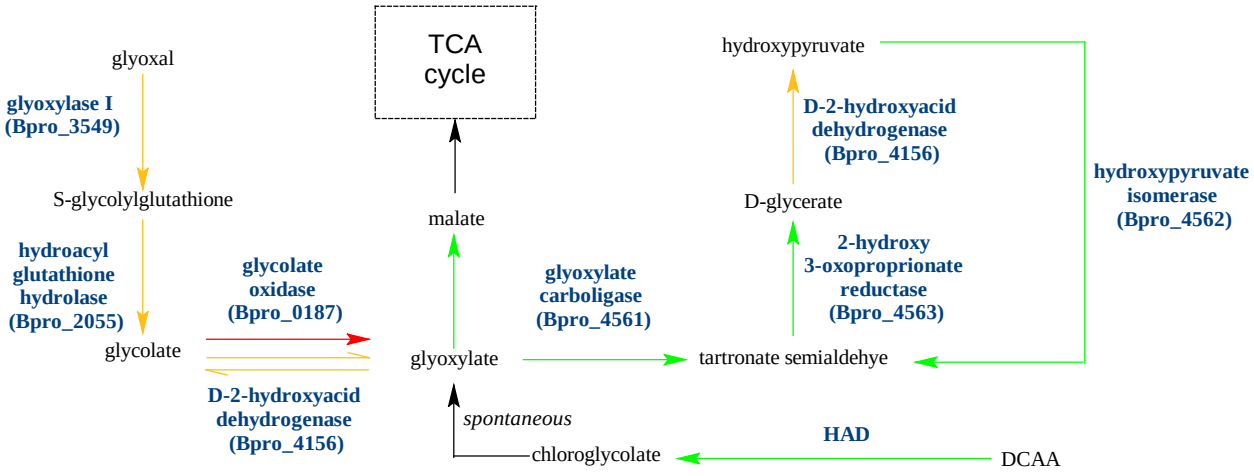

Figure 4.23. Pathways involved in glyoxal and glyoxylate transformation. Green, orange and red arrows indicate protein expressions elevated, moderately elevated and reduced by cDCE in WT cultures, respectively.

Table 4.4. Proteins involved in proposed glyoxal transformation pathway.

Locus Tag	Protein Description	115/114	p[a]	EF[a]	116/114	p[a]	EF[a]	117/114	p[a]	EF[a]
Bpro_4561	glyoxylate carboligase [b]	0.293	1	---	0.335	1	---	0.335	1	---
Bpro_4562	hydroxypyruvate isomerase [b,c]	0.009	1	---	0.059	2	1.989	0.053	2	2.182
Bpro_4563	2-hydroxy-3-oxopropionate reductase	0.239	2	1.094*	0.051	5	3.652*	0.060	4	3.210*
Bpro_2055	hydroxyacylglutathione hydrolase	0.785	2	1.052	1.162	2	1.086	1.065	2	1.163
Bpro_3549	glyoxalase I [b,c]	0.830	1	---	0.524	1	---	0.637	1	---
Bpro_0187	glycolate oxidase FAD binding subunit [b]	1.153	1	---	1.757	1	---	1.404	1	---
Bpro_4156	D- 2-hydroxyacid dehydrogenase [b,c]	0.861	1	---	0.982	1	---	1.052	1	---

[a] p = number of peptides associated with the protein; EF = error factor
[b] manual checking done with BLASTP
[c] MS/MS intensity peaks $\geq 10^4$
(*) indicates ratio that is significantly different from 1 at a 95% confidence level. Error factors with brackets [ ] indicate that the peptide match ratios do not appear to come from a sample with a normal distribution.

4.6.1 Knockout system proteome

Kanamycin was not added in the second transfer to avoid the expression of stress-related proteins due to the presence of kanamycin instead of cDCE. Despite this, the abundance level of kanamycin-resistance protein (neomycin phosphotransferase) was elevated in both KO cultures. Another protein associated with the insert that was seen in the KO cultures was the OriT binding protein (Appendix D). Five peptides associated with CHMO that are upstream and downstream of the insertion point were identified in KO cultures, and two of them yielded weak spectra or negative intensities. No formation of LacZ was reported, consistent with the sequence results (Appendix A) because of a one-nucleotide addition in the insert. Both *nagR* and *nagR2* knockout CJ2 strains were reported to produce LacZ (Jeon et al., 2006). An enzyme encoded downstream of the *chmo* gene in the cyclohexanol operon (i.e. zinc-binding alcohol dehydrogenase, ChnD) was identified in the KO cultures, with five peptides attributed to it, which further confirms the earlier quantitative PCR results (Giddings, 2010) and transcription data (Figure 4.24). The degradation of CAP by hydrolase (Bpro_5566) has been demonstrated through enzymatic assay. Both iTRAQ and RT-PCR data indicate that this hydrolase, while significantly present in both KO cultures, was not elevated in abundance compared to levels in the two WT cultures. This means that either the reduced protein levels were nonetheless sufficient to support CAP degradation in the KO strain, or else CAP catalysis can be achieved as well by other hydrolases in JS666.

From iTRAQ data and RT-PCR work (Figure 4.24), it can be judged that there was insignificant cross-contamination across the samples — always a concern in such

work. WT is kanamycin-sensitive and KO was initially grown in media containing kanamycin. Kanamycin resistance in the KO strains is catalyzed by neomycin phosphotransferase (GI number: 108796622). This protein was identified by one peptide, and its MS/MS intensity peaks were 6772, 944, 79372 and 32096 for 114, 115, 116 and 117, respectively (115/114 = 0.19; 116/114 = 10.142; 117/114 = 4.632). The presence of small peaks in the 114 and 115 samples of neomycin phosphotransferase may be due to background noise and impurities of iTRAQ reagents (Wiese et al., 2007) or minimal percentage error of impurities even after correction. The iTRAQ report shows CHMO protein was reduced almost 7-fold in KO cultures compared to WT cultures (Table 4.2). Furthermore, based on RT-PCR work, where primers were designed to target the intact region of the native *chmo* before and after the KO insertion point, intact *chmo* amplicons were not seen in KO samples even after 35 cycles. The detection limit of the gel is approximately 10 ng as indicated by the marker at 564 bp. Alcohol dehydrogenase (ChnD), a gene in the same operon, was 10-fold lower in KO cultures vs. cDCE-degrading WT cultures; nevertheless RT-PCR work shows *chnD* amplicons in all samples (30 and 35 cycles).

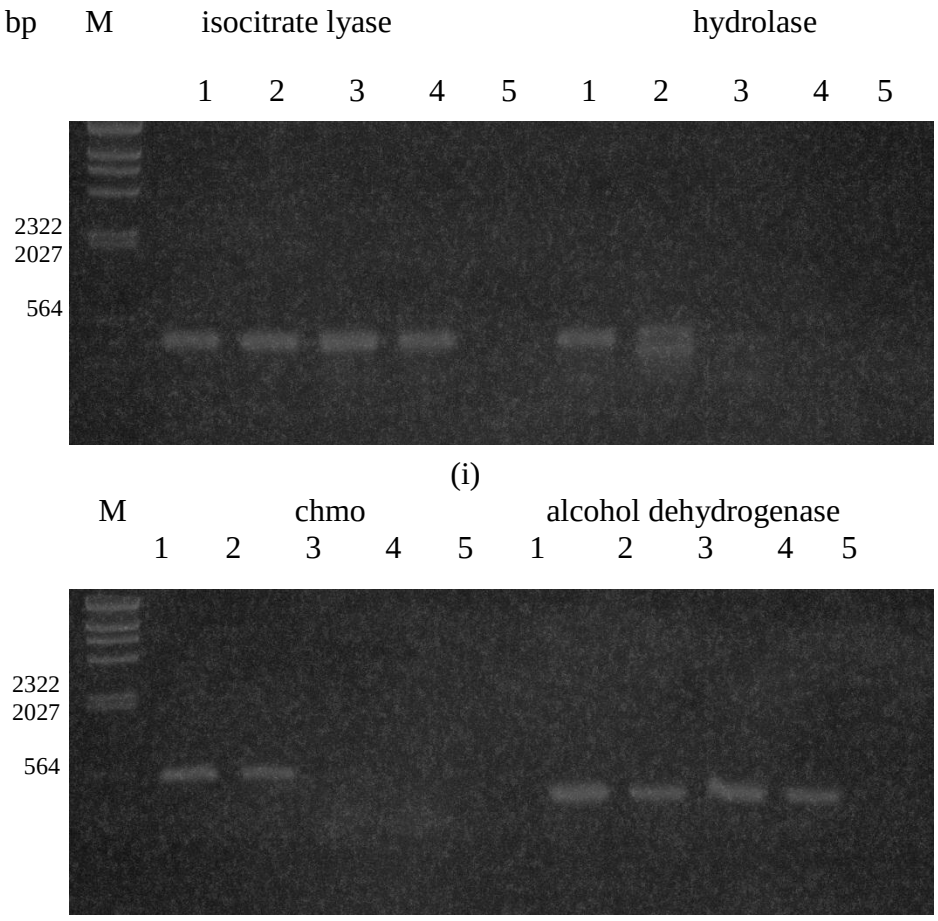

Figure 4.24. RT-PCR of 35 cycles using 300 ng of cDNA template and corresponding primer pairs for WT and KO cultures grown for iTRAQ study. cDNA was synthesized with a mixture of gene-specific reverse primers. M: Lambda DNA/HindIII marker; 1: WT grown in CAP and cDCE; 2: WT grown in CAP; 3: KO grown in CAP and cDCE; 4: KO grown in CAP; 5: water blank.

In Figure 4.24, multiple amplicons were observed in lane 2 (hydrolase) with 35-cycles but not with 30-cycle RT-PCR (data not shown). This implies that there were unintentional priming sites or high levels of *chnD* transcripts. The proteome level of hydrolase in CAP-grown WT cultures was 10-fold higher than in cultures grown on

cDCE and CAP. The absence of hydrolase amplicons from KO strains in RT-PCR but detectable protein in iTRAQ may be due to lack of correlation between transcripts and proteins. mRNA in bacteria degrades rapidly (within minutes) whereas proteins can survive much longer (Taniguchi et al., 2010). The additional sequence of the insert in the polycistronic mRNA may hinder the formation of secondary structure of original mRNA at 5'-end, thus limiting its stability, which leaves mRNA open for endoribonuclease E's attack (Rauhut and Klug, 1999). The *chnC* (hydrolase) gene is at the 5'-terminal of the polycistronic mRNA, followed by the *chnB* (*chmo*) gene.

4.6.2 Stress related to the presence of cDCE and its degradation

cDCE exposure to cells led to expression of stress related proteins, associated with heat shock and oxidative stress. In the cDCE-degrading WT culture, a heat-shock protein, Hsp20 (Bpro_1199) was elevated in abundance almost 2-fold when compared to the CAP-degrading WT culture. Conversely, this enzyme was elevated 2-fold in both KO cultures compared to the cDCE-degrading WT culture. Glutaredoxins were moderately elevated in cDCE-degrading WT cultures compared to CAP-grown WT cultures (Table 4.5). Thioredoxin reductase (Bpro_3801) was elevated in WT cells degrading cDCE+CAP vs. WT cells degrading CAP and this enzyme is responsible in reducing thioredoxin. Both glutaredoxin and thioredoxin catalyze the reversible oxidation of two vicinal protein-SH groups to a sulfide bridge and thioredoxin system provides defense against oxidative damage due to oxygen metabolism (Holmgren, 1989).

Results reported for peroxidases, which provide protection against oxidative stress, were varied. The abundance of heme peroxidase (Bpro_2396) was reduced 2.4-fold in cDCE-degrading WT cultures when comparing to CAP-grown WT cultures. Yet, this enzyme was elevated 2.4-fold when compared to KO cultures in the presence of cDCE and CAP. Jennings et al. (2009) reported 14.8-fold upregulation of heme peroxidase transcripts. Another peroxidase was elevated up-to 3-fold in both KO strains when compared to the cDCE-degrading WT cultures. The protein levels of catalase/peroxidase ortholog (KatG, Bpro_0678, hydroperoxidase I) were similar across all four cultures tested. KatG was elevated in alkane-grown *M. chubuense* cells (proteomics) (Coleman et al., 2011). The expression of a universal stress protein (Bpro_3227) was reduced in cDCE-degrading WT cultures even though Jennings et al. (2009) reported 3-fold transcript upregulation. Unfolded and destabilized proteins caused by stresses can be repaired by bacterial chaperones. DnaK was elevated 1.3-fold more in the cDCE-degrading WT cultures than in WT cultures growing on cDCE and CAP (Table 4.5).

Both WT cultures produced approximately similar relative amounts of molecular chaperones (GroEL and Cpn10, Table 4.5), which perhaps were constitutively expressed by the cells regardless of the presence or absence of the solvents. A DnaK homolog and Cpn10 were identified in *M. chubuense* strain NBB4 by comparing spot patterns on 2D gels (Coleman et al., 2011). The expression of global regulator for starvation conditions (encoded by *dps*) was reduced when comparing cDCE-degrading WT cells with the rest (Table 4.5) but in *E. coli* with a monooxygenase-and-glutathione system, Dps were induced in both proteomics and transcriptomics works (Lee et al., 2006; Lee et al., 2010).

Sigma 70 (encoded by *RpoD*) was repressed in cDCE-degrading WT cultures vs. CAP-grown cultures (Table 4.5). It serves as a housekeeping sigma factor that is responsible for transcribing most genes in cells. Transcription of *rpoD* was reduced during stationary growth phase when compared to that of in the exponential phase in *E. coli* (Rahman et al., 2008) and in *Streptococcus agalactiae* (Sitkiewicz and Musser, 2009), which may indicate a slowing of gene transcription.

Table 4.5. Ratios of selected proteins involved in biological stresses.

Locus Tag	Protein Description	115/114	p[a]	EF[a]	116/114	p[a]	EF[a]	117/114	p[a]	EF[a]
Bpro_3126	molecular chaperone DnaK	0.802	20	[1.091]	0.593	20	1.075*	0.627	20	1.062*
Bpro_2031	ATP-dependent protease ATP-binding subunit ClpX	0.864	2	1.231	0.935	2	1.422	0.753	2	1.742
Bpro_1400	Ferritin and Dps	1.148	2	1.098	3.526	2	1.151	3.733	2	1.176
Bpro_0759	chaperonin GroEL	1.040	38	[1.128]	0.553	37	[1.099]	0.677	37	[1.094]
Bpro_0760	chaperonin Cpn10 GroES	1.039	7	1.076	0.541	7	1.052	0.647	7	1.093
Bpro_1032	heat shock protein HtpX [b,c]	1.290	1	---	1.153	1	---	1.067	1	---
Bpro_1303	heat-inducible transcription repressor [b,c]	1.138	1	---	1.167	1	---	1.246	1	---
Bpro_1199	heat shock protein Hsp20	0.551	10	1.064*	1.970	10	1.054*	2.175	10	1.061*
Bpro_3187	Hsp33 protein [b,c]	0.927	1	---	1.019	1	---	1.140	1	---
Bpro_2651	putative heat shock protein	0.943	2	1.280	0.487	3	1.349	0.485	2	1.017*
Bpro_0614	heat shock protein 90 [b,c]	1.255	1	---	1.003	1	---	1.330	1	---
Bpro_3337	DNA mismatch repair protein MutS	1.362	3	[1.229]	0.846	3	1.136	0.999	3	1.105
Bpro_3097	sigma 70 (RpoD)	1.423	5	1.046*	1.128	5	1.136	1.166	5	1.055*
Bpro_2396	heme peroxidase	2.414	2	1.066	0.407	2	1.057	1.345	2	1.009
Bpro_0678	catalase/peroxidase HPI [b]	0.979	1	---	1.054	1	---	0.939	1	---

[a] p = number of peptides associated with the protein; EF = error factor
[b] manual checking done with BLASTP
[c] MS/MS intensity peaks $\geq 10^4$
(*) indicates ratio that is significantly different from 1 at a 95% confidence level. Error factors with brackets [ ] indicate that the peptide match ratios do not appear to come from a sample with a normal distribution.

Table 4.5 (continued)

Locus Tag	Protein Description	115/114	p[a]	EF[a]	116/114	p[a]	EF[a]	117/114	p[a]	EF[a]
Bpro_4841	peroxidase	1.051	3	1.056	2.994	3	1.074*	2.870	3	1.063*
Bpro_2856	glutaredoxin	0.836	5	1.066*	1.427	5	1.295*	1.468	4	1.129*
Bpro_0848	glutaredoxin-like protein [b,c]	0.676	1	---	0.747	1	---	0.802	1	---
Bpro_0643	NADPH-glutathione reductase	0.862	2	1.124	0.869	2	1.075	0.843	2	1.274
Bpro_2337	phosphoadenylylsulfate reductase (thioredoxin) [b,c]	0.949	1	---	0.578	1	---	0.676	1	---
Bpro_2263	thioredoxin	0.847	7	1.136*	1.059	7	1.172	1.016	7	1.244
Bpro_3369	thioredoxin [b,c]	1.267	1	---	0.846	1	---	0.889	1	---
Bpro_4628	thioredoxin	1.031	4	1.291	1.246	4	1.128*	1.184	4	1.056*
Bpro_3801	thioredoxin reductase	0.732	5	1.049*	0.966	5	1.041	1.015	5	1.037
Bpro_3227	universal stress protein	1.708	4	1.069	1.886	4	1.097	2.157	4	1.106

[a] p = number of peptides associated with the protein; EF = error factor
[b] manual checking done with BLASTP
[c] MS/MS intensity peaks $\geq 10^4$
(*) indicates ratio that is significantly different from 1 at a 95% confidence level. Error factors with brackets [ ] indicate that the peptide match ratios do not appear to come from a sample with a normal distribution.

Proteins related to reduced glutathione (GSH) synthesis are summarized in Figure 4.25 and Table 4.6. GSH is a tripeptide that consists of cysteine, glutamate and glycine. There are several hypothesized functions of bacterial GSTs during degradation of chlorinated ethenes. 4-aminobutyrate aminotransferase (Bpro_2912) was significantly elevated in WT cells degrading CAP+cDCE vs. WT cells degrading CAP. The elevation of this enzyme indicates that the cells may have been producing more L-glutamate from α-ketoglutarate and 4-aminobutanoate (Figure 4.25 and Table 4.6). The enzyme (Bpro_4540) involved in synthesis of GSH from γ-glutamylcysteine and glycine was moderately elevated in WT cultures degrading cDCE vs. WT cultures degrading CAP-only. In addition, NADPH-dependent glutathione reductase (Bpro_0643) involved in conversion of glutathione disulfide to GSH was also fairly elevated in WT degrading cDCE vs. all other cultures, which suggests that the production of GSH in cell cultures degrading cDCE was increased. The enzyme converts glutathione disulfide to GSH and is regulated by the LysR regulator in the upstream gene. In an *E. coli* strain expressing monooxygenase and glutathione systems, glutamate-cysteine ligase (encoded by *gshA*, JS666 homolog: Bpro_4583) was induced in both proteomic and transcriptomic studies (Lee et al., 2006; Lee et al., 2010). In JS666, another glutamate-cysteine ligase (Bpro_3399) was identified and had elevated expression in cDCE-degrading WT cultures vs. CAP-degrading WT cultures.

The GST-like protein and PNPox are transcribed in the opposite direction. GST (Bpro_0645) was elevated the cDCE-degrading cells compared to the others. This protein was identified by only one peptide, and its MS/MS intensity peaks were 117817, 62390, 2302 and 2854 for 114, 115, 116 and 117, respectively. Cysteine desulfurase (IscS) plays

a central role in the delivery of sulfur to a variety of metabolic pathway and its relative abundance in WT degrading cDCE and CAP was not significant, versus the other three conditions, even though it was fairly elevated in both proteomic and transcriptomic works of *E. coli* cells co-expressing TOM-Green and IsoILR (Lee et al., 2006; Lee et al., 2010).

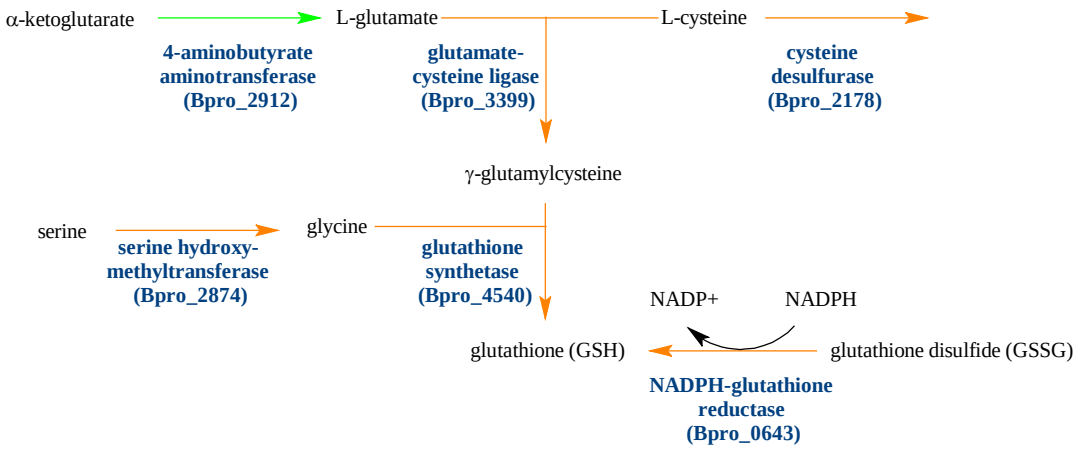

Figure 4.25. Synthesis pathway for reduced glutathione (GSH) in strain JS666. Green and orange respectively arrows indicate protein abundaces highly and moderately elevated in WT cultures grown in cDCE and CAP vs. CAP only.

Table 4.6. Ratios of proteins involved in GSH synthesis and several GST-like proteins.

Locus Tag	Protein Description	115/114	p[a]	EF[a]	116/114	p[a]	EF[a]	117/114	p[a]	EF[a]
Bpro_2912	4-aminobutyrate aminotransferase	0.407	5	1.311	1.022	5	1.085	1.445	5	1.071
Bpro_3399	glutamate-cysteine ligase [b,c]	0.803	1	---	1.161	1	---	1.085	1	---
Bpro_2178	cysteine desulfurase IscS	0.907	2	1.038	0.689	2	1.076	0.912	2	1.030
Bpro_2417	glutathione-dependent formaldehyde-activating, GFA	0.708	8	1.184*	2.187	8	1.101*	2.310	8	1.084*
Bpro_0824	GST-like	1.612	6	1.090*	1.164	6	1.081*	1.178	6	[1.070]
Bpro_2563	putative GST-related protein	1.924	6	1.119*	1.538	4	1.013*	1.284	5	1.044*
Bpro_0643	NADPH-glutathione reductase	0.862	2	1.124	0.869	2	1.075	0.843	2	1.274
Bpro_0645	GST-like [b,c]	0.724	1	---	0.017	1	---	0.024	1	---
Bpro_0243	GST -like	0.976	3	1.025	1.034	3	1.052	1.053	3	1.002*
Bpro_4661	GST -like [b,c]	0.961	1	---	1.156	1	---	1.309	1	---
Bpro_4540	glutathione synthetase [b,c]	0.804	1	---	1.027	1	---	1.136	1	---
Bpro_0387	GST-like [b]	0.733	1	---	0.412	1	---	0.486	1	---
Bpro_2168	lactoylglutathione lyase [b,c]	0.913	1	---	1.349	1	---	1.239	1	---
Bpro_2055	hydroxyacylglutathione hydrolase	0.785	2	1.052	1.162	2	1.086	1.065	2	1.163
Bpro_2874	serine hydroxymethyltransferase [b,c]	0.921	1	---	0.700	1	---	0.850	1	---

[a] p = number of peptides associated with the protein; EF = error factor
[b] manual checking done with BLASTP
[c] MS/MS intensity peaks $\geq 10^4$
(*) indicates ratio that is significantly different from 1 at a 95% confidence level. Error factors with brackets [ ] indicate that the peptide match ratios do not appear to come from a sample with a normal distribution.

4.6.3 Central metabolism

The genome of JS666 contains a complete glycolytic pathway, a tricarboxylic acid (TCA) cycle and a glyoxylate bypass. It also contains a pentose phosphate pathway, missing a gene that confers 6-phosphogluconolactonase. Two ribulose bisphosphate carboxylase homologs are also present in the genome (Mattes et al., 2008).

Fatty acids are the main components of bacterial lipids. The degradation of CAP yields adipate, which is further oxidized through β-oxidation to generate acetyl-CoA and succinyl-CoA. These two intermediates are fed into the TCA or glyoxylate cycles to generate precursor metabolites. The thiolase-mediated conversion of 3-oxoadipyl-CoA to succinyl-CoA (via Bpro_1231) was elevated up-to 8-fold in WT cells degrading cDCE and CAP when compared to the both KO cultures and 1.1-fold when compared to WT cells degrading CAP (Table 4.7). A similar enzyme is involved in conjugation of acetyl-CoA to acyl-CoA groups. In *E. coli* containing monooxygenase and glutathione systems, cDCE repressed fatty acid synthesis, gluconeogenesis, and the TCA cycle (Lee et al., 2006). In cDCE-degrading WT cells, cDCE-degradation caused an elevation of malate synthase, which converts glyoxylate to malate, by 2-fold when comparing to the WT degrading CAP or to both KO cultures.

Abundance of isocitrate lyase was reduced 2-fold in cDCE-degrading WT cells versus non-cDCE-degrading cells (both WT and KO), suggesting an ample (and spontaneous) production of glyoxylate from chloroglycolate (Figure 4.26), which is a result of dehalogenation of dichloroacetate by HAD. The abundance of glycolate oxidase, responsible for transformation of glycolate (a possible product of cDCE-epoxide hydrolysis) to glyoxylate was reduced approximately up-to 1.75-fold in cDCE-degrading

WT cells when compared to the other three conditions. D-2-hydroxyacid dehydrogenase (Bpro_4156) may act as a glyoxylate reductase that can catalyze similar reaction as glycolate oxidase. The abundance of pyruvate dehydrogenase, which catalyzes the production of acetyl-CoA from pyruvate, was higher in WT than in KO strains. A summary of central metabolism pathways is depicted in Table 4.7 and Figure 4.26.

Table 4.7. Ratios of selected important proteins involved in central metabolism.

Locus Tag	Protein Description	115/114	p[a]	EF[a]	116/114	p[a]	EF[a]	117/114	p[a]	EF[a]
Bpro_3592	aconitate hydratase	0.870	7	1.041*	1.794	8	1.073*	1.929	8	1.042*
Bpro_0187	glycolate oxidase FAD binding subunit [b]	1.153	1	---	1.757	1	---	1.404	1	---
Bpro_2942	isocitrate dehydrogenase	0.765	9	[1.294]	0.933	9	1.027*	0.763	9	[1.119]
Bpro_2101	isocitrate lyase	2.494	9	[1.088]	2.114	9	1.075*	2.177	9	[1.102]
Bpro_4517	malate synthase G	0.556	8	[1.062]	0.594	8	1.124*	0.684	8	1.204*
Bpro_0160	phosphoenolpyruvate carboxykinase	0.452	7	1.314*	0.666	7	[1.350]	0.792	7	1.142*
Bpro_3665	phosphoenolpyruvate carboxylase	0.789	16	[1.064]	1.444	16	1.055*	1.324	16	[1.089]
Bpro_3184	phosphopyruvate hydratase	1.001	9	1.082	0.742	9	1.086*	0.754	9	1.081*
Bpro_2672	pyruvate dehydrogenase subunit E1	1.209	4	1.068*	0.585	4	1.043*	0.699	4	1.108*
Bpro_4634	pyruvate kinase [b,c]	0.936	1	---	0.347	1	---	0.403	1	---
Bpro_3602	succinate dehydrogenase subunit A	0.921	7	[2.794]	1.483	8	[12.001]	1.025	7	1.303
Bpro_4681	succinyl-CoA synthetase subunit α	0.333	4	[1.377]	1.123	4	1.216	1.016	4	1.100
Bpro_4682	succinyl-CoA synthetase subunit β	0.914	17	1.057*	1.078	18	[1.964]	1.050	17	1.067*
Bpro_3605	type II citrate synthase	1.165	12	1.095*	2.990	9	1.284*	3.170	13	1.253*
Bpro_1231	β-ketoadipyl CoA thiolase	0.888	9	1.079*	0.124	9	1.354*	0.134	8	1.327*

[a] p = number of peptides associated with the protein; EF = error factor
[b] manual checking done with BLASTP
[c] MS/MS intensity peaks $\geq 10^4$
(*) indicates ratio that is significantly different from 1 at a 95% confidence level. Error factors with brackets [ ] indicate that the peptide match ratios do not appear to come from a sample with a normal distribution.

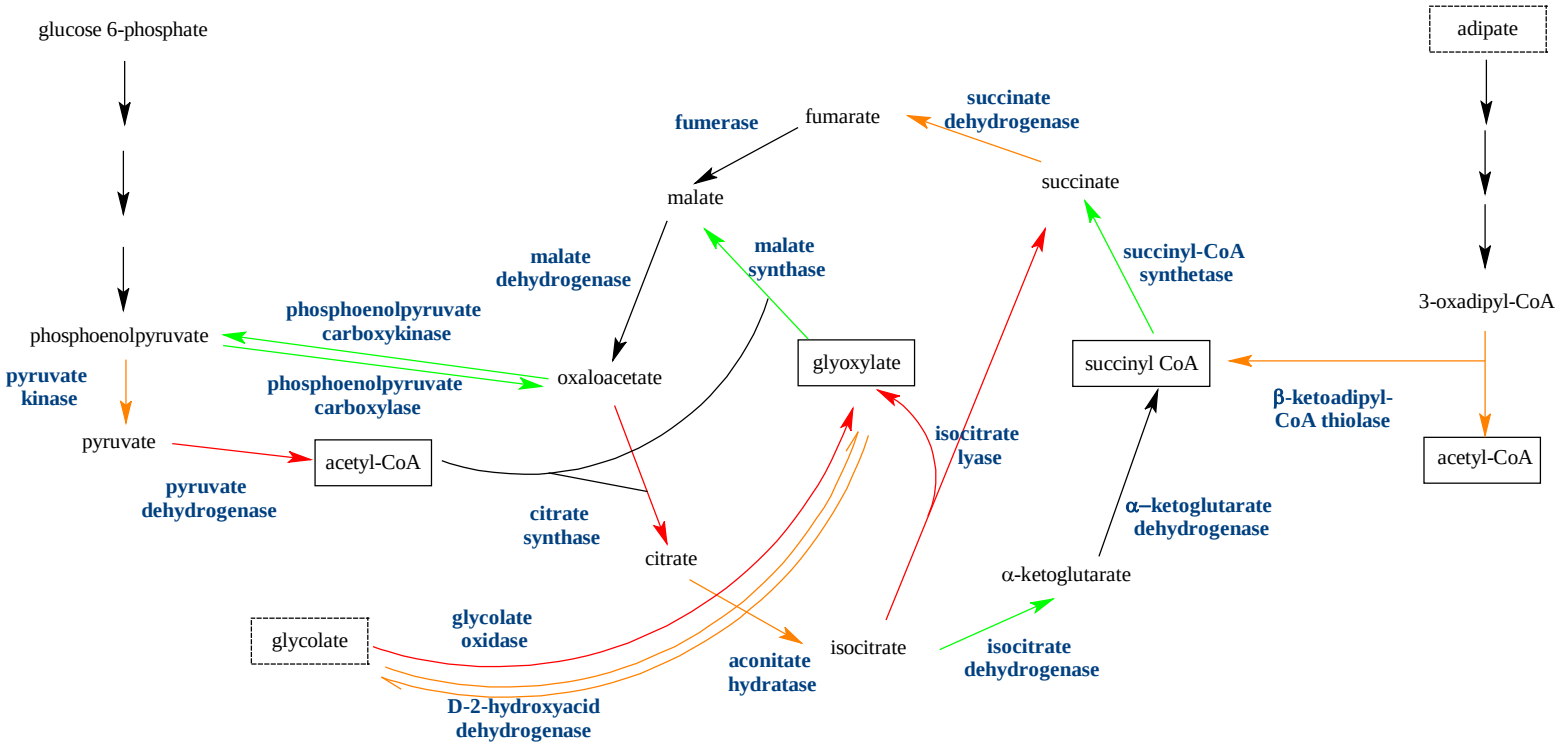

Figure 4.26. Selected important central metabolic pathways (gluconeogenesis, TCA and glyoxylate pathways). Green and orange arrows respectively indicate highly and moderately elevated protein expressions in WT cultures grown in cDCE and CAP vs. CAP only. Red arrows indicate reduced expression, and proteins that were not reported are represented by black arrows.

CHAPTER 5

5. DISCUSSION

5.1 Investigating the roles of the *chmo* gene and genes in the cyclohexanol operon during cDCE degradation by strain JS666

One of the aims of this study was to determine the involvement of the *chmo* gene during cDCE degradation by knocking out the *chmo* homolog of JS666 and conducting CHMO enzymatic assays. CHMO, an FMO from strain JS666, showed activity on CYHX; nonetheless, no activity was confirmed with cDCE. This confirms the work of Alexander (2010), and certainly suggests that CHMO is not involved in the first step of cDCE degradation. However, different cellular environments in both *E. coli* and JS666 strains may have contributed to the outcome of the experiments.

Overlays of 2D gel images comparing proteins extracted from cDCE-grown and non-cDCE-grown cells, and subsequent analysis of differing proteins by mass-spectrometry, revealed the presence of multiple spots with slightly different isoelectric points for CHMO, HAD and GST (Jennings et al., 2009). This suggests that these upregulated proteins were modified post-translationally, which could include the covalent attachment of phosphate, lipids or proteins to the amino acids. It is possible that modification is necessary for cDCE epoxidation by CHMO. Nevertheless the observation that CHMO-catalyzed conversion of CYHX to CAP proves that the protein was functional. We note that no cDCE activity was observed in cell extracts of JS666, suggesting that this activity is not easily assayed *in vitro* (Nishino, 2011). Lack of a

positive result with *E. coli* overexpressing CHMO cannot prove that CHMO is not involved in cDCE epoxidation; it merely fails to prove involvement.

The *chmo*-knockout study demonstrated that the KO strain was incapable of growing on cDCE, CYHX, cyclohexanol and EtOH after several days of incubation. Our enzymatic assays with dehydrogenases (ChnA and ChnD), encoded by genes downstream of *chmo,* demonstrated that these enzymes are capable of transforming cyclohexanol to CYHX and EtOH to acetaldehyde. This suggests some impairment of ChnA and/or ChnD in the KO strain, in addition to the intended loss of functional CHMO.

Several pieces of evidence indicate that the genes downstream of *chmo* were transcribed and translated in the KO strain: (i) Quantitative- and RT-PCR studies showed transcription of a sequence of *chmo* after the insert and of *chnD*; (ii) iTRAQ data identified CHMO peptides after the insert, as well as those from ChnD; and (iii) no palindromic transcription termination sequence is present in the suicide vector, implying that transcription would be expected to continue until the RNA polymerase hit the next termination sequence, which is located after the *chnD* gene.

Though there is evidence that genes downstream of *chmo* (and peptides from the altered *chmo*) continued to be expressed in the KO strain, it does not mean that levels of expression, translation, and resulting enzyme function were unimpaired in the cyclohexanol operon and other operons that share similar regulation. Indeed, the iTRAQ results showed an 80-90% reduction in the abundance of ChnD protein in the KO strain, compared to WT. Since peptides from the altered *chmo* were also about 90% reduced in abundance in the KO, this suggests that the downstream, short-chain dehydrogenase (*chnA*) was probably similarly affected, since it is located between *chmo* and *chnD* on the

JS666 genome. Peptides from *chnC* (the hydrolase adjacent upstream of *chmo*) were also reduced in abundance in the KO, but less so. Since the KO strain is quite capable of growth on CAP, the approximately 70-75% reduction in abundance of this hydrolase (Bpro_5566, ChnC), which was shown in enzyme assays to be active on CAP, is either insufficient to cause deleterious effect on growth, or else there are other hydrolases in JS666 that serve this same purpose.

The impaired translation of genes downstream of an insert has been noted in other studies. For example, the inactivation of cyclopentanone 1,2-monooxygenase (*cpnB*) in *Comamonas* sp. NCIMB9872 resulted a mutant strain incapable of utilizing cyclopentanone and cyclopentanol (Iwaki et al., 2002b), and yet the cyclopentanol dehydrogenase gene (*cpnA*) is located downstream of *cpnB*. In our study, the relatively low abundance of ChnD (though still detectable) might explain the KO strain's inability to grow on EtOH. Also, protein conformation matters to function, and iTRAQ studies cannot tell us whether the resulting, detectable ChnD was even functional in the KO strain

ChnD is responsible for metabolizing 6-HHA to 6-oxohexanoate; therefore, one has to reconcile the impairment of ChnD in the KO with the KO's observed capability to grow on CAP. The first step in CAP degradation is hydrolase-mediated conversion to 6-HHA. We speculate that any of all of the following might be true:

- The abundances of ChnC and ChnD, though reduced in the KO, were nonetheless sufficient for the conversions of CAP and 6-HHA, respectively, but that higher amounts of ChnD are needed to initiate the degradation of EtOH or cyclohexanol.

- There was not only a decrease in abundance of ChnD in the KO, versus the WT, but also a change in ChnD conformation affecting its function. It might have retained activity on 6-HHA, but not on cyclohexanol or EtOH.
- ChnA (undetected in both WT and KO strains through iTRAQ) was far more impaired in the KO than was ChnD, and that ChnA normally has a greater role in cyclohexanol and EtOH degradation than does ChnD. We were unable to conduct separate over-expression studies with ChnA to assay its function separate from that of ChnD.
- 6-HHA is a straight-chain fatty acid that can be further metabolized by other enzymes, apart from ChnD, through multiple pathways (Kunz and Weimer, 1983). Loss of ChnD (and presumably of ChnA) function might have been critical to degradations of cyclohexanol and EtOH, but not to degradation of 6-HHA.

The transformation of DCAL into DCET by ChnD was demonstrated in our study through whole-cell enzymatic assays. The interconversion of DCAL and DCET (or DCAA) could be further tested through purifying the dehydrogenases and conducting enzymatic assays with different cofactors (i.e. NAD^+, NADH or NADPH). This should eliminate the background conversion of DCAL to DCET in *E. coli* cells and configure the conversion of DCET to DCAL by supplementing with excess NAD^+. In our enzymatic assay, succinate was supplied to the *E. coli,* and this could have decreased the NAD^+/NADH ratio. The co-administration of succinate in excess with cDCE in WT cells was shown to slow down cDCE-degradation. Succinate usage supplies excess NADH that

may shift the degradation from DCAL towards formation of DCET instead of DCAA. This might stall cDCE-degradation before DCET is transformed back into DCAL.

In this study, we also investigated the possible role of hydrolase (ChnC) as an epoxide hydrolase. Negative results from hydrolysis assays of different epoxides with ChnC perhaps imply involvement of other hydrolases or perhaps abiotic hydrolysis of the epoxides. Preliminary evidence from another hydrolase (Bpro_4478) was insufficient to conclude anything about involvement of epoxide hydrolases as detoxification agents.

Even though the downstream genes are transcribed and translated, the protein abundances (i.e. ChnD, P450) were found to be low in the KO strain that was exposed to cDCE. We speculate that this may be due to the regulatory network's being affected by the knockout. Bpro_5567 is a putative Fis-family transcriptional regulator, a gene upstream of *chmo* that is transcribed in the opposite direction. Fis is a small DNA-binding and -bending protein that can enhance the promoter activity if the promoter has a Fis-binding capability in the presence of other activators.

5.2 Strain JS666's responses to different substrates and conditions

High concentrations of cDCE and the presence of metabolites produced by cDCE oxidation partially inhibited the growth of strain JS666, even in the presence of co-substrates such as succinate or CAP as reported in Figure 4.4 and Figure 4.7, respectively. The explanations for the inhibitory effect of cDCE on growth may be due to membrane stress caused by high concentrations of cDCE and/or the presence of inadequate amounts of bacterial detoxification agents or repair mechanisms to handle the damaging effects of oxidative metabolites. The growth of strain CJ2 was also retarded by

a high initial concentration of naphthalene (78 μM), but grew well at naphthalene concentrations ≤ 55 μM. In their investigations, the researchers also showed that the metabolites produced as a result of naphthalene oxidation also caused growth inhibition (Pumphrey and Madsen, 2007). The degradation of cDCE produces several chlorinated metabolites, such as cDCE-epoxide, DCAL and DCAA, before they are completely mineralized (2 moles of chloride ion produced per a mole of cDCE consumed). These metabolites (e.g., cDCE-epoxide) may be more reactive than the parent compound itself. Metabolites produced as a result of aromatic oxidation by other bacteria, for example, are more soluble than their parent compounds and prone to form adducts to the DNA and proteins (Schweigert et al., 2001).

Strain JS666's adaptation to the toxicity of cDCE and/or its metabolites (e.g., cDCE-epoxide) may cause delay in cDCE degradation. Epoxide catabolic genes in strain JS666 have yet to be identified. Epoxyalkane:coenzyme-M transferase catalyzes the transformation of epoxyethane and VC-epoxide to acetyl-CoA in *Mycobacterium* strains and many other VC degraders (Coleman and Spain, 2003b; Coleman and Spain, 2003a; Danko et al., 2006; Mattes et al., 2007). BLASTP search for similar enzymes in strain JS666 failed to return any highly matched proteins. In addition, other detoxification mechanisms in strain JS666 have not yet been established. Highly induced GST-like protein (Bpro_0645) has shown no activity with cDCE (Jennings et al., 2009), and neither hydrolase tested in this showed any promising results. Giddings (2012) also observed an immediate increase of *gst* transcripts after exposure of JS666 to EtOH or DCA when there was no associated degradation, suggesting that GST may be involved in stress due to presence of solvent, rather than to metabolites. Other possible roles for GST that have

yet to be tested include metabolite-detoxification by conjugating to epoxide or DCAL (Dowsley et al., 1995).

In our cDCE-starvation study, the observed lag time could possibly be related to a microbial acclimation phase, where necessary transcriptional expression and enzymatic induction are achieved. *P. putida* strain JS644 exhibited an extended lag period prior to growth on *p*-nitrophenol. The cause of the delay was due to an uninduced *p*-nitrophenol monooxygenase, which was dependant on the accumulation of hydroquinone, a *p*-nitrophenol metabolite (Nishino and Spain, 1993). Giddings (2012) observed low targeted transcript levels of JS666 (i.e. *aceA, gst, chmo, pnpox, rpoB, had* and *p450*) following cDCE starvation, and they rose simultaneously as cDCE-degradation resumed.

The addition of succinate provided mixed results in alleviating the extended lag in strain JS666. In CYHX-grown cultures, the addition of succinate helped inititate cDCE degradation. A similar phenomenon was observed during co-metabolic propene oxidation in ethene-grown *Mycobacterium* sp. strain E3 cultures and in VC metabolism in *Nocardioides* sp. strain JS614 (Mattes et al., 2007). Succinate-grown *Ralstonia pickettii* PKO1 readily utilized benzene when 1.25 mM succinate was supplied (Bucheli-Witschel et al., 2009). This implies that the JS666's growth on CYHX induced enzymes responsible for cDCE-degradation, and that addition of succinate (1 mM) provided ATP and/or NADH (or NADPH) for initial attack on cDCE – or carbon for enzyme synthesis/repair. The demand for NADH (or NADPH) in the initial catabolic step is greater than the NADH demand for cellular maintenance and respiration, as observed also in bacteria expressing toluene monooxygenases. Toluene oxygenation requires a net consumption of NADH for the initial ring cleavage (Johnson et al., 2006). On the other

hand, succinate-grown cultures of JS666 did not start degrading cDCE until after 15 days (Figure 4.22). JS666 has been observed to have an extended lag period to cDCE-degradation when grown previously on acetate or glycolate. When the strain was grown on cDCE with 10 mM succinate as co-substrate, the cultures exhibited "bad behavior" with respect to cDCE-degradation. When CYHX or EtOH was supplied as co-substrate, the cells quickly exhibited cDCE-degradation and sustained it through multiple additions. Excess succinate (10 mM) may disrupt the NAD^+/NADH ratio in the cells, shifting the cDCE-degradation pathways towards unfavorable ones. This hypothesis has yet to be tested.

5.3 Monitoring translational changes in strain JS666 during aerobic cDCE degradation

iTRAQ was conducted to determine whether the proteins encoded downstream of *chmo* were translated and to explore the proteome changes during cDCE degradation. This study complements previous proteomic and transcriptomic analyses conducted by Jennings et al. (2009). In our study, the concentration of CAP was limited to 2 mM so that the cells would readily degrade both CAP and cDCE simultaneously, avoiding diauxic metabolism. The peptide samples were tagged with an excess label and were let sit for at least an hour to ensure complete tagging before hydrolysis. The presence of small peaks in the 114 and 115 samples of neomycin phosphotransferase and OriT may be due to background noise and impurities of iTRAQ reagents (Wiese et al., 2007) or minimal percentage error of impurities even after correction.

The *had* gene has been suggested as a good bioindicator for monitoring cDCE and DCA degradations (Giddings, 2012). Giddings observed that *had* transcripts were upregulated when either cDCE or DCA was degraded and downregulated when degradation stopped. The increased abundance of HAD by cDCE was also confirmed by our iTRAQ data. Even though P450 catalyzes the initial attack on cDCE and DCA, the gene encoding it was reported to have a low degree of upregulation (Giddings, 2012). In RT-PCR study, Alexander (2010) reported mixed levels of *p450* transcription by the cells exposed to cDCE compared to cells grown on other substrates. The reduction of P450 abundance (in our iTRAQ study) in cDCE-degrading cells may be due to the formation of a damaging and reactive enzyme-substrate complex, which is a dead-end product due to an irreversible porphyrin *N*-alkylation with one carbon atom of the ethenes (de Visser et al., 2004). The formation of a suicide complex could reduce the abundance of the P450 in the cells. In any event, protein abundance does not necessarily correlate with transcript abundance. Given that transcription of *p450* is not all that highly upregulated by cDCE (only 3.5-fold) (Jennings et al., 2009), it is unsurprising if differences in the standing crop of P450 protein among cultures do not perfectly reflect previously reported differences in transcript abundance.

A study on stress-related proteins in engineered *E. coli* strains suggested that the presence of these proteins improves cDCE metabolism (Lee et al., 2010). The data suggest that the response to cDCE degradation is similar to the response to reactive oxygen species. In the previous omics analyses (Jennings et al., 2009), cDCE elevated the abundances of GST, which was reported as modestly elevated in our iTRAQ study. Proteins involved in GST system were moderately elevated by cDCE-degradation and

these GST-like proteins identified in the iTRAQ results may be responsible for glutathione conjugation to cDCE or cDCE-derivatives. GST-like protein (Bpro_0387), which shares 37% amino acid identity (coverage at C-terminal) with IsoILR1 of *Rhodococcus* AD45, was found to be fairly elevated in cDCE-degrading cells.

Cells' exposure to toxic substances can cause both elevation and reduction of abundances of many ribosomal proteins. Elevated expression of these proteins may be due to the presence of misfolded proteins in the cells. Proteases attack misfolded proteins for recycling amino acids, and cells have to generate more enzymes to replace inactive ones. The induction of DnaK in cDCE-degrading cells helps in the refolding of misfolded proteins (Hesterkamp and Bukau, 1998), in addition to preventing proteins' misfolding and aggregation (Agashe and Hartl, 2000). In KO cultures, the increase in abundance of ribosomal subunit proteins may be a general response to translational limitations caused by the addition of the insert and extra genes (Wood and Peretti, 1990).

Overall, iTRAQ study enhanced our understanding of proteome changes caused by the presence of cDCE and its reactive products in strain JS666. It generally supported the previous study by Jennings et al. (2009). Its more important contribution, however, was to provide information concerning transcription and translation of potentially important genes adjacent to the *chmo* insert in the KO strain. From this, it was found that translation of an upstream *chnC* (encoding a hydrolase) was lowered significantly, though apparently not so impaired as to prevent the KO strain from growing on CAP. On the other hand, translation of a downstream *chnD* (encoding an alcohol dehydrogenase) – and by inference the short-chain dehydrogenase (ChnA) whose encoding gene is between *chmo* and *chnD* – was decreased 80-90% in the KO. Though detectable, the lower ChnD

and/or ChnA abundances (or effects on their conformation) in the KO strain might explain the loss of its ability to degrade (and grow on) EtOH. By extension, this suggests a role for ChnD and/or ChnA in cDCE degradation, although likely not in carrying out the first step in the process. Though we could not demonstrate a role for CHMO in cDCE degradation, we cannot be said to have proven there is none.

5.4 Updated cDCE-degradation pathways

Multiple cDCE-degradation pathways have been proposed (Jennings et al., 2009) and updated with the discovery of the oxidative function of cyctochrome P450 (Shin, 2010). Figure 5.1 presents the updated pathways, reflecting results from this dissertation research and earlier studies.

In initial attack, cDCE is broken down into DCAL and cDCE-epoxide by P450. DCAL can be further degraded to DCAA by aldehyde dehydrogenase(s). Originally, the activity of dehydrogenase was confirmed by enzyme assay in JS666 cell extract; however, the specific dehydrogenase was not determined (Jennings et al., 2009). From the iTRAQ report, the aldehyde dehydrogenase that may be responsible for oxidizing DCAL is Bpro_3952. DCAA is then transformed into chloroglycolate by haloacid dehalogenases (Bpro_0530 and Bpro_5186) or hydrolase (Bpro_4478) before spontaneous conversion to glyoxylate (Goldman et al., 1968; Chan et al., 2010). It is also possible that DCAL can be conjugated to glutathione by GST, which has yet to be tested (Dowsley et al., 1995). Our enzymatic assay with ChnD demonstrated the conversion of DCAL to DCET. The DCET-to-DCAL transformation by the same enzyme has not been

tested and is a subject for future study. The metabolic pathway for DCET (other than the oxidation to DCAL) is still not known in JS666.

There are two potential pathways for cDCE-epoxide metabolism: (i) hydrolysis either abiotically or by a hydrolase to 1,2-dichloroethane-1,2-diol; or (ii) glutathione conjugation by GSTs. Both of these pathways are hypothesized to form glyoxal. We can also speculate the two-step conversion of glyoxal to glycolate is catalyzed by glyoxalase I (Bpro_3549) and hydroxyacylglutathione hydrolase (Bpro_2055), as their putative functions are primarily conversion of methylglyoxal to D-lactate (Clugston et al., 1998).

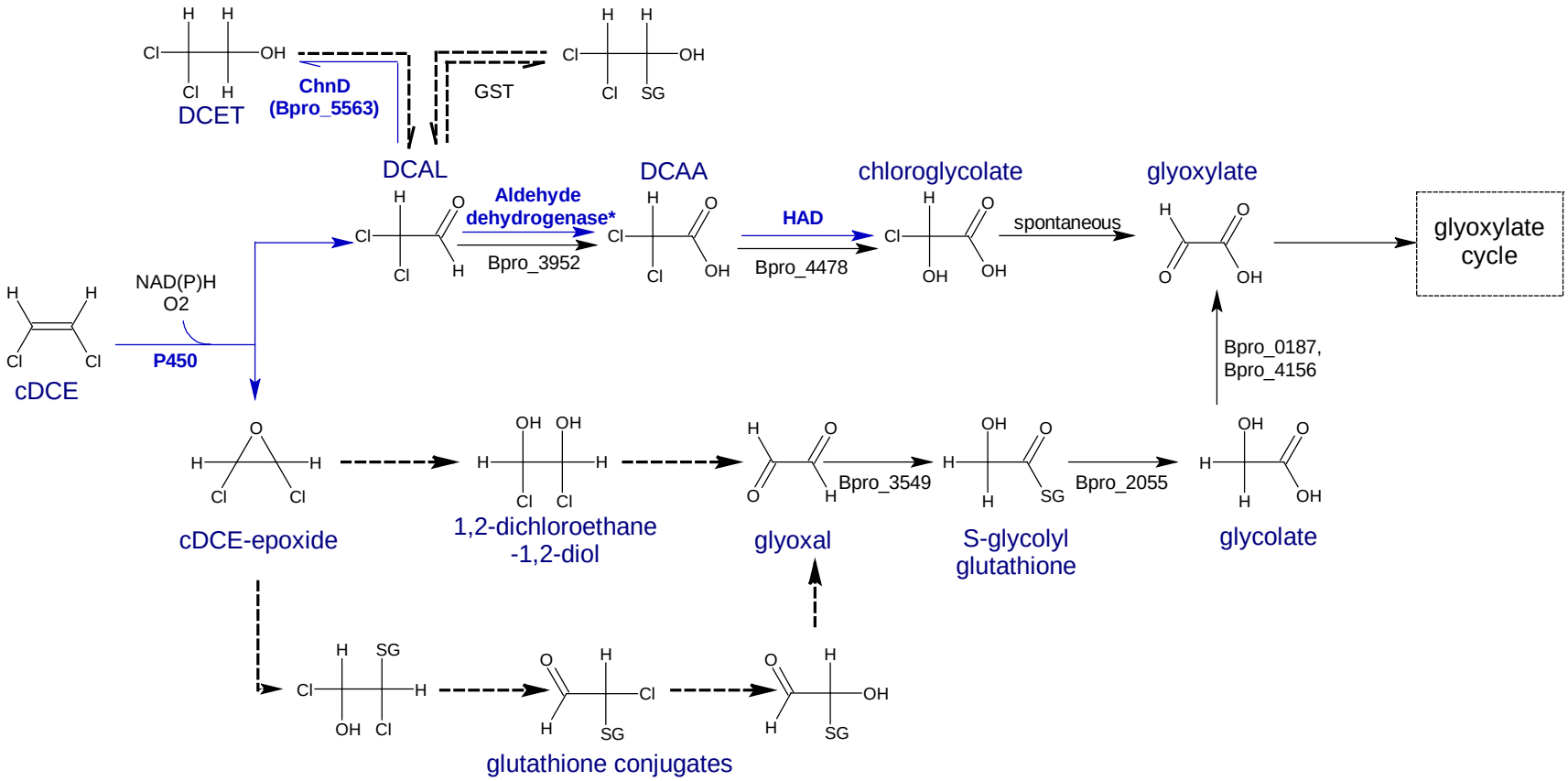

Figure 5.1. Updated proposed cDCE-degradation pathway(s) by strain JS666. ChnD (Bpro_5563) = zinc-binding alcohol dehydrogenase; Bpro_3952 = aldehyde dehydrogenase; Bpro_4478 = hydrolase; Bpro_3549 = glyoxylase I; Bpro_2055 = hydroxyacylglutathione hydrolase (glyoxylase II); Bpro_0187 = glycolate oxidase; Bpro_4156 = D-2-hydroxyacid dehydrogenase. Blue arrows indicate pathways that have been demonstrated with enzymatic assays (in whole-cell *E. coli* or JS666 cell extracts – marked with *). Black arrows indicate pathways that are deduced from iTRAQ study. Dotted arrows indicate pathways that have not been yet elucidated.

CHAPTER 6

6. CONCLUSIONS

6.1 Summary and conclusions

We conclude the following:

(i) Knocking out *chmo* in JS666 conclusively prevented the KO from degrading either cDCE or CYHX (as would be expected); however, it also prevented degradation of cyclohexanol and EtOH. Degradation and growth on CAP (encoded by a hydrolase gene, *chnC*, upstream of the KO insert) was unaffected. This strongly suggests a role for *chmo* and/or either of two dehydrogenases encoded downstream of it in the cyclohexanol-degradation operon.

(ii) iTRAQ studies showed that translation of the adjacent upstream *chnC* (encoding an hydrolase) was lowered significantly, though apparently not so impaired as to prevent the KO strain from growing on CAP. On the other hand, translation of a downstream *chnD* (encoding a dehydrogenase) – and by inference the short-chain dehydrogenase *chnA* whose encoding gene is between *chmo* and *chnD* – was decreased 80-90% in the KO. Though detectable, the lower ChnD and/or ChnA abundances (or effects on their conformation) in the KO strain might explain the loss of its ability to degrade (and grow on) EtOH. By extension, this suggests a role for ChnD and/or ChnA in cDCE degradation, although likely not in carrying out the first step in the process.

(iii) CHMO itself was not demonstrated to be directly involved in the epoxidation of cDCE. So far, we have determined no direct role for this enzyme in cDCE-degradation by strain JS666, though it cannot be said we have proven there is none.

(iv) Hydrolase (Bpro_5566, ChnC) has been successfully cloned and demonstrated activity with CAP, but no activity was yet found with epoxides. ChnD (Bpro_5563, zinc-binding alcohol dehydrogenase), encoded by a gene downstream of *chmo* gene, is capable of transforming DCAL to DCET. It is also active with EtOH and 6-HHA.

(v) We speculate that the elevation of *chmo* expression in the presence of cDCE may be due to the presence of chlorinated alkanal (i.e. DCAL) that induces any operon encoding alcohol dehydrogenases (i.e. ChnA and ChnD), including the cyclohexanol operon of JS666. [Note: DCAL is one of the products of cDCE oxidation by P450, as demonstrated by Shin (2010)].

(vi) We speculate that knocking out *chmo* may have disrupted the NAD^+/NADH ratio, affecting the DCET/DCAA transformation ratio, shifting the reaction towards unfavorable pathways and slowing cDCE oxidation (in the time-frame of our experiments).

(vii) We speculate that knocking out *chmo* affected the regulatory systems that the JS666 strain shares between cyclohexanol and p450 operons.

(viii) When WT and KO cultures were grown on acetate, the presence of cDCE had virtually no effect. It did not impact bacterial growth by either strain, nor was cDCE degraded by either.

(ix) When the strain was grown on cDCE with 10 mM succinate administered as co-substrate, the cultures exhibited “bad behavior” with respect to cDCE-degradation. When CYHX or EtOH was supplied as co-substrate, the cells quickly exhibited cDCE-degradation and sustained it through multiple cDCE additions.

(x) High concentrations of cDCE and the presence of metabolites produced by cDCE oxidation partially inhibited the growth of JS666, even in the presence of co-substrates such as succinate or CAP. JS666’s adaptation to the toxicity of cDCE and/or its metabolites (e.g., cDCE-epoxide) may cause delay in cDCE degradation.

(xi) The observed (cDCE-degradation) lag time in the starvation study or in the cells that were previously grown in acetate, succinate or glycolate could possibly be related to a microbial acclimation phase, where necessary transcriptional expression and enzymatic induction are achieved.

(xii) The addition of succinate provided varied results in alleviating the extended lag in JS666. Succinate-grown cultures of JS666 when supplied with cDCE did not start degrading cDCE until after 15 days. On the other hand, in CYHX-grown cultures, the addition of succinate helped inititate cDCE degradation. This implies that the growth on CYHX induced enzymes responsible for cDCE-degradation and addition of succinate provided ATP and/or cofactors for initial attack on cDCE or carbon for enzyme synthesis/repair.

(xiii) Detoxification mechanisms of cDCE-metabolites in strain JS666 have not been fully studied. Other possible roles for GST (Bpro_0645) that have yet to be tested include metabolite-detoxification by conjugating to epoxide or DCAL.

(xiv) iTRAQ revealed several proteins that may be involved in cDCE-degradation pathways, such as an aldehyde dehydrogenase (Bpro_3952) and enzymes involved in glyoxal metabolism. This also supports the idea of glyoxal formation from hydrolysis of cDCE-epoxide.

(xv) Our iTRAQ study also confirms that HAD, not P450, is a prime candidate for bioindicator for cDCE-degradation, even though P450 initiates the attack on cDCE.

(xvi) Isocitrate lyase expression was reduced in cDCE-degrading cells indicating that possible flux of glyoxylate formation through dehalogenation of DCAA and hydrolysis of cDCE-epoxide.

(xvii) Several proteins involved in glutathione synthesis were moderately elevated by cDCE-degradation. Proteins involved in glyoxylate metabolism were highly elevated in the WT cells degrading CAP+cDCE vs. WT cells degrading CAP.

(xviii) cDCE-degradation pathways in JS666 were updated with new information gathered from our enzymatic and iTRAQ studies.

6.2 Suggestions for future studies

6.2.1 Improving overexpression of enzymes in the cyclohexanol operon and others.

The dehydrogenases' activities can be better characterized by conducting the assays with purified enzymes. The purified enzymes should be then tested with substrates such as acetaldehyde, EtOH, 2-chloroethanol, DCET, chloroacetaldehyde, and DCAL, among others. This will avoid the interconversion of aldehydes to alcohols by the *E. coli* cells as demonstrated in our results. Apart from cyclic ketones, CHMO also should be tested on hydrazine, tertiary amines and organic sulfur compounds, expanding the roles of CHMO from strain JS666 in biocatalysis and bioremediation processes. CHMO can be co-expressed with molecular chaperones and subsequently purified for a better characterization of the enzyme. The induction of GST (Bpro_0645) in omic studies is yet to be elucidated. The purified enzyme should be tested with cDCE-epoxide, DCAL and other chlorinated aliphatic byproducts.

From iTRAQ work, several cDCE-induced proteins may be involved in cDCE degradation, such as aldehyde dehydrogenase (Bpro_3952) and several hydrolases (Bpro_4478 and Bpro_5259). Preliminary results with Bpro_4478 showed no activity with cDCE-epoxide (above the significant activity of the controls), nonetheless the epoxide should also be tested with purified enzyme. In strain JS666, an adjacent gene to the P450 system is a pyrrolo-quinoline-quinone containing alcohol dehydrogenase (PQQ, Bpro_5302) which shares 50% amino-acid identity with an alcohol dehydrogenase from *Pseudomonas stutzeri*. This enzyme was postulated to catalyze the oxidation of

chloroethanol (Dijk et al., 2004) and can be tested in future studies, alongside aldehyde dehydrogenase (Bpro_4570).

The fate of DCAL in strain JS666 should be further investigated. This will provide clear evidence on how the pathways are shifting. Several co-substrates can be administered along with DCAL to study the effects of different substrates on DCAL degradation and will further answer why EtOH sped up the cDCE degradation while succinate slowed it down, when both substrates provide reduced cofactors for cDCE degradation.

6.2.2 Epoxidation of chlorinated compounds by chemically-synthesized hydroperoxyflavin

The epoxidation of cDCE by hydroperoxyflavin can be tested by reacting chemically synthesized 4a-hydroperoxy 5-ethyl 3-methyllumiflavin (compound 6.1.1 in Figure 6.1) and cDCE. The synthesis of compound 6.1.1 can be viewed in the original paper by Kemal and Bruice (1976) through a series of chemical syntheses. Figure 6.1 shows an example of epoxidation of an alkene by flavin hydroperoxide by reacting 2,3-dimethyl 2-butene and compound 40.1 in $CHCl_3$ yielding up to 50% of epoxialkane and 18% of flavin's corresponding alcohol (Bruice et al., 1983). This study will confirm the epoxidation ability of FMOs (including CHMO). If the chemical epoxidation from the above-mentioned experiment were successful; and in order to understand the unsuccessful attempts of cDCE epoxidation by CHMO, several considerations should be further analyzed: (i) the conformation of the CHMO, (ii) post-translational modification of the enzyme and (iii) the optimal conditions for the enzymatic assays.

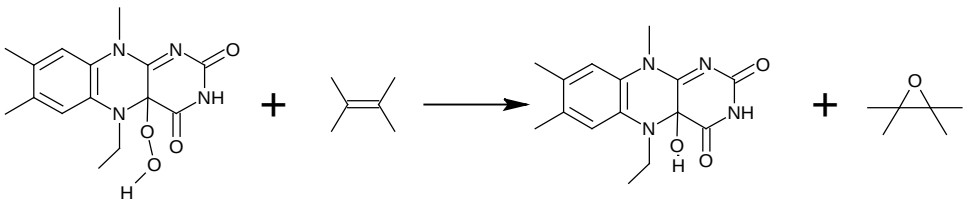

Figure 6.1. 4a-hydroperoxy 5-ethyl 3-methyllumiflavin was reacted with 2,3-dimethyl 2-butene producing corresponding epoxide and flavin's corresponding alcohol (Bruice et al., 1983).

6.2.3 Protein and mRNA relationships during cDCE-oxidation by strain JS666

Transcriptional and translational changes in both WT and KO strains can be better understood by coupling iTRAQ with microarray studies. From both transcriptomic and proteomic analyses, we will gain comprehensive understanding about the initial response of both strains towards cDCE and its degradation products, the correlation between proteins and mRNAs and enzymatic activity on cDCE, its products and on different biological conditions such as pH, temperature and oxidative substrates.

CHAPTER 7

7. APPENDICES

Appendix A: Sequencing results for *chmo*-knockout mutant

The original *chmo* gene sequence is presented below. Underlined is ocmoF primer sequence and the highlighted sequence is the internal part that has been cloned into pVIK110 (suicide vector):

atgaccctggcaacacaagacagccacccaacccagaccgactacgacgcggtggtcgtgggtgccggcttcggcggactctacat
gctgcacaaactgcgcaacgagctcggcatgaacgttcgcgtctttgacaaggccggcgacgtcggcggcacctggtactggaacc
gctaccccggcgccctgtccgacaccgagagctttgtgtactgctactcattcgacaaagccctgctgcaggaatggcagtgggaca
cgcgctacgtcacgcagccgcagattctgtcttacctgaaccacgtggcggaccggctggacctgcgccgcgacatcgagttcaaca
ccggcgtcacgggcgcccggtttgatgaaaagcgcaatctctgg**gaaatccagaccgataccga**taaaaccgtcacggccagata
cctgatcacggcactgggcctgctgtcggccaccaacgtgc**ccaacatcaagggcatcgagactt**tccagggtgcgcaataccata
ccggcgcctggcctgaaggcgttgatttcaagggcaagcgggtcggcgtcattggcaccggctccaccggccttcaggtgatcacgg
ctctcgccccgcaggccagccacctgacggtattccagcgctcgccgcagtacagtgtgccggtcggcaacggcccggtcagcccg
gactacgtcaagtccgtcaaacagaactacgagcagatctggaaggacgtgcgcagctcggtggtggccttcggcttcaaggagag
cagcgtgccggccatgagcgtgtcggaagaagagcgccgcgccgtttaccagaaagcctgggacaccggcggcggctttcgcttca
tgtttgaaacctttgc**gacattgccaccagcgaaga**agccaacgaaaccgccgctgcgttcattcgcggcaagatcgccgagattg
tcaaagacccggaaactgcccgcaagctgacaccgaccgacctgtatgccaagcggccgctgtgtgacagcggctactacgccatt
tacaaccgtgacaatgtcgccttggtcgatgtcaaggcgaccccgattaccgaaatcacgcccaggggcatcaagacgtcggacgg
cgtggaacacgaattggacgtgctgatcttcgccaccggctttgacgcggtggacggcaactacaccaaaattgacctgcgcgggc
gcaacggcaagacgatcaaggacaagtggaaagccggcccgaccagctacctgggcgtggcgagcgcggactacccgaacttgt
tcatgatcctcggacccaacggcccttcaccaacctcccgccgagcatcgagacgcaggtcgagtggatctccgatctgatcaagc
acatgaacgacaccggccgccagctcgttgaagccacccacgaaggcgaagacggctggaccgccacctgcaacgaaattgccg
gctacacgctgttcccgaaagccgattcgtggatcttcggcgcgaacatcccgggcaaagccaggacagtgatgttttacctggccg
gcctgggagcctacactcaaaaactgaacgaggtgacgagcaccggctacccaggttttgagatccgctaa

A part of pVIK110 sequence is provided below. The double-underlined sequence is the VXR primer sequence in reverse. The underlined sequences are restriction enzyme sites used for cloning (XbaI and SalI, respectively):

gaattcccgggagagctcgatatcgcatgcggtacc**tctaga**agaagcttgggatccgtcgaccggggatcc**gtcgac**ctgcagcc
aagcttnnngtcgttttacaacgtcgtgactgggaaaaccctggcgttacccaacttaatcgccttgcagcacatccccctttcgcca
gctggcgtaatagcgaagaggcccgcaccgatcgcccttcccaacagttgcgcagcctgaatggcgaatggcgctttgcctggtttc
cggcaccagaagcggtgccggaaagctggctggagtgcgatcttcctgaggccgatactgtcgtcgtcccctcaaactggcagatg
cacggttacgatgcgcccatctacaccaacgta**acctatcccattacggtcaa**tccgccgtttgttcccacggagaatccgacgggtt
gttactcgctcacatttaatgttgatgaaagctggctacaggaaggccagacgcgaattatttttgatggcgttaactcggcgtttcat
ctgtggtgcaacgggcgctgggtcggttacggccaggacagtcgtttgccgtctgaatttgacctgagcgcatttttacgcgccggag
aaaaccgcctcgcggtgatggtgctgcgttggagtgacggcagttatc

After recombination, the sequence of the *chmo* gene will be theoretically as follows, where the resulting PCR band will be from the dotted- to the double-underlined sequences.

atgaccctggcaacacaagacagccacccaacccagaccgactacgacgcggtggtcgtgggtgccggcttcggcggactctacat
gctgcacaaactgcgcaacgagctcggcatgaacgttcgcgtctttgacaaggccggcgacgtcggcggcacctggtactggaacc
gctaccccggcgccctgtccgacaccgagagctttgtgtactgctactcattcgacaaagccctgctgcaggaatggcagtgggaca
cgcgctacgtcacgcagccgcagattctgtcttacctgaaccacgtggcggaccggctggacctgcgccgcgacatcgagttcaaca
ccggcgtcacgggcgcccggtttgatgaaaagcgcaatctctgg**gaaatccagaccgataccga**taaaaccgtcacggccagata
cctgatcacggcactgggcctgctgtcggccaccaacgtgc**ccaacatcaagggcatcgagactt**tccagggtgcgcaataccata
ccggcgcctggcctgaaggcgttgatttcaagggcaagcgggtcggcgtcattggcaccggctccaccggccttcaggtgatcacgg
ctctcgccccgcaggccagccacctgacggtattccagcgctcgccgcagtacagtgtgccggtcggcaacggcccggtcagcccg
gactacgtcaagtccgtcaaacagaactacgagcagatctggaaggacgtgcgcagctcggtggtggccttcggcttcaaggagag
cagcgtgccggccatgagcgtgtcggaagaagagcgccgcgccgtttaccagaaagcctgggacaccggcggcggctttcgcttca
tgtttgaaacctttgc**gacattgccaccagcgaaga**gtcgac**ctgcagccaagcttnnngtcgttttacaacgtcgtgactgggaa
aaccctggcgttacccaacttaatcgccttgcagcacatccccctttcgccagctggcgtaatagcgaagaggcccgcaccgatcgc
ccttcccaacagttgcgcagcctgaatggcgaatggcgctttgcctggtttccggcaccagaagcggtgccggaaagctggctggag
tgcgatcttcctgaggccgatactgtcgtcgtcccctcaaactggcagatgcacggttacgatgcgcccatctacaccaacgta**acct
atcccattacggtcaa**tccgccgtttgttcccacggagaatccgacgggttgttactcgctcacatttaatgttgatgaaagctggcta
caggaaggccagacgcgaattatttttgatggcgttaactcggcgtttcatctgtggtgcaacgggcgctgggtcggttacggccag
gacagtcgtttgccgtctgaatttgacctgagcgcatttttacgcgccggagaaaaccgcctcgcggtgatggtgctgcgttggagtg
acggcagttatc

This is the result of the sequence using the forward primer ocmoF.

>83_1390366__091.ab1
CACGCNANCTGAT**ACGGCACTGGGCC**TGCTGTCGGCCACCAACGTGCCCAACATCAAGGGCATCG
AGACTTTCCAGGGTGCGCAATACCATACCGGCGCCTGGCCTGAAGGCGTTGATTTCAAGGGCAAG
CGGGTCGGCGTCATTGGCACCGGCTCCACCGGCCTTCAGGTGATCACGGCTCTCGCCCCGCAGGCC
AGCCACCTGACGGTATTCCAGCGCTCGCCGCAGTACAGTGTGCCGGTCGGCAACGGCCCGGTCAG
CCCGGACTACGTCAAGTCCGTCAAACAGAACTACGAGCAGATCTGGAAGGACGTGCGCAGCTCGG
TGGTGGCCTTCGGCTTCAAGGAGAGCAGCGTGCCGGCCATGAGCGTGTCGGAAGAAGAGCGCCG
CGCCGTTTACCAGAAAGCCTGGGACACCGGCGGCGGCTTTCGCTTCATGTTTGAAACCTTTTGCGA
CATTGCCACCAGCGAAGAAGTCGACCTGCAGCCAAGCTTGCTCCCGTCGTTTTACAACGTCGTGACT
GGGAAAACCCTGGCGTTACCCAACTTAATCGCCTTGCAGCACATCCCCCTTTCGCCAGCTGGCGTAA
TAGCGAAGAGGCCCGCACCGATCGCCCTTCCCAACAGTTGCGCAGCCTGAATGGCGAATGGCGCTT
TGCCTGGTTTC**CGGCACCAGAA**GCGGTGCCGGAAAGCTGGCTGGAGTGCGATCTTCCTGAGGCCG
ATACTGTCGTCGTCCCCTCAAACTGGCAGATGCACGGTTACGATGCGCCCATCTACACCAACGTGAC
CTATCCCATTNACGGNTCAAAANNTNNNNNTTTNNNNTTNNNTNNNNTTTNTNNNNNNNNNNT
NTNNNNTNNNNNTTNNNTTTATNTTNTTNTTTTTNTNTNNTNNNNNNTTTNNNTNNNNNNTNTN
TNNNNNNNTNNNNNTTTNTTNTNTNNNNTTNNTANNNNNTTTTNNNNNNNNNANNNTANTNN
TTTNTNTNNTNTNNNTNNTNNTNNTNTTTTTNNNTANTTNNNNNNNNTTNTNTNNTNNNNTNNT
NNTNNNTNTNTNTNNNNTTNTTNTTTNTNTTTNTTNTNNTNTNNNTNNTTTANNNNNNTCTTTTNNT
NTTTATCNNNNTTTTTNNN

And this is using the reverse primer VXR

>84_1390367__089.ab1
NGGTAGGCGCATGATACCGTGCATCTGCCAGTTTTGAGGGGACGACGACAGCTATCGGCCTCAGGA
AGATCGCACTCCAGCCAGCTTTCCGGCACCGCGTTCTGGTGCCGGAAACCAGGCAAAGCGCCATTCG
CCATTCAGGCTGCGCAACTGTTGGGAAGGGCGATCGGTGCGGGCCTCTTCGCTATTACGCCAGCTG
GCGAAAGGGGGATGTGCTGCAAGGCGATTAAGTTGGGTAACGCCAGGGTTTTCCCAGTCACGACGT
TGTAAAACGACGGGAGCAAGCTTGGCTGCAGGTCGACTTCTTCGCTGGTGGCAATGTCGCAAAAGG
TTTCAAACATGAAGCGAAAGCCGCCGCCGGTGTCCCAGGCTTTCTGGTAAACNGCGCGGCGCTCTTC
TTCCGACACGCTCATGGCCGGCACGCTGCTCTCCTTGAAGCCGAAGGCCACCACCGAGCTGCGCACG
TCCTTCCAGATCTGCTCGTAGTTCTGTTTGACGGACTTGACGTAGTCCGGGCTGACCGGGCCGTTGC
CNACCGGCACACTGTACTGCGGCGAGCGCTGGAATACCGTCAGGTGGCTGGCCTGCGGGGCGAGA
GCCGTGATCACCTGAAGGCCGGTGGAGCCGGTGCCAATGACGCCGACCCGCTTGCCCTTGAAATCA
ACGCCTTCAGGCCAGGCGCCGGTATGGTATTGCGCACCCTGGAAAGTCTCGATGCCCTTGATGTTGG
GCACGTTGGTGGCCGACAGCAGGCCCAGTGCCGTGATCAGGTATCTGGCCGTGACGGTTTTATCGG
TATCGGTCCTGGATTTCAANNNNNNNNNNNTTNTNNNATNTNTCTNNTANANTATANTNCANATT
NTTNTTTTTTNNTNTNTNTTTNTNNNNTTAANTTTTTTTNNCTTANATTTATTTCTAANNNANCNAN
NNTTTNTTANNNANTNAGNTNNNCATTTANNATTTNTTTAANTTANTTTNTNTNNTTTANNTTNNT
ATNTTANTNATTTCNTTNNCATNNNANNNTATTNAANNANNTNNTTATNTTNATNNNTNATTTTNN
NNANTNNTTNANNNTNNTNCNTTCNATNNTTNTNTNTTTTTTATNCAATTNNTTNANATATNTACT
TNATNTTCTATAANTCTATTNTTNAA

The result of alignment of the sequence using the ocmoF primer and the resulting band sequence gives:

```
>lcl|4411
Length=837
Score = 1417 bits (767),  Expect = 0.0
Identities = 790/801 (98%), Gaps = 7/801 (0%)
Strand=Plus/Plus
Query  9     CTGAT-ACGGCACTGGGCCTGCTGTCGGCCACCAACGTGCCCAACATCAAGGGCATCGAG  67
             ||||| ||||||||||||||||||||||||||||||||||||||||||||||||||||||
Sbjct  433   CTGATCACGGCACTGGGCCTGCTGTCGGCCACCAACGTGCCCAACATCAAGGGCATCGAG  492

Query  68    ACTTTCCAGGGTGCGCAATACCATACCGGCGCCTGGCCTGAAGGCGTTGATTTCAAGGGC  127
             ||||||||||||||||||||||||||||||||||||||||||||||||||||||||||||
Sbjct  493   ACTTTCCAGGGTGCGCAATACCATACCGGCGCCTGGCCTGAAGGCGTTGATTTCAAGGGC  552

Query  128   AAGCGGGTCGGCGTCATTGGCACCGGCTCCACCGGCCTTCAGGTGATCACGGCTCTCGCC  187
             ||||||||||||||||||||||||||||||||||||||||||||||||||||||||||||
Sbjct  553   AAGCGGGTCGGCGTCATTGGCACCGGCTCCACCGGCCTTCAGGTGATCACGGCTCTCGCC  612

Query  188   CCGCAGGCCAGCCACCTGACGGTATTCCAGCGCTCGCCGCAGTACAGTGTGCCGGTCGGC  247
             ||||||||||||||||||||||||||||||||||||||||||||||||||||||||||||
Sbjct  613   CCGCAGGCCAGCCACCTGACGGTATTCCAGCGCTCGCCGCAGTACAGTGTGCCGGTCGGC  672

Query  248   AACGGCCCGGTCAGCCCGGACTACGTCAAGTCCGTCAAACAGAACTACGAGCAGATCTGG  307
             ||||||||||||||||||||||||||||||||||||||||||||||||||||||||||||
Sbjct  673   AACGGCCCGGTCAGCCCGGACTACGTCAAGTCCGTCAAACAGAACTACGAGCAGATCTGG  732

Query  308   AAGGACGTGCGCAGCTCGGTGGTGGCCTTCGGCTTCAAGGAGAGCAGCGTGCCGGCCATG  367
             ||||||||||||||||||||||||||||||||||||||||||||||||||||||||||||
Sbjct  733   AAGGACGTGCGCAGCTCGGTGGTGGCCTTCGGCTTCAAGGAGAGCAGCGTGCCGGCCATG  792

Query  368   AGCGTGTCGGAAGAAGAGCGCCGCGCCGTTTACCAGAAAGCCTGGGACACCGGCGGCGGC  427
             ||||||||||||||||||||||||||||||||||||||||||||||||||||||||||||
Sbjct  793   AGCGTGTCGGAAGAAGAGCGCCGCGCCGTTTACCAGAAAGCCTGGGACACCGGCGGCGGC  852

Query  428   TTTCGCTTCATGTTTGAAACCTTTTGCGACATTGCCACCAGCGAAGAAGTCGACCTGCAG  487
             |||||||||||||||||||||||||||||||||||||||||||||| ||||||||||||||
Sbjct  853   TTTCGCTTCATGTTTGAAACCTTTTGCGACATTGCCACCAGCGAAG-AGTCGACCTGCAG  911

Query  488   CCAAGCTTGCTCCCGTCGTTTTACAACGTCGTGACTGGGAAAACCCTGGCGTTACCCAAC  547
             |||||| |  |   ||||||||||||||||||||||||||||||||||||||||||||||
Sbjct  912   CCAAGC-T--TNNNGTCGTTTTACAACGTCGTGACTGGGAAAACCCTGGCGTTACCCAAC  968

Query  548   TTAATCGCCTTGCAGCACATCCCCCTTTCGCCAGCTGGCGTAATAGCGAAGAGGCCCGCA  607
             ||||||||||||||||||||||||||||||||||||||||||||||||||||||||||||
Sbjct  969   TTAATCGCCTTGCAGCACATCCCCCTTTCGCCAGCTGGCGTAATAGCGAAGAGGCCCGCA  1028

Query  608   CCGATCGCCCTTCCCAACAGTTGCGCAGCCTGAATGGCGAATGGCGCTTTGCCTGGTTTC  667
             ||||||||||||||||||||||||||||||||||||||||||||||||||||||||||||
Sbjct  1029  CCGATCGCCCTTCCCAACAGTTGCGCAGCCTGAATGGCGAATGGCGCTTTGCCTGGTTTC  1088

Query  668   CGGCACCAGAAGCGGTGCCGGAAAGCTGGCTGGAGTGCGATCTTCCTGAGGCCGATACTG  727
             ||||||||||||||||||||||||||||||||||||||||||||||||||||||||||||
Sbjct  1089  CGGCACCAGAAGCGGTGCCGGAAAGCTGGCTGGAGTGCGATCTTCCTGAGGCCGATACTG  1148

Query  728   TCGTCGTCCCCTCAAACTGGCAGATGCACGGTTACGATGCGCCCATCTACACCAACGTGA  787
             |||||||||||||||||||||||||||||||||||||||||||||||||||||||||| |
Sbjct  1149  TCGTCGTCCCCTCAAACTGGCAGATGCACGGTTACGATGCGCCCATCTACACCAACGTAA  1208
```

```
Query  788   CCTATCCCATTNACGGNTCaa  808
             |||||||||| |||| ||||
Sbjct  1209  CCTATCCCATT-ACGG-TCAA  1227
```

Starting from:

gaaatccagaccgataccgataaaaccgtcacggccagatacctgatc**acggcactgggcc**tgctgtcggccaccaacgtgc
ccaacatcaagggcatcgagactttccagggtgcgcaataccataccggcgcctggcctgaaggcgttgatttcaagggcaa
gcgggtcggcgtcattggcaccggctccaccggccttcaggtgatcacggctctcgccccgcaggccagccacctgacggtat
tccagcgctcgccgcagtacagtgtgccggtcggcaacggcccggtcagcccggactacgtcaagtccgtcaaacagaacta
cgagcagatctggaaggacgtgcgcagctcggtggtggccttcggcttcaaggagagcagcgtgccggccatgagcgtgtcg
gaagaagagcgccgcgccgtttaccagaaagcctgggacaccggcggcggctttcgcttcatgtttgaaacctttgc**gacat**
tgccaccagcgaagaa**gtcgac**ctgcagccaagcttgctcccgtcgttttacaacgtcgtgactgggaaaaccctggcgttac
ccaacttaatcgccttgcagcacatccccctttcgccagctggcgtaatagcgaagaggcccgcaccgatcgcccttcccaac
agttgcgcagcctgaatggcgaatggcgctttgcctggtttc**cggcaccagaa**gcggtgccggaaagctggctggagtgcgat
cttcctgaggccgatactgtcgtcgtcccctcaaactggcagatgcacggttacgatgcgcccatctacaccaacgta**acctat**
cccattacggtcaa

Underlined nucleotide indicates an insertion. Highlighted sequence indicates the alignment results of theoretical and actual sequences. Note that the sequence started before the insert (between two bolded sequences). Red nucleotide sequence corresponds to that of in the result above. Alignment result using the reverse primer was not shown.

Appendix B: Synthesis of epoxides using peracid and identification of the GC peaks

Peracid epoxidation of chlorinated ethenes has been commonly utilized in many studies as confirmation of compound elution in gas chromatography methods. TCE, VC and DCEs have been reacted with mCPBA and yielded their corresponding epoxides. In one study, 1,1-DCE-epoxide was chemically synthesized by reacting its parent compound with mCPBA at 60°C for 3 hours (Liebler and Guengerich, 1983). A similar approach was used to synthesize *trans*-DCE-epoxide (Janssen et al., 1988) and cDCE-epoxide (Verce et al., 2002). Epoxide can also be synthesized at low temperature, such as in one study where octene-1,2-oxide was synthesized at 0°C (Guengerich and Mason, 1980).

The chemical synthesis of epoxide is useful to confirm the GC elution times of epoxide peaks resulting from oxidation of chlorinated ethenes by monooxygenases. In our studies, the distilled mixture from the synthesis was also used to provide epoxide substrate for hydrolase enzymatic assays. DCEs were reacted with mCPBA at 50 – 60°C until the formation of a white precipitate of chlorobenzoic acid was observed. Several peaks were detected through GC-FID (equipped with an 8-ft x 1/8-inch stainless-steel column packed with 1% SP-1000 on 60/80 Carbopack B (Supelco), isothermal run at 160°C, 30 mL/min N_2); and by process of elimination, the peaks corresponding to expected residual starting materials, impurities and byproducts (e.g., chlorobenzene) could be identified, most of which either eluted after the normal monitoring period or not at all, with the column employed. After eliminating these, we found there remained two unattributed peaks (at retention times of 2.8 min and 3.5 min, with the earlier peak being

much larger than the later one), whether the starting substrate was cDCE or tDCE. Both peaks had highly similar, DCE-epoxide-like mass spectra. The presence of two peaks may indicate the formation of both *cis*- and *trans*-cDCE isomers during synthesis. The synthesis of tDCE-epoxide yielded peaks with similar retention times and similar relative sizes (Figure B1 and Figure B2).

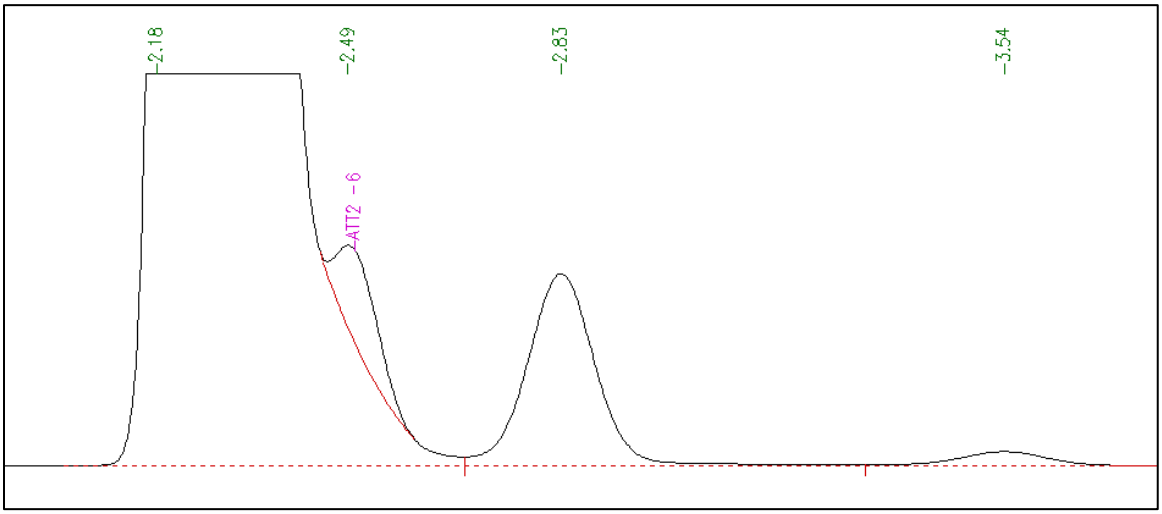

Figure B.1. GC result from product of cDCE epoxidation (headspace of vapor above the organic mixture injection to packed column). Peak assignments: 2.18 min (remaining cDCE); 2.49 min (probably MEHQ stabilizer in the cDCE stock, since it's present in vapors above cDCE-only); 2.83 min (putative DCE epoxide); 3.54 min (putative DCE epoxide).

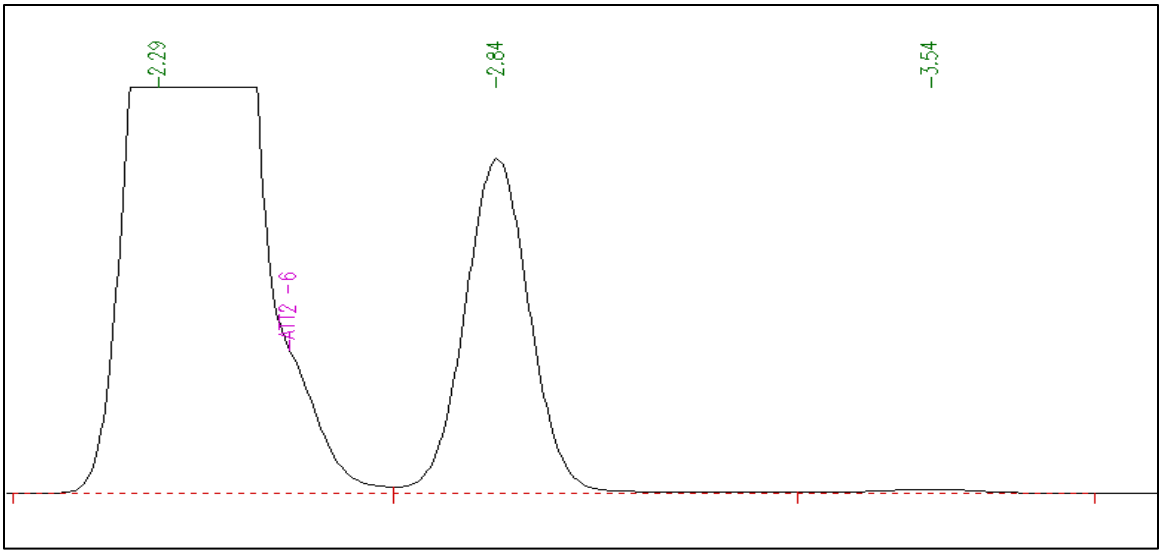

Figure B.2. GC result from product of tDCE epoxidation (headspace of vapor above the organic mixture injection to packed column). Peak assignments: 2.29 min (remaining tDCE); 2.84 min (putative DCE epoxide); 3.54 min (putative DCE epoxide).

DCE-epoxides were confirmed by GC-MS equipped with a DB-5ms column in other studies (Verce et al., 2002; Shin, 2010) and also in our study (Figures B3 and B4). The mass spectra of DCE-epoxides were originally reported by Griesbaum and co-workers (Griesbaum et al., 1975), and similar observations were reported by other researchers (Janssen et al., 1988; van Hylckama Vlieg et al., 1996). The mass spectrum of cDCE-epoxide contains several significant peaks at lower mass than the molecular ion (*m/e* 112), i.e. at *m/e* 83 ($CHCl_2^+$), 77 ($C_2H_2OCl^+$), 48 ($HCCl^+$) and 29 (HCO^+). The mass spectral fragmentation of epoxides may share similarities with their behavior under pyrolytic and photolytic conditions. Both pyrolysis and photolysis of epoxyethane produce methyl and formyl radicals, presumably through the formation of acetaldehyde. Correspondingly, three significant peaks were reported for epoxyethane, at *m/e* 44 (M^+),

29 (CHO^+) and 15 (CH_3^+). Detailed review of mass spectrometry of aliphatic epoxides can be found elsewhere (Brown et al., 1966).

Some researchers hypothesize that during epoxidation by peracid, the oxygen atom is added in a concerted manner involving a symmetrical transition state (i.e. to both olefinic carbons simultaneously), whereas other researchers have provided evidence for asymmetrical epoxidation (i.e., initially involving O attack at only one carbon). In that case, it is possible that during the insertion of an oxygen molecule, thermal motion enables C–C rotation to occur, thus enabling production of both epoxide isomers. One of the isomers may be preferential during chemical synthesis — regardless of whether the starting material is cDCE or tDCE. Biological epoxidation, however, might preserve isomerism of the initial DCE substrate.

In addition to the epoxides, chlorobenzene was identified (not shown in Figures B1 and B2, which focus only on earlier-eluting peaks) in DCE-epoxide synthesis, which was also detected during other peracid reactions (Ray et al., 2008). Another possibility of a compound having similar mass to DCE-epoxide is 1,2-dichloroethenol (ClHC=CClOH) or 2,2-dichloroethenol ($Cl_2C=CH_2$). Incomplete oxygen molecule insertion may result in such byproducts; nonetheless this assumption is merely speculative and more investigations would have to be made to confirm this.

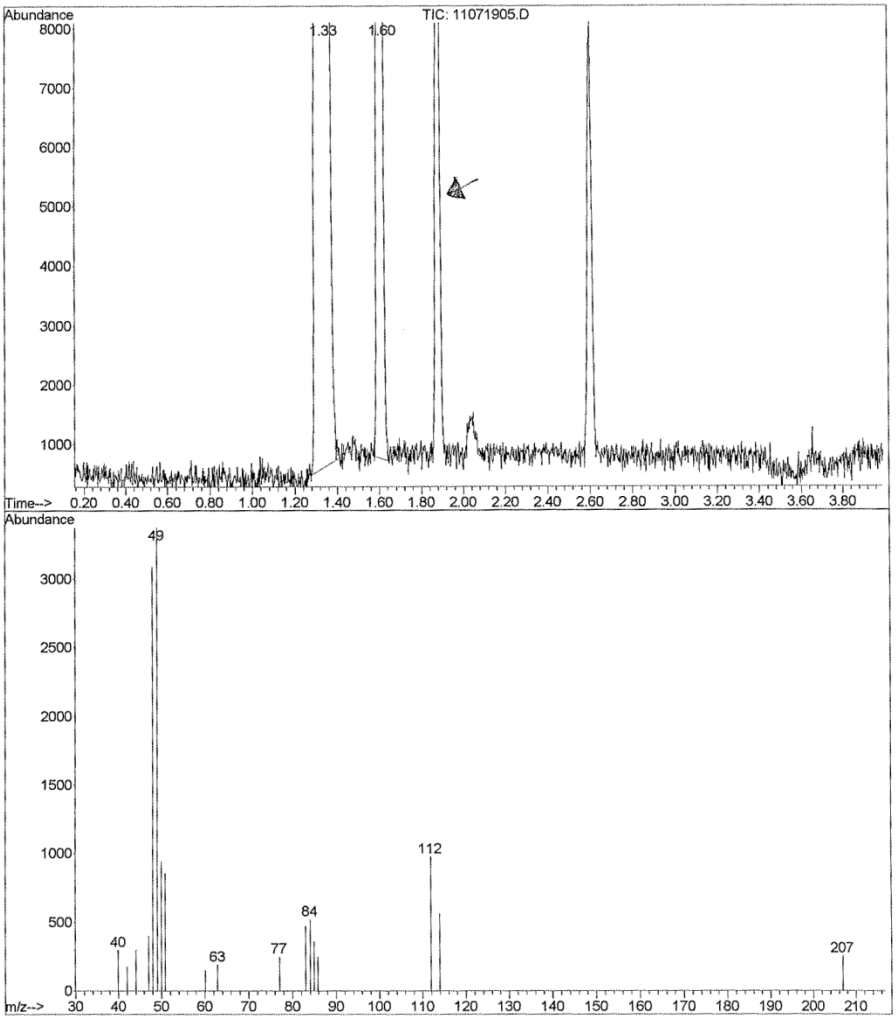

Figure B.3. Chromatography and spectrometry profiles of the chemically synthesized cDCE-epoxide (headspace of vapor above the organic mixture injection) by the GC-MS equipped with a DB-5ms column. The arrow shows the first epoxide peak with its mass spec profile at the bottom.

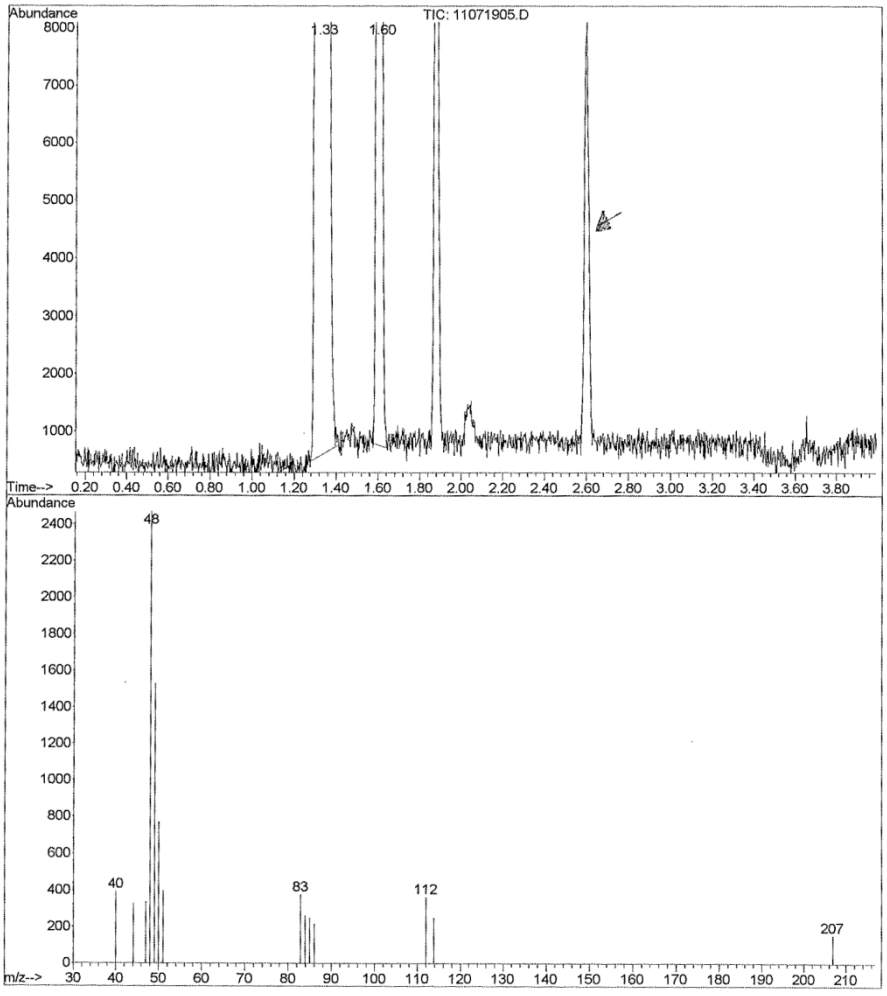

Figure B.4. Chromatography and spectrometry profiles of the chemically synthesized cDCE-epoxide (headspace of vapor above the organic mixture injection) by the GC-MS equipped with a DB-5ms column. The arrow shows the second epoxide peak with its mass spec profile at the bottom.

The DCE epoxides produced are expected to be relatively stable at neutral pH with a reported half-life of about 72 hours (Janssen et al., 1988), as opposed to the half-lives of VC-epoxide and TCE-epoxide, which are 78 and 21 seconds, respectively (van Hylckama Vlieg et al., 1996). Abiotic transformation of VC-epoxide to glycolaldehyde was reported by Guengerich et al. (1979). The abiotic release of chloride ions from cDCE-epoxide has also been demonstrated (Canada et al., 2002b). In our study, the abiotic rearrangement of DCE-epoxide was studied by monitoring the disappearance of both GC-peaks and the formation of chloride ions as follows. Ten microliters of DCE-epoxide synthesis mixture (from cDCE as starting substrate) was injected into 50 mL chloride-free phosphate buffer (20 mM, pH 7.2). 1 mL of headspace was drawn out for GC measurements (of DCE-epoxides), and 3 mL of liquid was sampled for triplicate measurements of chloride ions. After almost 18 hours of incubation, approximately 6 times the initial chloride concentration was measured (Figure B5). Both putative DCE-epoxide peaks at 2.8 and 3.5 min were monitored, and after 18 hours, both peaks had diminished approximately 30% from their respective, initial values. The cDCE peak was used as internal standard.

We concluded that, since both peaks have the MS spectrum expected of DCE epoxides and both decay abiotically as expected of DCE epoxides, then both likely represent DCE epoxides.

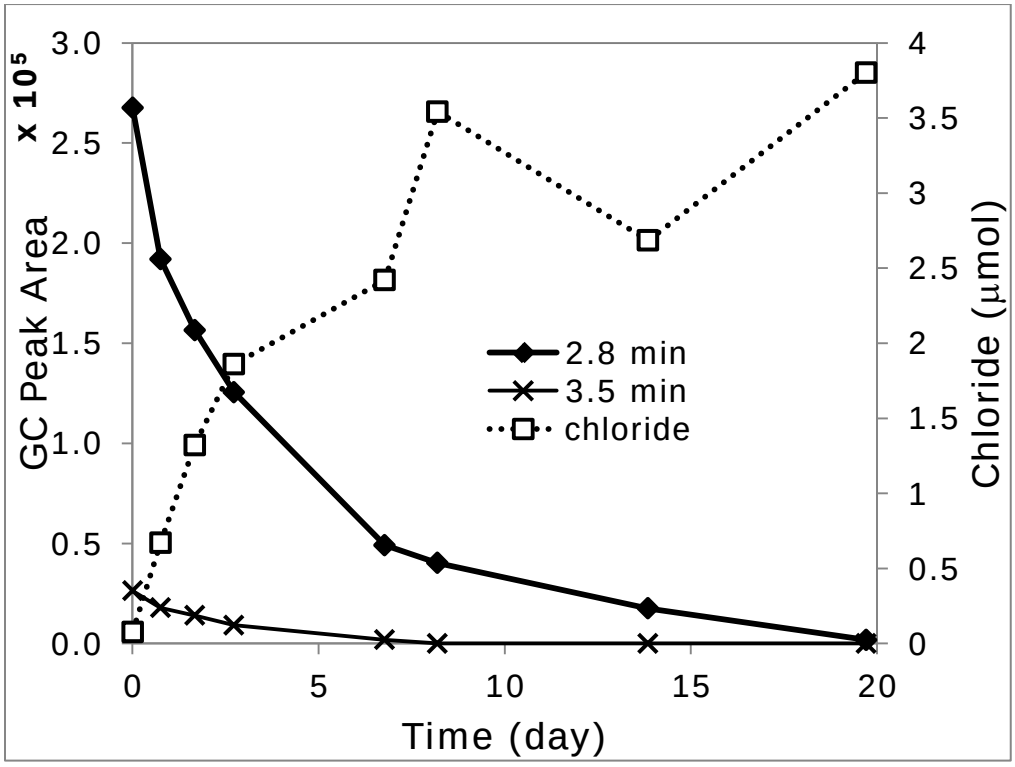

Figure B.5. The disappearance of DCE-epoxide peaks at 2.8 and 3.5 min and the formation of chloride ions.

Appendix C: Protocols for iTRAQ

C.1 Protein digestion and iTRAQ labeling

A total of 100 µg protein of each sample was denatured, reduced with 5 mM tris-(2-carboxylethyl) phosphine at 37 ºC for 1 hour, and the cysteine residues were blocked with 8 mM methyl methanethiosulfonate for 10 min at room temperature. Protein samples were digested with 10 µg of sequence-grade-modified trypsin at 37ºC for 16 hours. Efficiency of protein digestion was assessed by SDS-PAGE using undigested and digested samples. Tryptic peptides from four different samples (WT grown in cDCE and CAP, WT grown in CAP, KO grown in cDCE and CAP, KO grown in CAP) were each labeled with iTRAQ reagents 114, 115, 116, and 117, respectively according to the manufacturer's protocols (document #4351918A and 4350831C downloaded from http://docs.appliedbiosystems.com/search.taf; Applied Biosystems, Foster City, CA). The labeled samples were then combined and fractionated via high pH reverse phase liquid chromatography as described below.

C.2 High pH reverse phase (hpRP) fractionation

The pooled iTRAQ-labeled peptides were pretreated with SCX cartridges (AB Sciex, Framingham, MA) and desalted by Sep-Pak SPE for hpRP separation. The hpRP chromatography was carried out using a Dionex UltiMate 3000 HPLC system with a built-in micro fraction collection option in its autosampler and UV detection (Sunnyvale, CA). The iTRAQ-tagged tryptic peptides were reconstituted in buffer A (20 mM

ammonium formate pH 9.5 in water), and loaded onto an XTerra MS C18 column (3.5 µm, 2.1x150 mm, Waters) with 20 mM ammonium formate (NH_4FA), pH 9.5 as buffer A and 80% ACN/20% 20 mM NH_4FA as buffer B. The LC was performed using a gradient from 10-45% of buffer B in 30 min at a flow rate 200 µL/min.(Gilar et al., 2005a; Gilar et al., 2005b) Forty-eight fractions were collected at 1 min intervals and pooled into a total of 24 fractions based on the UV absorbance at 214 nm. All of the fractions were dried and reconstituted in 20 µL of 2% ACN/0.5% FA for nanoLC-MS/MS analysis**.** Fractions were pooled into the final 10 fractions by disparate first dimension fractions (retention time multiplexing) as reported recently. All ten pooled peptide fractions were dried and reconstituted in 2% ACN, 0.5% formic acid for subsequent nanoLC-MS/MS.

C.3 Nano-scale reverse phase chromatography and tandem mass spectrometry (nanoLC-MS/MS)

The nanoLC-MS/MS analysis was carried out using a LTQ-Orbitrap Velos (Thermo-Fisher Scientific, San Jose, CA) mass spectrometer equipped with nano ion source using high energy collision dissociation (HCD). The Orbitrap was interfaced with an UltiMate3000 RSLCnano system (Dionex, Sunnyvale, CA). An aliquot of hpRP peptide fractions (2.0 – 10.0 µL) was injected onto a PepMap C18 trap column (5 µm, 300 µm × 5 mm, Dionex) at 20 µL/min flow rate for on-line desalting and then separated on a PepMap C-18 RP nano column (3 µm, 75µm x 15cm), and eluted in a 90 min gradient of 5% to 38% acetonitrile (ACN) in 0.1% formic acid at 300 nL/min., followed by a 3-min ramping to 95% ACN-0.1%FA and a 5-min holding at 95% ACN-0.1%FA. The column was re-equilibrated with 2% ACN-0.1%FA for 20 min prior to the next run.

The eluted peptides were detected by Orbitrap through a nano ion source containing a 10-µm analyte emitter (NewObjective, Woburn, MA). The Orbitrap Velos was operated in positive ion mode with nano spray voltage set at 1.5 kV and source temperature at 275 °C. Either internal calibration using the background ion signal at *m/z* 445.120025 as a lock mass or external calibration for FT mass analyzer was performed. The instrument was operated in data-dependent acquisition (DDA) mode using FT mass analyzer for one survey MS scan for precursor ions, followed by ten data-dependent HCD-MS/MS scans for precursor peptides with multiple charged ions above a threshold ion count of 7500 with normalized collision energy of 45%. MS survey scanned at a resolution of 30,000 (fwhm at *m/z* 400), for the mass range of *m/z* 400-1400, and MS/MS scanned at 7,500 resolution for the mass range, *m/z* 100-2000. All data were acquired under Xcalibur 2.1 operation software (Thermo-Fisher Scientific).

C.4 Data processing, protein identification and data analysis

All MS and MS/MS raw spectra from iTRAQ experiments were processed using Proteome Discoverer 1.2 (PD1.2, Thermo), and the spectra from each DDA file were output as an MGF file for subsequent database search using in-house license Mascot Deamon (version 2.3.02, Matrix Science, Boston, MA). The bacterial "protein non-redundancy" sequence database was used, containing 10,348,164 sequence entries downloaded from NCBI (http://www.NCBI.com) on Jan. 21st, 2010. "Combine with customized mutant sequences" was used for database search. The default search settings used for 4-plex iTRAQ quantitative processing and protein identification in Mascot server were: one mis-cleavage for full trypsin with fixed MMTS modification of

cysteine, fixed 4-plex iTRAQ modifications on lysine and N-terminal amines and variable modifications of methionine oxidation and 4-plex iTRAQ on tyrosine.

The peptide mass tolerance and fragment mass tolerance values were 30 ppm and 100 mmu, respectively. To estimate the false discovery rate (FDR) for a measure of identification certainty in each replicate set, an automatic decoy database search was performed in Mascot by choosing the decoy checkbox in which a random sequence of database is generated and tested for raw spectra along with the real database. To reduce the probability of false peptide identification, the significant scores at 99% confidence interval for the peptides defined by a Mascot probability analysis (www.matrixscience.com/help/scoring_help.html#PBM) greater than "identity" were used as a filter and the resulting peptides are considered to be confidently identified peptides and used for protein identifications. Furthermore, proteins identified in all four iTRAQ experiments, which contained at least two peptides with a p value of < 0.001 (expectation value) as determined by Mascot probability analysis were further analyzed. Intensities of the reporter ions from iTRAQ tags upon fragmentation were used for quantification, and the relative quantitation ratios were normalized to the median ratio for the 4-plex in each set of experiments.

Appendix D: iTRAQ Reports

Table D.1. Selected proteins reported in iTRAQ studies. (*) indicates ratio that is significantly different from 1 at a 95% confidence level. Error factors with brackets [ ] indicate that the peptide match ratios do not appear to come from a sample with a normal distribution; p is number of peptides; EF = error factor.

Locus Tag	Protein Description	115/114	p	EF	116/114	p	EF	117/114	p	EF
Bpro_5301	cytochrome P450	1.587	7	1.193*	0.180	7	1.524*	0.370*	7	1.180*
Bpro_5566	hydrolase	10.493	3	1.819*	0.282	3	1.653*	0.485*	3	1.283*
Bpro_5565	flavin-containing monooxygenase FMO	2.994	9	[1.182]	0.140	6	[2.421]	0.148*	7	1.371*
Bpro_5563	zinc-binding alcohol dehydrogenase	0.770	5	1.104*	0.100	5	1.535*	0.139*	5	1.319*
Bpro_5186	haloacid dehalogenase, type II	0.155	12	[1.212]	0.142	12	1.160*	0.150*	12	1.142*
Bpro_0056	haloacid dehalogenase, type II	0.804	2	1.023*	0.651	2	1.007*	0.828	2	1.030
Bpro_2101	isocitrate lyase	2.494	9	[1.088]	2.114	9	1.075*	2.177	9	[1.102]
Bpro_0645	glutathione S-transferase-like	0.724	1	---	0.017	1	---	0.024	1	---
Bpro_0646	pyridoxamine 5'-phosphate oxidase	1.165	1	---	0.450	1	---	0.401	1	---
Bpro_4442	DNA-directed RNA polymerase subunit beta	1.088	22	1.077*	0.949	22	1.090*	0.909	22	[1.088]
Bpro_0086	2,5-dioxopentanoate dehydrogenase (NAD+)	0.738	3	1.022*	0.702	3	1.059*	0.654	3	1.234
Bpro_4478	hydrolase	0.507	1	---	0.806	1	---	1.033	1	---
<u>Aldehyde and alcohol dehydrogenases</u>										
Bpro_3952	aldehyde dehydrogenase	0.385	23	1.081*	0.055	22	1.380*	0.081	23	1.228*
Bpro_2290	aldehyde dehydrogenase	1.141	6	1.046*	1.057	6	1.038*	1.061	6	1.061
Bpro_3422	aldehyde dehydrogenase	1.379	2	1.178	1.038	3	1.136	1.014	2	1.081
Bpro_4691	aldehyde dehydrogenase	0.849	1	---	1.334	1	---	1.329	1	---
Bpro_2298	aldehyde dehydrogenase	0.824	2	1.036	0.828	2	1.481	0.854	2	1.387
Bpro_4702	aldehyde dehydrogenase	0.934	2	1.064	1.377	2	1.482	1.655	2	1.057*
Bpro_3129	zinc-binding alcohol dehydrogenase	0.387	1	---	0.906	1	---	0.757	1	---

Table D.1 (continued)

Locus Tag	Protein Description	115/114	p	EF	116/114	p	EF	117/114	p	EF
Bpro_2526	iron-containing alcohol dehydrogenase	0.546	3	1.178*	0.834	3	1.070*	1.081	3	1.074
Bpro_0360	zinc-binding alcohol dehydrogenase	0.735	1	---	1.176	1	---	1.132	1	---
Bpro_5563	zinc-binding alcohol dehydrogenase	0.770	5	1.104*	0.100	5	1.535*	0.139	5	1.319*
Bpro_3853	zinc-binding alcohol dehydrogenase	0.800	7	1.055*	1.907	8	1.113*	1.987	8	1.120*
Bpro_3259	zinc-binding alcohol dehydrogenase	0.806	5	[1.053]	0.710	4	1.051*	0.789	5	1.060*
Bpro_2634	zinc-binding alcohol dehydrogenase	1.122	5	1.043*	5.900	5	1.201*	5.295	5	1.187*
Bpro_4700	iron-containing alcohol dehydrogenase	1.129	4	1.094	1.604	4	1.123*	1.857	4	1.114*
Bpro_2565	zinc-binding alcohol dehydrogenase	1.536	4	1.157*	1.400	4	1.126*	1.438	4	1.182*
Bpro_3062	zinc-containing alcohol dehydrogenase	2.949	2	1.173	1.519	2	1.23	1.545	2	1.17
Bpro_2135	zinc-binding alcohol dehydrogenase	3.422	4	1.170*	0.901	4	1.042*	0.859	4	[1.068]
Proteins from suicide vector										
108796622	neomycin phosphotransferase	0.190	1	---	10.142	1	---	4.632	1	---
53793959	oriT-binding protein	---	0	---	79.075	2	2.407	84.455	2	2.359
Ribosomal proteins										
Bpro_4443	50S ribosomal protein L7/L12	1.470	8	1.243*	0.686	8	1.134*	0.675	8	1.123*
Bpro_4445	50S ribosomal protein L1	1.187	9	1.059*	0.603	9	1.052*	0.669	9	1.062*
Bpro_0259	50S ribosomal protein L2	0.975	5	1.020*	0.605	5	[1.049]	0.677	5	[1.111]
Bpro_1292	50S ribosomal protein L25P	1.186	9	1.063*	0.526	9	1.111*	0.581	8	1.068*

Table D.1 (continued)

Locus Tag	Protein Description	115/114	p	EF	116/114	p	EF	117/114	p	EF
Bpro_0257	50S ribosomal protein L4	1.039	12	1.050*	0.552	12	1.125*	0.635	12	1.049*
Bpro_4113	50S ribosomal protein L13	1.020	8	[1.101]	0.576	7	1.077*	0.557	8	1.102*
Bpro_0487	50S ribosomal protein L5	1.088	9	1.025*	0.638	9	1.061*	0.607	8	1.032*
Bpro_2105	50S ribosomal protein L20	1.126	4	1.068*	0.493	4	1.046*	0.470	4	1.139*
Bpro_0485	50S ribosomal protein L14P	1.017	4	1.245	0.553	4	1.248*	0.625	4	1.197*
Bpro_3034	50S ribosomal protein L9P	1.018	9	1.069	0.560	9	1.084*	0.527	9	1.160*
Bpro_0493	50S ribosomal protein L30P	1.139	3	1.036*	0.502	3	[1.104]	0.592	3	1.057*
Bpro_0256	50S ribosomal protein L3P	1.098	7	1.085*	0.588	6	1.128*	0.650	7	[5.488]
Bpro_3802	50S ribosomal protein L28	1.116	5	1.022*	0.562	5	1.035*	0.590	5	1.040*
Bpro_0838	50S ribosomal protein L27	1.077	3	1.058	0.442	3	1.220*	0.464	3	1.111*
Bpro_1101	50S ribosomal protein L11P methyltransferase	0.787	3	1.207	0.823	3	1.173	0.874	3	1.122
Bpro_0490	50S ribosomal protein L6P	1.053	6	[1.408]	0.493	6	1.155*	0.569	6	1.091*
Bpro_2261	50S ribosomal protein L31P	1.146	4	1.052*	0.479	4	1.120*	0.585	3	1.045*
Bpro_0258	50S ribosomal protein L23P	0.947	2	1.068	0.600	2	1.027	0.470	2	1.021*
Bpro_0494	50S ribosomal protein L15P	0.929	2	1.101	0.584	2	1.241	0.472	2	1.226
Bpro_4444	50S ribosomal protein L10	1.120	2	1.079	0.683	2	1.393	0.662	2	1.026*
Bpro_0839	50S ribosomal protein L21P	1.262	1	---	0.558	1	---	0.474	1	---
Bpro_0027	50S ribosomal protein L19	1.118	2	1.747	2.883	2	1.214	4.030	2	1.115*
Bpro_0260	30S ribosomal protein S19P	0.304	4	[2.160]	0.704	4	1.192*	0.382	4	1.322*
Bpro_2695	30S ribosomal protein S2P	1.099	5	1.120	0.736	5	1.163*	0.721	4	1.065*
Bpro_3570	30S ribosomal protein S20P	0.413	1	---	1.101	1	---	0.934	1	---
Bpro_0499	30S ribosomal protein S11	0.687	3	1.322	0.792	3	1.122	0.677	3	1.185

Table D.1 (continued)

Locus Tag	Protein Description	115/114	p	EF	116/114	p	EF	117/114	p	EF
Bpro_0252	30S ribosomal protein S7	0.928	7	1.032*	0.754	7	1.043*	0.638	7	1.033*
Bpro_0262	30S ribosomal protein S3	0.847	5	1.169	0.624	5	1.130*	0.646	5	1.108*
Bpro_1789	30S ribosomal protein S1	0.521	5	[1.193]	0.902	5	1.039*	0.813	5	1.064*
Bpro_0492	30S ribosomal protein S5	0.996	3	1.463	0.636	3	1.217	0.457	3	1.174*
Bpro_3261	30S ribosomal protein S15	0.959	5	1.021*	0.634	5	1.062*	0.662	5	1.036*
Bpro_0255	30S ribosomal protein S10	0.958	3	1.029	0.703	3	1.014*	0.753	3	1.018*
Bpro_0500	30S ribosomal protein S4	1.042	1	---	0.594	1	---	0.620	1	---
Bpro_4112	ribosomal protein S9	0.980	1	---	0.758	1	---	0.755	1	---
Bpro_2692	ribosome recycling factor	0.992	4	1.052	1.192	4	1.102*	1.178	4	1.091*
Bpro_0771	ribosome biogenesis GTP-binding protein YsxC	0.827	1	---	1.143	1	---	1.199	1	---
<u>Central metabolism</u>										
Bpro_0086	2,5-dioxopentanoate dehydrogenase (NAD+)	0.738	3	1.022*	0.702	3	1.059*	0.654	3	1.234
Bpro_0195	6-phosphogluconate dehydrogenase, NAD-binding	1.041	5	1.065	0.726	5	[1.079]	0.745	5	1.090*
Bpro_1231	Beta-ketoadipyl CoA thiolase	0.888	9	1.079*	0.124	9	1.354*	0.134	8	1.327*
Bpro_1287	fructose-bisphosphate aldolase	1.647	1	---	0.556	1	---	0.568	1	---
Bpro_0753	glucose-6-phosphate isomerase	0.738	2	1.016*	0.801	2	1.133	0.774	2	1.227
Bpro_4517	malate synthase G	0.556	8	[1.062]	0.594	8	1.124*	0.684	8	1.204*
Bpro_0643	NADPH-glutathione reductase	0.862	2	1.124	0.869	2	1.075	0.843	2	1.274
Bpro_0160	phosphoenolpyruvate carboxykinase	0.452	7	1.314*	0.666	7	[1.350]	0.792	7	1.142*

Table D.1 (continued)

Locus Tag	Protein Description	115/114	p	EF	116/114	p	EF	117/114	p	EF
Bpro_3665	phosphoenolpyruvate carboxylase	0.789	16	[1.064]	1.444	16	1.055*	1.324	16	[1.089]
Bpro_4634	pyruvate kinase	0.936	1	---	0.347	1	---	0.403	1	---
Bpro_4827	transketolase	0.833	4	1.100*	0.985	4	1.146	1.037	3	1.056
Bpro_2140	acetyl-CoA acetyltransferase	1.122	18	[1.099]	2.674	21	[2.289]	2.245	20	[2.334]
Bpro_3678	L-lactate dehydrogenase (cytochrome)	1.056	1	---	0.928	1	---	0.821	1	---
Bpro_2055	hydroxyacylglutathione hydrolase	0.785	2	1.052	1.162	2	1.086	1.065	2	1.163
Bpro_0187	glycolate oxidase FAD binding subunit	1.153	1	---	1.757	1	---	1.404	1	---
Bpro_3592	aconitate hydratase	0.870	7	1.041*	1.794	8	1.073*	1.929	8	1.042*
Bpro_2942	isocitrate dehydrogenase	0.765	9	[1.294]	0.933	9	1.027*	0.763	9	[1.119]
<u>Proteins involved in biological stresses</u>										
Bpro_3126	molecular chaperone DnaK	0.802	20	[1.091]	0.593	20	1.075*	0.627	20	1.062*
	ATP-dependent protease ATP-binding subunit									
Bpro_2031	ClpX	0.864	2	1.231	0.935	2	1.422	0.753	2	1.742
Bpro_1400	Ferritin and Dps	1.148	2	1.098	3.526	2	1.151	3.733	2	1.176
Bpro_0759	chaperonin GroEL	1.040	38	[1.128]	0.553	37	[1.099]	0.677	37	[1.094]
Bpro_1032	heat shock protein HtpX	1.290	1	---	1.153	1	---	1.067	1	---
Bpro_1303	heat-inducible transcription repressor	1.138	1	---	1.167	1	---	1.246	1	---
Bpro_1199	heat shock protein Hsp20	0.551	10	1.064*	1.970	10	1.054*	2.175	10	1.061*
Bpro_2651	putative heat shock protein	0.943	2	1.280	0.487	3	1.349	0.485	2	1.017*
Bpro_0614	heat shock protein 90	1.255	1	---	1.003	1	---	1.330	1	---

Table D.1 (continued)

Locus Tag	Protein Description	115/114	p	EF	116/114	p	EF	117/114	p	EF
Bpro_0948	DNA repair protein RadC	0.772	1	---	1.260	1	---	0.929	1	---
Bpro_3337	DNA mismatch repair protein MutS	1.362	3	[1.229]	0.846	3	1.136	0.999	3	1.105
Bpro_3097	sigma 70 (RpoD)	1.423	5	1.046*	1.128	5	1.136	1.166	5	1.055*
Bpro_3187	Hsp33 protein	0.927	1	---	1.019	1	---	1.140	1	---
Bpro_2396	heme peroxidase	2.414	2	1.066	0.407	2	1.057	1.345	2	1.009
Bpro_0678	catalase/peroxidase HPI	0.979	1	---	1.054	1	---	0.939	1	---
Bpro_4841	peroxidase	1.051	3	1.056	2.994	3	1.074*	2.870	3	1.063*
Bpro_4561	glyoxylate carboligase	0.293	1	---	0.335	1	---	0.335	1	---
Bpro_4563	2-hydroxy-3-oxopropionate reductase	0.239	2	1.094*	0.051	5	3.652*	0.060	4	3.210*
Bpro_4562	hydroxypyruvate isomerase	0.009	1	---	0.059	2	1.989	0.053	2	2.182
Bpro_3549	glyoxalase I	0.830	1	---	0.524	1	---	0.637	1	---
Bpro_0266	alkyl hydroperoxide reductase/ Thiol specific antioxidant/ Mal allergen	0.936	3	1.054	1.417	4	1.3	1.447	4	1.087*
Bpro_2187	alkyl hydroperoxide reductase/ Thiol specific antioxidant/ Mal allergen	0.892	6	1.050*	0.817	6	1.053*	0.868	6	1.031*
Bpro_2856	glutaredoxin	0.836	5	1.066*	1.427	5	1.295*	1.468	4	1.129*
Bpro_0848	glutaredoxin-like protein	0.676	1	---	0.747	1	---	0.802	1	---
Bpro_2337	phosphoadenylylsulfate reductase (thioredoxin)	0.949	1	---	0.578	1	---	0.676	1	---
Bpro_2263	thioredoxin	0.847	7	1.136*	1.059	7	1.172	1.016	7	1.244
Bpro_3369	thioredoxin	1.267	1	---	0.846	1	---	0.889	1	---
Bpro_4628	thioredoxin	1.031	4	1.291	1.246	4	1.128*	1.184	4	1.056*
Bpro_3801	thioredoxin reductase	0.732	5	1.049*	0.966	5	1.041	1.015	5	1.037

Table D.1 (continued)

Locus Tag	Protein Description	115/114	p	EF	116/114	p	EF	117/114	p	EF
Proteins involved in iron-sulfur cluster assembly										
Bpro_4271	FeS assembly protein SufD	0.656	1	---	1.120	1	---	1.514	1	---
Bpro_4109	iron-sulfur cluster insertion protein ErpA	0.793	3	1.079*	0.839	3	1.049*	0.905	3	1.049
Bpro_3557	(2Fe-2S)-binding	0.865	1	---	0.890	1	---	0.984	1	---
Bpro_2178	cysteine desulfurase IscS	0.907	2	1.038	0.689	2	1.076	0.912	2	1.030
Bpro_2335	sulfate adenylyltransferase subunit 1	0.916	5	[1.089]	0.421	4	1.049*	0.558	5	1.138*
Bpro_2628	sulfur compound chelating protein SoxZ	0.924	2	1.01	0.815	2	1.037	0.915	2	1.084
Bpro_2337	phosphoadenylylsulfate reductase (thioredoxin)	0.949	1	---	0.578	1	---	0.676	1	---
Bpro_2182	Fe-S protein assembly chaperone HscA	0.976	2	1.043	0.940	2	1.003*	1.195	2	1.176
Bpro_2336	sulfate adenylyltransferase subunit 2	1.019	2	1.339	0.444	2	1.095	0.548	2	1.167
Proteins involved in glutathione synthesis										
Bpro_3399	glutamate-cysteine ligase	0.803	1	---	1.161	1	---	1.085	1	---
Bpro_2178	cysteine desulfurase IscS	0.907	2	1.038	0.689	2	1.076	0.912	2	1.030
Bpro_2417	glutathione-dependent formaldehyde-activating, GFA	0.708	8	1.184*	2.187	8	1.101*	2.310	8	1.084*
Bpro_0824	glutathione S-transferase-like	1.612	6	1.090*	1.164	6	1.081*	1.178	6	[1.070]
Bpro_2563	putative glutathione S-transferase-related protein	1.924	6	1.119*	1.538	4	1.013*	1.284	5	1.044*
Bpro_0643	NADPH-glutathione reductase	0.862	2	1.124	0.869	2	1.075	0.843	2	1.274
Bpro_0243	glutathione S-transferase-like	0.976	3	1.025	1.034	3	1.052	1.053	3	1.002*

Table D.1 (continued)

Locus Tag	Protein Description	115/114	p	EF	116/114	p	EF	117/114	p	EF
Bpro_4661	glutathione S-transferase-like	0.961	1	---	1.156	1	---	1.309	1	---
Bpro_4540	glutathione synthetase	0.804	1	---	1.027	1	---	1.136	1	---
Bpro_0387	glutathione S-transferase-like	0.733	1	---	0.412	1	---	0.486	1	---
Bpro_2168	lactoylglutathione lyase	0.913	1	---	1.349	1	---	1.239	1	---
Bpro_2055	hydroxyacylglutathione hydrolase	0.785	2	1.052	1.162	2	1.086	1.065	2	1.163
Bpro_4156	D-isomer specific 2-hydroxyacid dehydrogenase, NAD-binding	0.861	1	---	0.982	1	---	1.052	1	---

CHAPTER 8

8. REFERENCES

Abe, Y., R. Aravena, J. Zopfi, O. Shouakar-Stash, E. Cox, J. D. Roberts and D. Hunkeler (2009). Carbon and Chlorine Isotope Fractionation during Aerobic Oxidation and Reductive Dechlorination of Vinyl Chloride and *cis*-1,2-Dichloroethene. *Environmental Science & Technology*. **43**(1): 101-107.

Agashe, V. R. and F. U. Hartl (2000). Roles of molecular chaperones in cytoplasmic protein folding. *Seminars in Cell & Developmental Biology*. **11**(1): 15-25.

Alexander, A. K. (2010). Bioremediation and Biocatalysis with *Polaromonas* sp. strain JS666. PhD Dissertation, University of Iowa.

Alvarez-Cohen, L. and P. L. McCarty (1991). Effects of toxicity, aeration, and reductant supply on trichloroethylene transformation by a mixed methanotrophic culture. *Appl. Environ. Microbiol.* **57**(1): 228-235.

Attar, M., D. Dong, K.-H. J. Ling and D. D.-S. Tang-Liu (2003). Cytochrome P450 2C8 and Flavin-containing Monooxygenases are Involved in the Metabolism of Tazarotenic Acid in Humans. *Drug Metabolism and Disposition*. **31**(4): 476-481.

Baba, T., T. Ara, M. Hasegawa, Y. Takai, Y. Okumura, M. Baba, K. A. Datsenko, M. Tomita, B. L. Wanner and H. Mori (2006). Construction of *Escherichia coli* K-12 in-frame, single-gene knockout mutants: the Keio collection. *Mol Syst Biol*. **2**.

Baeyer, A. and V. Villiger (1899). Einwirkung des Caro'schen Reagens auf Ketone. *Berichte der deutschen chemischen Gesellschaft*. **32**(3): 3625-3633.

Bagley, D. M. and J. M. Gossett (1990). Tetrachloroethene transformation to trichloroethene and *cis*-1,2-dichloroethene by sulfate-reducing enrichment cultures. *Appl. Environ. Microbiol.* **56**(8): 2511-2516.

Bloom, Y., R. Aravena, D. Hunkeler, E. Edwards and S. K. Frape (2000). Carbon Isotope Fractionation during Microbial Dechlorination of Trichloroethene, *cis*-1,2-Dichloroethene, and Vinyl Chloride: Implications for Assessment of Natural Attenuation. *Environmental Science & Technology*. **34**(13): 2768-2772.

Bonse, G., T. Urban, D. Reichert and D. Henschler (1975). Chemical reactivity, metabolic oxirane formation and biological reactivity of chlorinated ethylenes in the isolated perfused rat liver preparation. *Biochemical Pharmacology*. **24**(19): 1829-1834.

Bradley, P. M. (2003). History and Ecology of Chloroethene Biodegradation: A Review. *Bioremediation Journal*. **7**(2): 81-109.

Bradley, P. M. and F. H. Chapelle (1999). Aerobic Microbial Mineralization of Dichloroethene as Sole Carbon Substrate. *Environmental Science & Technology*. **34**(1): 221-223.

Brown, P., J. Kossanyi and C. Djerassi (1966). Mass spectrometry in structural and stereochemical problems—CXVIII: Aliphatic epoxides. *Tetrahedron*. **22, Supplement 8**(0): 241-267.

Bruice, T. C., J. B. Noar, S. S. Ball and U. V. Venkataram (1983). Monooxygen donation potential of 4a-hydroperoxyflavins as compared with those of a percarboxylic acid and other hydroperoxides. Monooxygen donation to olefin, tertiary amine, alkyl sulfide, and iodide ion. *Journal of the American Chemical Society*. **105**(8): 2452-2463.

Brzostowicz, P. B., M. B. Blasko and P. R. Rouvière (2002). Identification of two gene clusters involved in cyclohexanone oxidation in *Brevibacterium epidermidis* strain HCU. *Applied Microbiology and Biotechnology*. **58**(6): 781-789.

Brzostowicz, P. C., K. L. Gibson, S. M. Thomas, M. S. Blasko and P. E. Rouviere (2000). Simultaneous Identification of Two Cyclohexanone Oxidation Genes from an Environmental *Brevibacterium* Isolate Using mRNA Differential Display. *J. Bacteriol.* **182**(15): 4241-4248.

Brzostowicz, P. C., D. M. Walters, S. M. Thomas, V. Nagarajan and P. E. Rouviere (2003). mRNA Differential Display in a Microbial Enrichment Culture: Simultaneous Identification of Three Cyclohexanone Monooxygenases from Three Species. *Appl. Environ. Microbiol.* **69**(1): 334-342.

Bucheli-Witschel, M., T. Hafner, I. Rüegg and T. Egli (2009). Benzene degradation by *Ralstonia pickettii* PKO1 in the presence of the alternative substrate succinate. *Biodegradation*. **20**(3): 419-431.

Bull, R. J., D. A. Reckhow, V. Rotello, O. M. Bull and J. Kim (2006) Use of Toxicological and Chemical Models to Prioritize DBP Research. 347.

Cai, H. and F. P. Guengerich (1999). Mechanism of Aqueous Decomposition of Trichloroethylene Oxide. *Journal of the American Chemical Society*. **121**(50): 11656-11663.

Canada, K. A., S. Iwashita, H. Shim and T. K. Wood (2002a). Directed Evolution of Toluene *ortho*-Monooxygenase for Enhanced 1-Naphthol Synthesis and Chlorinated Ethene Degradation. *J Bacteriol*. **184**(2): 344-349.

Canada, K. A., S. Iwashita, H. Shim and T. K. Wood (2002b). Directed Evolution of Toluene ortho-Monooxygenase for Enhanced 1-Naphthol Synthesis and Chlorinated Ethene Degradation. *J. Bacteriol.* **184**(2): 344-349.

Cashman, J. R. (2005). Some distinctions between flavin-containing and cytochrome P450 monooxygenases. *Biochemical and Biophysical Research Communications*. **338**(1): 599-604.

Chan, W. Y., M. Wong, J. Guthrie, A. V. Savchenko, A. F. Yakunin, E. F. Pai and E. A. Edwards (2010). Sequence- and activity-based screening of microbial genomes for novel dehalogenases. *Microbial Biotechnology*. **3**(1): 107-120.

Chartrand, M. M. G., A. Waller, T. E. Mattes, M. Elsner, G. Lacrampe-Couloume, J. M. Gossett, E. A. Edwards and B. Sherwood Lollar (2005). Carbon Isotopic Fractionation during Aerobic Vinyl Chloride Degradation. *Environmental Science & Technology*. **39**(4): 1064-1070.

Chauhan, S., P. Barbieri and T. K. Wood (1998). Oxidation of Trichloroethylene, 1,1-Dichloroethylene, and Chloroform by Toluene/*o*-Xylene Monooxygenase from *Pseudomonas stutzeri* OX1. *Appl. Environ. Microbiol.* **64**(8): 3023-3024.

Cheesman, M. J., M. B. Kneller, E. J. Kelly, S. J. Thompson, C. K. Yeung, D. L. Eaton and A. E. Rettie (2001). Purification and Characterization of Hexahistidine-Tagged Cyclohexanone Monooxygenase Expressed in *Saccharomyces cerevisiae* and *Escherichia coli*. *Protein Expression and Purification*. **21**(1): 81-86.

Chen, Y. C., O. P. Peoples and C. T. Walsh (1988). *Acinetobacter* cyclohexanone monooxygenase: gene cloning and sequence determination. *J. Bacteriol.* **170**(2): 781-789.

Cheng, Q., S. M. Thomas, K. Kostichka, J. R. Valentine and V. Nagarajan (2000). Genetic Analysis of a Gene Cluster for Cyclohexanol Oxidation in *Acinetobacter* sp. Strain SE19 by In Vitro Transposition. *J. Bacteriol.* **182**(17): 4744-4751.

Chu, K.-H., S. Mahendra, D. L. Song, M. E. Conrad and L. Alvarez-Cohen (2004). Stable Carbon Isotope Fractionation during Aerobic Biodegradation of Chlorinated Ethenes. *Environmental Science & Technology*. **38**(11): 3126-3130.

Clugston, S. L., J. F. J. Barnard, R. Kinach, D. Miedema, R. Ruman, E. Daub and J. F. Honek (1998). Overproduction and Characterization of a Dimeric Non-Zinc Glyoxalase I from *Escherichia coli*: Evidence for Optimal Activation by Nickel Ions. *Biochemistry*. **37**(24): 8754-8763.

Coleman, N. V., T. E. Mattes, J. M. Gossett and J. C. Spain (2002a). Biodegradation of *cis*-Dichloroethene as the Sole Carbon Source by a β-Proteobacterium. *Applied and Environmental Microbiology*. **68**(6): 2726-2730.

Coleman, N. V., T. E. Mattes, J. M. Gossett and J. C. Spain (2002b). Phylogenetic and Kinetic Diversity of Aerobic Vinyl Chloride-Assimilating Bacteria from Contaminated Sites. *Appl. Environ. Microbiol.* **68**(12): 6162-6171.

Coleman, N. V. and J. C. Spain (2003a). Distribution of the Coenzyme M Pathway of Epoxide Metabolism among Ethene- and Vinyl Chloride-Degrading *Mycobacterium* Strains. *Appl. Environ. Microbiol.* **69**(10): 6041-6046.

Coleman, N. V. and J. C. Spain (2003b). Epoxyalkane:Coenzyme M Transferase in the Ethene and Vinyl Chloride Biodegradation Pathways of *Mycobacterium* Strain JS60. *J. Bacteriol.* **185**(18): 5536-5545.

Coleman, N. V., S. Yau, N. L. Wilson, L. M. Nolan, M. D. Migocki, M.-a. Ly, B. Crossett and A. J. Holmes (2011). Untangling the multiple monooxygenases of *Mycobacterium chubuense* strain NBB4, a versatile hydrocarbon degrader. *Environmental Microbiology Reports*. **3**(3): 297-307.

Colonna, S., N. Gaggero, A. Bertinotti, G. Carrea, P. Pasta and A. Bernardi (1995). Enantioselective oxidation of 1,3-dithioacetals catalysed by cyclohexanone monooxygenase. *Journal of the Chemical Society, Chemical Communications*(11): 1123-1124.

Colonna, S., N. Gaggero, G. Carrea, G. Ottolina, P. Pasta and F. Zambianchi (2002). First asymmetric epoxidation catalysed by cyclohexanone monooxygenase. *Tetrahedron Letters*. **43**(10): 1797-1799.

Colonna, S., N. Gaggero, G. Carrea and P. Pasta (1997). A new enzymatic enantioselective synthesis of dialkyl sulfoxides catalysed by monooxygenases. *Chemical Communications*(5): 439-440.

Colonna, S., N. Gaggero, P. Pasta and G. Ottolina (1996). Enantioselective oxidation of sulfides to sulfoxides catalysed by bacterial cyclohexanone monooxygenases. *Chemical Communications*(20): 2303-2307.

Copeland, A., S. Lucas, A. Lapidus, K. Barry, J. C. Detter, T. Glavina del Rio, N. Hammon, S. Israni, E. Dalin, H. Tice, S. Pitluck, T. Brettin, D. Bruce, C. Han, R. Tapia, A. C. Munk, P. Gilna, J. Schmutz, F. Larimer, M. Land, L. Hauser, N. Kyrpides, I. Anderson and P. Richardson (2006). Complete sequence of chromosome of Polaromonas sp. JS666. Walnut Creek, US DOE Joint Genome Institute.

Corma, A., L. T. Nemeth, M. Renz and S. Valencia (2001). Sn-zeolite beta as a heterogeneous chemoselective catalyst for Baeyer-Villiger oxidations. *Nature*. **412**(6845): 423-425.

Costa, A. K. and K. M. Ivanetich (1982). The 1,2-dichloroethylenes: Their metabolism by hepatic cytochrome P-450 in vitro. *Biochemical Pharmacology*. **31**(11): 2093-2102.

Costa, A. K. and K. M. Ivanetich (1984). Chlorinated ethylenes: their metabolism and effect on DNA repair in rat hepatocytes. *Carcinogenesis*. **5**(12): 1629-1636.

Danko, A. S., C. A. Saski, J. P. Tomkins and D. L. Freedman (2006). Involvement of Coenzyme M during Aerobic Biodegradation of Vinyl Chloride and Ethene by *Pseudomonas putida* Strain AJ and *Ochrobactrum* sp. Strain TD. *Appl. Environ. Microbiol.* **72**(5): 3756-3758.

Darlington, R., L. Lehmicke, R. G. Andrachek and D. L. Freedman (2008). Biotic and Abiotic Anaerobic Transformations of Trichloroethene and *cis*-1,2-Dichloroethene in Fractured Sandstone. *Environmental Science & Technology*. **42**(12): 4323-4330.

Davey, J. F. and P. W. Trudgill (1977). The Metabolism of trans-Cyclohexan-1,2-diol by an Acinetobacter Species. *European Journal of Biochemistry*. **74**(1): 115-127.

de Visser, S. P., D. Kumar and S. Shaik (2004). How do aldehyde side products occur during alkene epoxidation by cytochrome P450? Theory reveals a state-specific multi-state scenario where the high-spin component leads to all side products. *Journal of Inorganic Biochemistry*. **98**(7): 1183-1193.

Dijk, J. A., J. Gerritse, G. Schraa and A. J. M. Stams (2004). Degradation pathway of 2-chloroethanol in *Pseudomonas stutzeri* strain JJ under denitrifying conditions. *Archives of Microbiology*. **182**(6): 514-519.

Dolfing, J. and D. B. Janssen (1994). Estimates of Gibbs free energies of formation of chlorinated aliphatic compounds. *Biodegradation*. **5**(1): 21-28.

Donoghue, N. A., D. B. Norris and P. W. Trudgill (1976). The Purification and Properties of Cyclohexanone Oxygenase from *Nocardia globerula* CL1 and *Acinetobacter* NCIB 9871. *European Journal of Biochemistry*. **63**(1): 175-192.

Donoghue, N. A. and P. W. Trudgill (1975). The Metabolism of Cyclohexanol by *Acinetobacter* NCIB 9871. *European Journal of Biochemistry*. **60**(1): 1-7.

Douglas, H. (1983). Studies on transformation of *Escherichia coli* with plasmids. *Journal of Molecular Biology*. **166**(4): 557-580.

Dowsley, T. F., P.-G. Forkert, L. A. Benesch and J. L. Bolton (1995). Reaction of glutathione with the electrophilic metabolites of 1,1-dichloroethylene. *Chemico-Biological Interactions*. **95**(3): 227-244.

Duba, A. G., K. J. Jackson, M. C. Jovanovich, R. B. Knapp and R. T. Taylor (1996). TCE Remediation Using In Situ, Resting-State Bioaugmentation. *Environmental Science & Technology*. **30**(6): 1982-1989.

Elango, V., H. D. Kurtz and D. L. Freedman (2011). Aerobic cometabolism of trichloroethene and *cis*-dichloroethene with benzene and chlorinated benzenes as growth substrates. *Chemosphere*. **84**(2): 247-253.

Ensign, S. A. (2001). Microbial Metabolism of Aliphatic Alkenes. *Biochemistry*. **40**(20): 5845-5853.

Ensign, S. A., M. R. Hyman and D. J. Arp (1992). Cometabolic degradation of chlorinated alkenes by alkene monooxygenase in a propylene-grown *Xanthobacter* strain. *Appl. Environ. Microbiol.* **58**(9): 3038-3046.

Forkert, P.-G., R. M. Baldwin, B. Millen, L. H. Lash, D. A. Putt, M. A. Shultz and K. S. Collins (2005). Pulmonary Bioactivation of Trichloroethylene to Chloral Hydrate: Relative Contributions of CYP2E1, CYP2F and CYP2B1. *Drug Metabolism and Disposition*. **33**(10): 1429-1437.

Fraaije, M. W., N. M. Kamerbeek, W. J. H. van Berkel and D. B. Janssen (2002). Identification of a Baeyer-Villiger monooxygenase sequence motif. *FEBS Letters*. **518**(1-3): 43-47.

Friedman, P. J. and J. R. Cooper (1960). The Role of Alcohol Dehydrogenase in the Metabolism of Chloral Hydrate. *Journal of Pharmacology and Experimental Therapeutics*. **129**(4): 373-376.

Fulco, A. J. (1991). $P450_{BM-3}$ and other Inducible Bacterial P450 Cytochromes: Biochemistry and Regulation. *Annual Review of Pharmacology and Toxicology*. **31**(1): 177-203.

Gao, J. and R. S. Skeen (1999). Glucose-induced biodegradation of *cis*-dichloroethylene under aerobic conditions. *Water Research*. **33**(12): 2789-2796.

Gay, P., D. Le Coq, M. Steinmetz, E. Ferrari and J. A. Hoch (1983). Cloning structural gene sacB, which codes for exoenzyme levansucrase of *Bacillus subtilis*: expression of the gene in *Escherichia coli*. *J. Bacteriol.* **153**(3): 1424-1431.

Giddings, C. G. S. (2010). Unpublished Work. Ithaca, NY, Cornell University.

Giddings, C. G. S. (2012). Bioremediation of *cis*-dichloroethene by *Polaromonas* sp. strain JS666. PhD Dissertation, Cornell University.

Giddings, C. G. S., F. Liu and J. M. Gossett (2010). Microcosm Assessment of *Polaromonas* sp. JS666 as a Bioaugmentation Agent for Degradation of *cis*-1,2-dichloroethene in Aerobic, Subsurface Environments. *Ground Water Monitoring & Remediation*. **30**(2): 106-113.

Gilar, M., P. Olivova, A. E. Daly and J. C. Gebler (2005a). Orthogonality of separation in two-dimensional liquid chromatography. *Anal Chem*. **77**(19): 6426-6434.

Gilar, M., P. Olivova, A. E. Daly and J. C. Gebler (2005b). Two-dimensional separation of peptides using RP-RP-HPLC system with different pH in first and second separation dimensions. *J Sep Sci*. **28**(14): 1694-1703.

Goldman, P., G. W. A. Milne and D. B. Keister (1968). Carbon-Halogen Bond Cleavage. *Journal of Biological Chemistry*. **243**(2): 428-434.

Gossett, J. M. (2010). Sustained Aerobic Oxidation of Vinyl Chloride at Low Oxygen Concentrations. *Environmental Science & Technology*. **44**(4): 1405-1411.

Griesbaum, K., R. Kibar and B. Pfeffer (1975). Synthese und Stabilität von 2,3-Dichloroxiranen. *Justus Liebigs Annalen der Chemie*. **1975**(2): 214-224.

Griffin, M. and P. W. Trudgill (1972). The metabolism of cyclopentanol by Pseudomonas N.C.I.B. 9872. *Biochemical Journal*. **129**(3): 595-603.

Guengerich, F. P. (1991). Reactions and significance of cytochrome P-450 enzymes. *Journal of Biological Chemistry*. **266**(16): 10019-10022.

Guengerich, F. P., W. M. Crawford and P. G. Watanabe (1979). Activation of vinyl chloride to covalently bound metabolites: roles of 2-chloroethylene oxide and 2-chloroacetaldehyde. *Biochemistry*. **18**(23): 5177-5182.

Guengerich, F. P. and P. S. Mason (1980). Alcohol dehydrogenase-coupled spectrophotometric assay of epoxide hydratase activity. *Analytical Biochemistry*. **104**(2): 445-451.

Harkness, M. R., A. A. Bracco, M. J. Brennan, K. A. DeWeerd and J. L. Spivack (1999). Use of Bioaugmentation To Stimulate Complete Reductive Dechlorination of Trichloroethene in Dover Soil Columns. *Environmental Science & Technology*. **33**(7): 1100-1109.

Hartmans, S. and J. A. De Bont (1992). Aerobic vinyl chloride metabolism in *Mycobacterium aurum* L1. *Appl. Environ. Microbiol.* **58**(4): 1220-1226.

Hasegawa, Y., Y. Nakai, T. Tokuyama and H. Iwaki (2000). Purification and Characterization of Cyclohexanone 1,2-Monooxygenase from *Exophiala jeanselmei* strain KUFI-6N. *Biosci. Biotechnol. Biochem.* **64**: 2696-2698.

Hesterkamp, T. and B. Bukau (1998). Role of the DnaK and HscA homologs of Hsp70 chaperones in protein folding in *E.coli*. *EMBO J.* **17**(16): 4818-4828.

Holliger, C., D. Hahn, H. Harmsen, W. Ludwig, W. Schumacher, B. Tindall, F. Vazquez, N. Weiss and A. J. B. Zehnder (1998a). *Dehalobacter restrictus* gen. nov. and sp. nov., a strictly anaerobic bacterium that reductively dechlorinates tetra- and trichloroethene in an anaerobic respiration. *Archives of Microbiology*. **169**(4): 313-321.

Holliger, C., G. Schraa, A. J. Stams and A. J. Zehnder (1993). A highly purified enrichment culture couples the reductive dechlorination of tetrachloroethene to growth. *Appl. Environ. Microbiol.* **59**(9): 2991-2997.

Holliger, C., G. Wohlfarth and G. Diekert (1998b). Reductive dechlorination in the energy metabolism of anaerobic bacteria. *FEMS Microbiology Reviews*. **22**(5): 383-398.

Holmgren, A. (1989). Thioredoxin and glutaredoxin systems. *The Journal of biological chemistry*. **264**(24): 13963-13966.

Hudrlik, P. F., A. M. Hudrlik, G. Nagendrappa, T. Yimenu, E. T. Zellers and E. Chin (1980). Silicon-directed Baeyer-Villiger reactions. Stereospecific synthesis of olefinic acids and esters. *Journal of the American Chemical Society*. **102**(22): 6894-6896.

Hunkeler, D., R. Aravena and E. Cox (2002). Carbon Isotopes as a Tool To Evaluate the Origin and Fate of Vinyl Chloride: Laboratory Experiments and Modeling of Isotope Evolution. *Environmental Science & Technology*. **36**(15): 3378-3384.

Hutson, D. H., E. C. Hoadley and B. A. Pickering (1971). The Metabolic Fate of [Vinyl-I-14C]Dichlorvos in the Rat after Oral and Inhalation Exposure. *Xenobiotica*. **1**(6): 593-611.

Irgens, R. L., J. J. Gosink and S. T. (1996). Polaromonas vacuolata gen. nov., sp. nov., a Psychrophilic, Marine, Gas Vacuolate Bacterium from Antarctica. *Int J Syst Bacteriol*. **46**(3): 822-826.

Iwaki, H., Y. Hasegawa, M. Teraoka, T. Tokuyama, H. Bergeron and P. C. K. Lau (1999). Identification of a Transcriptional Activator (ChnR) and a 6-Oxohexanoate Dehydrogenase (ChnE) in the Cyclohexanol Catabolic Pathway in *Acinetobacter* sp. Strain NCIMB 9871 and Localization of the Genes That Encode Them. *Appl. Envir. Microbiol.* **65**(11): 5158-5162.

Iwaki, H., Y. Hasegawa, M. Teraoka, T. Tokuyama, L. Bernard and C. K. Lau Peter (2002a). Cyclohexanol Biodegradation Genes: A Pathway of Opportunities. Biocatalysis in Polymer Science, American Chemical Society. **840:** 80-92.

Iwaki, H., Y. Hasegawa, S. Wang, M. M. Kayser and P. C. K. Lau (2002b). Cloning and Characterization of a Gene Cluster Involved in Cyclopentanol Metabolism in *Comamonas* sp. Strain NCIMB 9872 and Biotransformations Effected by *Escherichia coli*-Expressed Cyclopentanone 1,2-Monooxygenase. *Appl. Environ. Microbiol.* **68**(11): 5671-5684.

Janssen, D. B., G. Grobben, R. Hoekstra, R. Oldenhuis and B. Witholt (1988). Degradation of *trans*-1,2-dichloroethene by mixed and pure cultures of methanotrophic bacteria. *Applied Microbiology and Biotechnology*. **29**(4): 392-399.

Jennings, L. K. (2005). Culturing and enumeration of *Polaromonas* sp. strain JS666 for its use as a bioaaugmentation agent in the remediation of *cis*-dichloroethene-contaminated sites. MS Thesis, Cornell University.

Jennings, L. K. (2009). Proteomic and transcriptomic analyses reveal genes upregulated by *cis*-dichloroethene in *Polaromonas* JS666. PhD Dissertation, Cornell University.

Jennings, L. K., M. M. G. Chartrand, G. Lacrampe-Couloume, B. S. Lollar, J. C. Spain and J. M. Gossett (2009). Proteomic and Transcriptomic Analyses Reveal Genes

Upregulated by *cis*-Dichloroethene in *Polaromonas* sp. Strain JS666. *Appl. Environ. Microbiol.* **75**(11): 3733-3744.

Jeon, C. O., M. Park, H.-S. Ro, W. Park and E. L. Madsen (2006). The Naphthalene Catabolic (*nag*) Genes of *Polaromonas naphthalenivorans* CJ2: Evolutionary Implications for Two Gene Clusters and Novel Regulatory Control. *Appl. Environ. Microbiol.* **72**(2): 1086-1095.

Johnson, D., J. Park, J. Kukor and L. Abriola (2006). Effect of carbon starvation on toluene degradation activity by toluene monooxygenase-expressing bacteria. *Biodegradation*. **17**(5): 437-445.

Kalogeraki, V. S. and S. C. Winans (1997). Suicide plasmids containing promoterless reporter genes can simultaneously disrupt and create fusions to target genes of diverse bacteria. *Gene*. **188**(1): 69-75.

Kemal, C. and T. C. Bruice (1976). Simple synthesis of a 4a-hydroperoxy adduct of a 1,5-dihydroflavine: preliminary studies of a model for bacterial luciferase. *Proceedings of the National Academy of Sciences*. **73**(4): 995-999.

Kim, Y. and L. Semprini (2005). Cometabolic transformation of *cis*-1,2-dichloroethylene and *cis*-1,2-dichloroethylene epoxide by a butane-grown mixed culture. *Water Science & Technology*. **52**(8): 125-131.

Kostichka, K., S. M. Thomas, K. J. Gibson, V. Nagarajan and Q. Cheng (2001). Cloning and Characterization of a Gene Cluster for Cyclododecanone Oxidation in *Rhodococcus ruber* SC1. *J. Bacteriol.* **183**(21): 6478-6486.

Kunz, D. A. and P. J. Weimer (1983). Bacterial formation and metabolism of 6-hydroxyhexanoate: evidence of a potential role for omega-oxidation. *Journal of Bacteriology*. **156**(2): 567-575.

Landa, A. S., E. M. Sipkema, J. Weijma, A. A. Beenackers, J. Dolfing and D. B. Janssen (1994). Cometabolic degradation of trichloroethylene by *Pseudomonas cepacia* G4 in a chemostat with toluene as the primary substrate. *Appl. Environ. Microbiol.* **60**(9): 3368-3374.

Larson, J. L. and R. J. Bull (1989). Effect of ethanol on the metabolism of trichloroethylene. *Journal of Toxicology and Environmental Health*. **28**(4): 395-406.

Lee, D. H., M. D. Kim, W. H. Lee, D. H. Kweon and J. H. Seo (2004). Consortium of fold-catalyzing proteins increases soluble expression of cyclohexanone monooxygenase in recombinant *Escherichia coli*. *Applied Microbiology and Biotechnology*. **63**(5): 549-552.

Lee, H. J., J. M. Kim, S. H. Lee, M. Park, E. L. Madsen and C. O. Jeon (2011). Characterization of Gentisate-1,2-Dioxygenase in the Third Naphthalene

Catabolic Gene Cluster of *Polaromonas naphthalenivorans* CJ2: Role in Naphthalene Degradation. *Microbiology*.

Lee, J., L. Cao, S. Y. Ow, M. E. Barrios-Llerena, W. Chen, T. K. Wood and P. C. Wright (2006). Proteome Changes after Metabolic Engineering to Enhance Aerobic Mineralization of *cis*-1,2-Dichloroethylene. *Journal of Proteome Research*. **5**(6): 1388-1397.

Lee, J., S. R. Hiibel, K. F. Reardon and T. K. Wood (2010). Identification of stress-related proteins in *Escherichia coli* using the pollutant *cis*-dichloroethylene. *Journal of Applied Microbiology*. **108**(6): 2088-2102.

Lee, P. K. H., M. E. Conrad and L. Alvarez-Cohen (2007). Stable Carbon Isotope Fractionation of Chloroethenes by Dehalorespiring Isolates. *Environmental Science & Technology*. **41**(12): 4277-4285.

Lee, W.-H., Y.-C. Park, D.-H. Lee, K. Park and J.-H. Seo (2005). Simultaneous Biocatalyst Production and Baeyer-Villiger Oxidation for Bioconversion of Cyclohexanone by Recombinant *Escherichia coli* Expressing Cyclohexanone Monooxygenase. Twenty-Sixth Symposium on Biotechnology for Fuels and Chemicals. B. H. Davison, B. R. Evans, M. Finkelstein and J. D. McMillan, Humana Press**:** 827-836.

Liebler, D. C. and F. P. Guengerich (1983). Olefin oxidation by cytochrome P-450: evidence for group migration in catalytic intermediates formed with vinylidene chloride and *trans*-1-phenyl-1-butene. *Biochemistry*. **22**(24): 5482-5489.

Little, C. D., A. V. Palumbo, S. E. Herbes, M. E. Lidstrom, R. L. Tyndall and P. J. Gilmer (1988). Trichloroethylene Biodegradation by a Methane-Oxidizing Bacterium. *Appl. Environ. Microbiol.* **54**(4): 951-956.

Liu, F. (2009). Unpublished Work. Ithaca, NY, Cornell University.

Lorah, M. M. and L. D. Olsen (1998). Degradation of 1,1,2,2-Tetrachloroethane in a Freshwater Tidal Wetland: Field and Laboratory Evidence. *Environmental Science & Technology*. **33**(2): 227-234.

Lorah, M. M. and M. A. Voytek (2004). Degradation of 1,1,2,2-tetrachloroethane and accumulation of vinyl chloride in wetland sediment microcosms and in situ porewater: biogeochemical controls and associations with microbial communities. *Journal of Contaminant Hydrology*. **70**(1-2): 117-145.

Mattes, T., N. Coleman, A. Chuang, A. Rogers, J. Spain and J. Gossett (2007). Mechanism controlling the extended lag period associated with vinyl chloride starvation in *Nocardioides* sp. strain JS614. *Archives of Microbiology*. **187**(3): 217-226.

Mattes, T. E., A. K. Alexander, P. M. Richardson, A. C. Munk, C. S. Han, P. Stothard and N. V. Coleman (2008). The Genome of *Polaromonas* sp. Strain JS666:

Insights into the Evolution of a Hydrocarbon- and Xenobiotic-Degrading Bacterium, and Features of Relevance to Biotechnology. *Appl. Environ. Microbiol.* **74**(20): 6405-6416.

McManus, M. E., I. Stupans, W. Burgess, J. A. Koenig, P. M. Hall and D. J. Birkett (1987). Flavin-containing monooxygenase activity in human liver microsomes. *Drug Metabolism and Disposition*. **15**(2): 256-261.

Meunier, B. (1992). Potassium Monopersulfate - Just Another Primary Oxidant or A Highly Versatile Oxygen Atom Donor in Metalloporphyrin-Mediated Oxygenation and Oxidation Reactions. *New Journal of Chemistry*. **16**(1-2): 203-211.

Miller, E., G. Wohlfarth and G. Diekert (1997). Comparative studies on tetrachloroethene reductive dechlorination mediated by *Desulfitobacterium* sp. strain PCE-S. *Archives of Microbiology*. **168**(6): 513-519.

Miller, R. E. and F. P. Guengerich (1983). Metabolism of Trichloroethylene in Isolated Hepatocytes, Microsomes, and Reconstituted Enzyme Systems Containing Cytochrome P-450. *Cancer Research*. **43**(3): 1145-1152.

Mirza, I. A., B. J. Yachnin, S. Wang, S. Grosse, H. l. n. Bergeron, A. Imura, H. Iwaki, Y. Hasegawa, P. C. K. Lau and A. M. Berghuis (2009). Crystal Structures of Cyclohexanone Monooxygenase Reveal Complex Domain Movements and a Sliding Cofactor. *Journal of the American Chemical Society*. **131**(25): 8848-8854.

Morgan, E. T., V. Ullrich, A. Daiber, P. Schmidt, N. Takaya, H. Shoun, J. C. McGiff, A. Oyekan, C. J. Hanke, W. B. Campbell, C.-S. Park, J.-S. Kang, H.-G. Yi, Y.-N. Cha, D. Mansuy and J.-L. Boucher (2001). Cytochromes P450 and Flavin Monooxygenases—Targets and Sources of Nitric Oxide. *Drug Metabolism and Disposition*. **29**(11): 1366-1376.

Nelson, M. J., S. O. Montgomery, W. R. Mahaffey and P. H. Pritchard (1987). Biodegradation of trichloroethylene and involvement of an aromatic biodegradative pathway. *Appl. Environ. Microbiol.* **53**(5): 949-954.

Neumann, A., H. Scholz-Muramatsu and G. Diekert (1994). Tetrachloroethene metabolism of *Dehalospirillum multivorans*. *Archives of Microbiology*. **162**(4): 295-301.

Newman, L. M. and L. P. Wackett (1991). Fate of 2,2,2-trichloroacetaldehyde (chloral hydrate) produced during trichloroethylene oxidation by methanotrophs. *Appl. Environ. Microbiol.* **57**(8): 2399-2402.

Nishino, S. (2011). Personal communcation.

Nishino, S. F. and J. C. Spain (1993). Cell density-dependent adaptation of *Pseudomonas putida* to biodegradation of *p*-nitrophenol. *Environmental Science & Technology*. **27**(3): 489-494.

Novy, R. and B. Morris (2001) Use of glucose to control basal expression in the pET system innovations. *inNovations*, 16.

Oldenhuis, R., J. Y. Oedzes, J. J. van der Waarde and D. B. Janssen (1991). Kinetics of chlorinated hydrocarbon degradation by *Methylosinus trichosporium* OB3b and toxicity of trichloroethylene. *Appl. Environ. Microbiol.* **57**(1): 7-14.

Oldenhuis, R., R. L. Vink, D. B. Janssen and B. Witholt (1989). Degradation of chlorinated aliphatic hydrocarbons by *Methylosinus trichosporium* OB3b expressing soluble methane monooxygenase. *Appl. Environ. Microbiol.* **55**(11): 2819-2826.

Park, J., J. Lang, K. Thamaraiselvi, J. J. Kukor and L. M. Abriola (2008). Induction kinetics of aerobic toluene degradation as a function of carbon starvation history. *Process Biochemistry*. **43**(12): 1345-1351.

Park, M., Y. Jeon, H. H. Jang, H.-S. Ro, W. Park, E. L. Madsen and C. O. Jeon (2007). Molecular and Biochemical Characterization of 3-Hydroxybenzoate 6-Hydroxylase from *Polaromonas naphthalenivorans* CJ2. *Appl. Environ. Microbiol.* **73**(16): 5146-5152.

Prileschajew, N. (1909). Oxydation ungesättigter Verbindungen mittels organischer Superoxyde. *Berichte der deutschen chemischen Gesellschaft*. **42**(4): 4811-4815.

Pumphrey, G. M. and E. L. Madsen (2007). Naphthalene metabolism and growth inhibition by naphthalene in *Polaromonas naphthalenivorans* strain CJ2. *Microbiology*. **153**(11): 3730-3738.

Rahman, M., M. Hasan and K. Shimizu (2008). Growth phase-dependent changes in the expression of global regulatory genes and associated metabolic pathways in *Escherichia coli*. *Biotechnology Letters*. **30**(5): 853-860.

Rauhut, R. and G. Klug (1999). mRNA degradation in bacteria. *FEMS Microbiology Reviews*. **23**(3): 353-370.

Ray, K., S. M. Lee and L. Que Jr (2008). Iron-oxidation-state-dependent O–O bond cleavage of *meta*-chloroperbenzoic acid to form an iron(IV)-oxo complex. *Inorganica Chimica Acta*. **361**(4): 1066-1069.

Rial, D. V., D. A. Bianchi, P. Kapitanova, A. Lengar, J. B. van Beilen and M. D. Mihovilovic (2008). Stereoselective Desymmetrizations by Recombinant Whole Cells Expressing the Baeyer–Villiger Monooxygenase from *Xanthobacter* sp. ZL5: A New Biocatalyst Accepting Structurally Demanding Substrates. *European Journal of Organic Chemistry*. **2008**(7): 1203-1213.

Rosner, B., P. Mccarty and A. Spormann (1997). In Vitro Studies on Reductive Vinyl Chloride Dehalogenation by an Anaerobic Mixed Culture. *Appl. Environ. Microbiol.* **63**(11): 4139-4144.

Ross, P. L., Y. N. Huang, J. N. Marchese, B. Williamson, K. Parker, S. Hattan, N. Khainovski, S. Pillai, S. Dey, S. Daniels, S. Purkayastha, P. Juhasz, S. Martin, M. Bartlet-Jones, F. He, A. Jacobson and D. J. Pappin (2004). Multiplexed Protein Quantitation in *Saccharomyces cerevisiae* Using Amine-reactive Isobaric Tagging Reagents. *Molecular & Cellular Proteomics*. **3**(12): 1154-1169.

Rui, L., L. Cao, W. Chen, K. F. Reardon and T. K. Wood (2004a). Active Site Engineering of the Epoxide Hydrolase from *Agrobacterium radiobacter* AD1 to Enhance Aerobic Mineralization of *cis*-1,2-Dichloroethylene in Cells Expressing an Evolved Toluene *ortho*-Monooxygenase. *Journal of Biological Chemistry*. **279**(45): 46810-46817.

Rui, L., Y. M. Kwon, K. F. Reardon and T. K. Wood (2004b). Metabolic pathway engineering to enhance aerobic degradation of chlorinated ethenes and to reduce their toxicity by cloning a novel glutathione S-transferase, an evolved toluene *o*-monooxygenase, and γ-glutamylcysteine synthetase. *Environmental Microbiology*. **6**(5): 491-500.

Scheps, D., S. Honda Malca, H. Hoffmann, B. M. Nestl and B. Hauer (2011). Regioselective w-hydroxylation of medium-chain *n*-alkanes and primary alcohols by CYP153 enzymes from *Mycobacterium marinum* and *Polaromonas* sp. strain JS666. *Organic & Biomolecular Chemistry*. **9**(19): 6727-6733.

Schmidt, K. R., T. Augenstein, M. Heidinger, S. Ertl and A. Tiehm (2010). Aerobic biodegradation of *cis*-1,2-dichloroethene as sole carbon source: Stable carbon isotope fractionation and growth characteristics. *Chemosphere*. **78**(5): 527-532.

Schweigert, N., A. J. B. Zehnder and R. I. L. Eggen (2001). Chemical properties of catechols and their molecular modes of toxic action in cells, from microorganisms to mammals. *Environmental Microbiology*. **3**(2): 81-91.

Sharma, P. and P. McCarty (1996). Isolation and Characterization of a Facultatively Aerobic Bacterium That Reductively Dehalogenates Tetrachloroethene to *cis*-1,2-Dichloroethene. *Appl. Environ. Microbiol.* **62**(3): 761-765.

Sharpe, A. L. and D. E. Carter (1993). Substrate specificity of rat liver aldehyde dehydrogenase with chloroacetaldehydes. *Journal of Biochemical Toxicology*. **8**(3): 155-160.

Shim, H. and T. K. Wood (2000). Aerobic degradation of mixtures of chlorinated aliphatics by cloned toluene-*o*-xylene monooxygenase and toluene *o*-monooxygenase in resting cells. *Biotechnology and Bioengineering*. **70**(6): 693-698.

Shin, K. (2010). Biodegradation of Diphenylamine and *cis*-dichloroethene. PhD Dissertation, Georgia Institute of Technology.

Singh, H., F. Löffler and B. Fathepure (2004). Aerobic biodegradation of vinyl chloride by a highly enriched mixed culture. *Biodegradation*. **15**(3): 197-204.

Sitkiewicz, I. and J. Musser (2009). Analysis of growth-phase regulated genes in *Streptococcus agalactiae* by global transcript profiling. *BMC Microbiology*. **9**(1): 32.

Smith, M. A. and M. J. Bidochka (1998). Bacterial fitness and plasmid loss: the importance of culture conditions and plasmid size. *Canadian Journal of Microbiology*. **44**(4): 351-355.

Taniguchi, Y., P. J. Choi, G.-W. Li, H. Chen, M. Babu, J. Hearn, A. Emili and X. S. Xie (2010). Quantifying *E. coli* Proteome and Transcriptome with Single-Molecule Sensitivity in Single Cells. *Science*. **329**(5991): 533-538.

Tiehm, A., K. R. Schmidt, B. Pfeifer, M. Heidinger and S. Ertl (2008). Growth kinetics and stable carbon isotope fractionation during aerobic degradation of *cis*-1,2-dichloroethene and vinyl chloride. *Water Research*. **42**(10-11): 2431-2438.

USEPA (2011). 2011 Edition of the Drinking Water Standards and Health Advisories. O. W. U. S. E. P. Agency. Washington, DC, U.S. Environmental Protection Agency.

Vallon, O. (2000). New sequence motifs in flavoproteins: Evidence for common ancestry and tools to predict structure. *Proteins: Structure, Function, and Bioinformatics*. **38**(1): 95-114.

Van Beilen, J. B., F. Mourlane, M. A. Seeger, J. Kovac, Z. Li, T. H. M. Smits, U. Fritsche and B. Witholt (2003). Cloning of Baeyer-Villiger monooxygenases from *Comamonas*, *Xanthobacter* and *Rhodococcus* using polymerase chain reaction with highly degenerate primers. *Environmental Microbiology*. **5**(3): 174-182.

van Hylckama Vlieg, J., W. de Koning and D. Janssen (1996). Transformation Kinetics of Chlorinated Ethenes by *Methylosinus trichosporium* OB3b and Detection of Unstable Epoxides by On-Line Gas Chromatography. *Appl. Environ. Microbiol.* **62**(9): 3304-3312.

van Hylckama Vlieg, J. E. T. and D. B. Janssen (2001). Formation and detoxification of reactive intermediates in the metabolism of chlorinated ethenes. *Journal of Biotechnology*. **85**(2): 81-102.

Vancheeswaran, S., R. U. Halden, K. J. Williamson, J. D. Ingle and L. Semprini (1999). Abiotic and Biological Transformation of Tetraalkoxysilanes and Trichloroethene/*cis*-1,2-Dichloroethene Cometabolism Driven by Tetrabutoxysilane-Degrading Microorganisms. *Environmental Science & Technology*. **33**(7): 1077-1085.

Vannelli, T., M. Logan, D. M. Arciero and A. B. Hooper (1990). Degradation of halogenated aliphatic compounds by the ammonia-oxidizing bacterium *Nitrosomonas europaea*. *Appl. Environ. Microbiol.* **56**(4): 1169-1171.

Verce, M. F., C. K. Gunsch, A. S. Danko and D. L. Freedman (2002). Cometabolism of *cis*-1,2-Dichloroethene by Aerobic Cultures Grown on Vinyl Chloride as the Primary Substrate. *Environmental Science & Technology*. **36**(10): 2171-2177.

Verce, M. F., R. L. Ulrich and D. L. Freedman (2000). Characterization of an Isolate That Uses Vinyl Chloride as a Growth Substrate under Aerobic Conditions. *Appl. Environ. Microbiol.* **66**(8): 3535-3542.

Wackett, L. P., G. A. Brusseau, S. R. Householder and R. S. Hanson (1989). Survey of microbial oxygenases: trichloroethylene degradation by propane-oxidizing bacteria. *Appl. Environ. Microbiol.* **55**(11): 2960-2964.

Wackett, L. P. and D. T. Gibson (1988). Degradation of trichloroethylene by toluene dioxygenase in whole-cell studies with *Pseudomonas putida* F1. *Appl. Environ. Microbiol.* **54**(7): 1703-1708.

Wakasugi, T., T. Miyakawa, F. Suzuki, S. Itsuno and K. Ito (1993). Preparation of Dichloroacetaldehyde Cyclic Trimer and Its Depolymerization. *Synthetic Communications*. **23**(9): 1289-1294.

Walton, A. Z. and J. D. Stewart (2004). Understanding and Improving NADPH-Dependent Reactions by Nongrowing Escherichia coli Cells. *Biotechnology Progress*. **20**(2): 403-411.

Wiese, S., K. A. Reidegeld, H. E. Meyer and B. Warscheid (2007). Protein labeling by iTRAQ: A new tool for quantitative mass spectrometry in proteome research. *PROTEOMICS*. **7**(3): 340-350.

Williams, D. E., M. K. Shigenaga and N. Castagnoli (1990). The role of cytochromes P-450 and flavin-containing monooxygenase in the metabolism of (*S*)-nicotine by rabbit lung. *Drug Metabolism and Disposition*. **18**(4): 418-428.

Wood, T. K. and S. W. Peretti (1990). Depression of protein synthetic capacity due to cloned-gene expression in *E. coli*. *Biotechnology and Bioengineering*. **36**(9): 865-878.

Yagi, J. M., D. Sims, T. Brettin, D. Bruce and E. L. Madsen (2009). The genome of *Polaromonas naphthalenivorans* strain CJ2, isolated from coal tar-contaminated sediment, reveals physiological and metabolic versatility and evolution through extensive horizontal gene transfer. *Environmental Microbiology*. **11**(9): 2253-2270.